APPENDIX A | INFORMATION QUALITY AND PEER REVIEW PROCEDURES

A.1 Ensuring Information Quality

The development of the technical documentation, Framework, Tool, and underlying analyses were conducted in accordance with EPA's Guidelines for Ensuring and Maximizing the Quality, Objectivity, Utility, and Integrity of Information Disseminated by the Environmental Protection Agency,[1] which follows Office of Management and Budget (OMB) guidelines[2] and implements the Information Quality Act (IQA) (Section 515 of Public Law 106–554).[3] The following section this Appendix describes the independent peer review that was performed on the technical documentation materials.

In accordance with OMB definitions, EPA defines the basic standard of information "quality" by the attributes objectivity, integrity, utility, and transparency. For products meeting a higher standard of quality, like this product, the Agency requires an appropriate level of transparency regarding data and methods in order to facilitate the reproducibility of information by qualified third parties. The EPA uses various established Agency processes (e.g., the Quality System, peer review requirements and processes) to ensure the appropriate level of objectivity, utility, integrity, and transparency for its products is based on the intended use of the information and the resources available.

Objectivity focuses on whether the disseminated information is being presented in an accurate, clear, complete, and unbiased manner, and as a matter of substance, is accurate, reliable, and unbiased. The technical documentation meets the standard for objectivity, due to activities described in the following:

a) The information disseminated was determined to be complete, accurate, and reliable based on internal quality control measures adopted by the expert modeling teams. This included quality checks throughout the chain of analytic steps, including developing and processing climate projections, calibrating and validating the sectoral impact models, and checking data to ensure that no errors occurred in the process to compile and summarize results.

[1] EPA, 2002: Guidelines for ensuring and maximizing the quality, objectivity, utility, and integrity of information disseminated by the Environmental Protection Agency. United States Environmental Protection Agency, EPA/260R-02-008. Available online at http://www.epa.gov/quality/informationguidelines/documents/EPA_InfoQualityGuidelines.pdf

[2] OMB, 2002: Office of Management and Budget Information Quality Guidelines. Executive Office of the President, Office of Management and Budget. Available online at http://www.whitehouse.gov/sites/default/files/omb/inforeg/iqg_oct2002.pdf

[3] The IQA requires the Office of Management and Budget and federal agencies to issue guidelines that "ensur[e] and maximize[e] the quality, objectivity, utility, and integrity of information (including statistical information) disseminated by Federal agencies" (Public Law 106-554; 44 U.S.C. 3516, note). The IQA does not impose its own standard of "quality" on agency information; instead, it requires only that an agency "issue guidelines" ensuring data quality. Following guidelines issued by the Office of Management and Budget, EPA released its own guidelines to implement the IQA: "Guidelines for Ensuring and Maximizing the Quality, Objectivity, Utility, and Integrity of Information Disseminated by the Environmental Protection Agency."

b) The information disseminated was determined to be clear, complete, and unbiased based on multiple rounds of independent review. Consistent with guidelines described in EPA's Peer Review Handbook,[4] the underlying sectoral modeling methodologies were peer-reviewed through scientific journal publication processes. In addition, the Temperature Binning Framework was subject to an external journal publication process. Citations for these publications can be found throughout the main sector chapters of the technical documentation and its appendices.

   The technical documentation in full was subject to a public comment period to ensure that the information summarized by EPA was technically supported, competently performed, properly documented, consistent with established quality criteria, and communicated clearly. This public review period was also intended to provide feedback and comments on the utility of the Framework.

   The technical documentation in full was subject to an independent, external peer review to ensure that the information summarized by EPA was technically supported, competently performed, properly documented, consistent with established quality criteria, and communicated clearly.

Integrity refers to security of information, such as the protection of information from unauthorized access or revision, to ensure that the information is not compromised through corruption or falsification. The technical documentation, Framework, Tool, and underlying analyses meet the standard for integrity due to the strategic steps taken to ensure that the data and information remained secure. These steps included the use of password protected data storage repositories, password protected data transfer technology, and multiple layers of data validation checks to ensure that the integrity was not compromised.

Utility is the usefulness of the information to the intended users. The technical documentation, Framework, Tool, and underlying analyses meet the standard for utility because the information disseminated provides insights (technical methods for quantifying physical and economic impacts) regarding the potential magnitude of the impacts of climate change. Understanding the risks posed by climate change can inform broader assessment reports and policy decisions designed to address these risks.

Transparency ensures access to and description of (1) the source of the data, (2) the various assumptions employed, (3) the analytic methods applied, and (4) the statistical procedures used. The report and its underlying analyses meet the standard for transparency for the following reasons:

a) The underlying datasets, sectoral impact models, and the methods supporting the Temperature Binning Framework have been published with open access in the peer-reviewed scientific literature, and are cited throughout the report. These papers, along with their online supplementary materials, provide detailed information on the sources of data used, assumptions employed, the analytic and

[4] EPA, 2015: Peer Review Handbook, 4th Edition, 2015. United States Environmental Protection Agency, Programs of the Office of the Science Advisor.

statistical methods applied, and important limitations regarding the approaches and/or how the results should be interpreted.

b) Appendix A for this Technical Documentation provides details on how results and output from each sectoral impact model (or impacts study) are formatted and adapted for usage in the Framework and Tool. This Appendix contains descriptions of the methodologies used in estimating impacts, assumptions used, and citations to the underlying literature where the reader can go for more information.

c) The technical documentation in full was subject to a public comment period to ensure the interested stakeholders had an opportunity to review and provide input on the methods of the Framework and Tool.

d) All data output associated with the illustrative analyses of this Technical Documentation have been posted on the following website. See https://www.epa.gov/cira/FrEDI

e) The R package for FrEDI has been posted on the following website. See https://www.github.com/USEPA/FrEDI

f) Reponses to all comments received during the public comment period. See https://cfpub.epa.gov/si/. Search using the report title.

g) Responses to all comments received during independent, expert peer review have been posted on the report's website. See https://cfpub.epa.gov/si/. Search using the report title. During their review period, expert peer reviewers were provided a copy of all comments received from the public comment period.

A.2 Consideration of Assessment Factors

When evaluating the quality, objectivity, and relevance of scientific and technical information, the considerations that EPA takes into account can be characterized by five general assessment factors, as found in A Summary of General Assessment Factors for Evaluating the Quality of Scientific and Technical Information, and the Guidance for Evaluating and Documenting the Quality of Existing Scientific and Technical Information.[5] The following section lays out how the assessment factors are considered to determine whether models and data are acceptable for their intended use in the technical documentation, Framework, Tool, and underlying analyses.

[5] USEPA. 2003. A Summary of General Assessment Factors for Evaluating the Quality of Scientific and Technical Information, and the Guidance for Evaluating and Documenting the Quality of Existing Scientific and Technical Information. Science Policy Council U.S. Environmental Protection Agency Washington, DC. EPA 100/B-03/001

Factor		How the Factor was Considered
Soundness	The extent to which the scientific and technical procedures, measures, methods or models employed to generate the information are reasonable for, and consistent with, the intended application.	• Used publicly available (to the maximum extent practicable) data reviewed for quality and accuracy with complete metadata available. Used data included in peer-reviewed publications. Ensured evaluation of the scientific and technical procedures, measures, and methods employed to generate the estimates produced by the sectoral impact models. • Considered the capabilities of integrated assessment, simple climate model, and sectoral impacts models to examine the key analytical questions of this report (i.e., physical effects, economic damages, and changes in risk from climate change) in a manner consistent with sound scientific theory and accepted approaches. • Considered the extent to which the models had been previously applied in projects of similar scope as the Climate change Impacts and Risk Analysis (CIRA) project. For example, the BenMAP model has been used in similar climate and health impact analyses, and the labor analysis has been employed in other multi-sector modeling projects (e.g., Hsiang et al. 2017). • Considered whether the data and code is available, made available by EPA, or determined to not be feasible as it is claimed as proprietary by a non-federal business. • Ensured soundness by selecting sectoral impacts models with the following criteria: sufficient understanding of how climate change affects the sector; the existence of data to support the methodologies; availability of modeling applications that could be applied in the CIRA-FrEDI framework; based on peer reviewed literature and datasets; and the economic, iconic, or cultural significance of impacts and damages in the sector to the U.S.
Applicability and Utility	The extent to which the information is relevant for the Agency's intended use.	• Ensured that CIRA-FrEDI uses applicable and relevant inputs and considers the capabilities of the integrated assessment, simple climate model, and sectoral impacts models to examine the key analytical questions of CIRA (i.e., changes in physical effects, economic damages, and risk associated with climate change). • Ensured that CIRA-FrEDI and its underlying analyses are relevant to their intended use so that the information disseminated provides insights and methods for quantifying the physical and economic impacts of climate change at national and regional levels. • Ensured sectoral impacts models are reasonable for, and consistent with, the intended application by being

Factor		How the Factor was Considered
		sufficiently flexible to ensure consistency in inputs and monetizing physical impacts. • Ensured that models have been applied in peer-reviewed, published studies of similar scope and rigor as CIRA, including those described in the Fourth National Climate Assessment.
Clarity and Completeness	The degree of clarity and completeness with which the data, assumptions, methods, quality assurance, sponsoring organizations and analyses employed to generate the information are documented.	• Ensured use of clear and complete inputs by considering the extent to which sectoral impacts models documented their key methods, assumptions, parameter values, limitations, sponsoring organizations/author affiliations, and funding information. • Ensured publications clearly and comprehensively describe analytic methods used and how they apply and build off existing bodies of research and underlying scientific and/or economic theories.
Uncertainty and Variability	The extent to which the variability and uncertainty (quantitative and qualitative) in the information or in the procedures, measures, methods or models are evaluated and characterized.	• Ensured inputs that appropriately characterize uncertainty and variability by considering the capabilities of sectoral impacts models to evaluate and characterize key sources of variability and uncertainty. Results of these analyses are described in the underlying journal articles, and also demonstrated in this report. • Reviewed the model documentation and peer-reviewed publications and determine if a model is sufficiently flexible and capable of evaluating important sources of uncertainty for climate change impacts analysis. • Addressed key sources of uncertainty such as projected emissions (high versus low); regional climate variability (uncertainty across general circulation models); climate sensitivity (different values for equilibrium climate sensitivity); structural uncertainty (multiple methods used to project climate, and models to estimate sectoral impacts); ability to capture variability in temperature and precipitation outcomes; and effects that increasing population and income can have on impact estimates. • Documented outcomes of sensitivity and uncertainty analyses, where applicable, in the presentation of results using ranges and confidence intervals.
Evaluation and Review	The extent of independent verification, validation and peer review of the information or of the	• Ensured use of independently verified and validated inputs by considering the extent to which models have been independently peer reviewed. • Reviewed the documentation associated with each model and determined if they have been independently peer

Factor		How the Factor was Considered
	procedures, measures, methods or models.	reviewed and published in scientific journals with procedures to ensure that the methods are technically supportable, properly documented, and consistent with established quality criteria. • Used scenarios and projections that have been independently verified and validated (e.g. scenarios and projections developed for the IPCC and its assessments, and then downscaled for the U.S. for used in the Fourth National Climate Assessment by the USGCRP Scenarios Working Group).

A.3 Peer Review of the Technical Documentation

Consistent with guidelines described in EPA's Peer Review Handbook,[6,7] this Technical Documentation was subject to a public review comment period, and an independent, external expert peer review. The Technical Documentation was subject to a public comment period to ensure that the information summarized by EPA was technically supported, competently performed, properly documented, consistent with established quality criteria, and communicated clearly. This public review period was also intended to provide feedback and comments on the utility of the Framework.

Similarly, the purpose of the expert peer review by independent, qualified, and objective experts was to ensure that the information summarized by EPA was technically supported, competently performed, properly documented, consistent with established quality criteria, and communicated clearly. The sectoral impact models and underlying the Technical Documentation, as well as the Temperature Binning Framework were previously peer reviewed and published in the research literature. However, the Technical Documentation provides comprehensive detail of the design, structure, and potential application of the Framework, and is therefore the focus of the public and expert review processes.

Public Review Period

A 30-day public comment period was held from April 15th through May 17th, 2021. All comments received were carefully reviewed, considered, and responded to.

Expert Peer Review

The expert review was managed by a contractor (ICF International) under the direction of a designated EPA peer review leader, who prepared a peer review plan, the scope of work for the review contract, and the charge for

[6] EPA, 2015: Peer Review Handbook, 4th Edition, 2015. United States Environmental Protection Agency, Programs of the Office of the Science Advisor. Available online at https://www.epa.gov/osa/peer-review-handbook-4th-edition-2015

[7] EPA has determined that this report falls under the classification of "influential scientific information," as defined by OMB and further described in the EPA Peer Review Handbook. This product is for science dissemination and communication purposes only and does not reflect analysis of nor recommendations regarding any particular policy.

the reviewers. Importantly, the EPA peer review leader played no role in producing any portion of the report. Reviewers worked individually (i.e., without contact with other reviewers, colleagues, or EPA) to prepare written comments in response to the charge questions. The reviewers were also provided with the public review comments for informational purposes.

The contractor identified, screened, and selected five reviewers who had no conflict of interest in performing the review, and who collectively met the technical selection criteria provided by EPA.

The peer review charge directed reviewers to provide responses to the following questions during the main review:

1. Does the introductory chapter clearly explain the purpose of the report and provide appropriate context for the rest of the documentation? If not, please provide recommendations for improvement.
2. The report has been written for an educated and semi-technical audience. Are the writing level and graphics appropriate for these audiences?
3. Does the report adequately explain the overall analytic framework of the temperature binning approach?
4. Do the text, figures, and tables clearly communicate the framework's structure and design? Are the requirements for input data, and the options for output/results summaries, clearly stated?
5. Does the report clearly convey both the conceptual basis for temperature binning and the specific data processing and analytic steps taken to execute the concept? Is it clear how both the EPA-sponsored CIRA sector studies, and other non-CIRA studies, can be incorporated in the framework?
6. Is the sector-specific approach to account for the role of socioeconomic driver data clear? Is it reasonable and well-supported?
7. Is the approach to estimating sector-specific and aggregate economic impact (damages) of specified temperature trajectories reasonable and suitable for the stated purposes?
8. Does the report adequately inform the reader about how uncertainty is addressed in the framework, including how results should be interpreted and used given the limitations?
9. Has EPA objectively used, applied, and documented the underlying data of the temperature binning framework? Has the Agency appropriately described the sensitivity of the findings to analytic assumptions?
10. Is the draft technical documentation report missing important information based on your review of the report?
11. Report Format: Please comment on whether any aspects of the layout help or hinder the reader to understand the content and key messages of the report.

APPENDIX B | DETAILS OF SECTORAL IMPACT STUDIES

B.1 Sector Data Overview

This appendix provides additional detail on the sectoral studies currently processed for the Framework and outlines the processing required to prepare the sectoral study results for inclusion in the Tool. This appendix will be updated over time as additional sectoral studies and their functions are incorporated into the Temperature Binning Framework. The sectors are presented in four groups: Health Sectors, Infrastructure Sectors, Water Resources Sectors, and Electricity Sectors. Sectors within each group often share data processing methods. **Table B-1** lists the 16 sectors by the four groups and summarizes the regional coverage of the sectoral impacts as well as identifies the GCMs used in the sectoral impact models. **Table 2** (impact types, socioeconomic drivers, adaptation scenarios), **Table 4** (links to population and GDP inputs), **Table 5** (time dependent scalars), and **Table 6** (valuation measures) in the main text also provide summarized information about the 16 sectors.

Application of the Framework is not limited to the sectors currently processed for the Tool. New sectors that meet the requirements outlined in Section 2 can be added to the tool following the process documented in this report. EPA is currently working with study authors to add three additional research studies to the sectoral scope of the Tool: 1) Two new sectors (violent and property crime; agriculture) and three sectors that overlap with estimates already in the Tool (labor, extreme temperature mortality, and coastal property) from Hsiang et al. (2017); 2) Coastal wind damage from changes in tropical storm activity, derived from Dinan (2017); and 3) Inland riverine flooding from an in-process update to Wobus et al. (2019). This expansion in sectoral scope remains a high priority option for inclusion in a future revision to the Tool.

TABLE B-1. REGIONAL COVERAGE AND GCMS USED BY SECTOR

		Regional Coverage							**GCMs Used**						
		Midwest	Northeast	Northern Plains	Northwest	Southeast	Southern Plains	Southwest	CanESM2	CCSM4	GFDL-CM3	GISS-E2-R	HadGEM2-ES	MIROC5	*SLR Scenarios*
Health	Air Quality	■	■	■	■	■	■	■		■	■				
	Extreme Temperature	■	■		■	■	■	■	■	■	■	■	■	■	
	Labor	■	■	■	■	■	■	■	■	■	■	■	■	■	
	Southwest Dust							■	■	■	■	■	■	■	
	Valley Fever		■	■	■	■	■	■	■	■	■	■	■	■	
	Wildfire	■	■	■	■	■	■	■	■	■		■	■	■	
Infrastructure	Asphalt Roads	■	■	■	■	■	■	■	*	*				*	
	Coastal Properties		■		■	■	■	■							■
	High Tide Flooding and Traffic		■		■	■	■	■							■
	Rail	■	■	■	■	■	■	■	■	■	■	■	■	■	
	Roads	■	■	■	■	■	■	■	■	■	■	■	■	■	
	Urban Drainage	■	■	■	■	■	■	■	■	■		■	■	■	
	Inland Flooding *	■	■	■	■	■	■	■	■		■		■	■	
	Hurricane Wind Damage		■			■	■			■	■		■	■	
Water Resources	Water Quality	■	■	■	■	■	■	■	■	■		■	■	■	
	Winter Recreation	■	■	■	■	■		■	■	■	■	■	■	■	
Electricity	Electricity Demand and Supply	■	■	■	■	■	■	■	■	■	■	■	■	■	
	Electricity Transmission and Distribution	■	■	■	■	■	■	■	■	■	■	■	■	■	

*The Asphalt Roads sector was not a part of the CIRA project but utilized three GCMs in common with the CIRA2.0 set of scenarios. The climate data for Asphalt Roads was bias corrected and downscaled using a different process than the method used in CIRA, therefore although the GCMs are the same, the integer degree arrival times differ slightly for this sector. The Inland Flooding sector used an ensemble of 14 GCMs (list provided in detailed write-up below), which includes four of the six GCMs listed in the table. The authors estimated arrival times and provided estimates of impacts by degree of warming for the mean of 14 GCM results for use in this work..

For each sector, the sections that follow provide a summary of the impact model as well as a citation to the underlying study, which can be referred to for more information. Next, the sub-impacts are presented for two socioeconomic scenarios (2010 and 2090, for sectors with differentiated impacts over time; see Sections 2.3 and 2.4 of the Technical Documentation for a description of the socioeconomic scenarios used in the underlying sectoral impacts modeling.). A flow diagram outlines the results processing steps. Finally, limitations introduced by the data processing steps are listed for each sector.

B.2 Health Sectors Data Processing

Air Quality

This sectoral study estimates mortality risk associated with changing air quality; specifically, ozone and fine particulate matter ($PM_{2.5}$) concentrations.

UNDERLYING DATA SOURCES AND LITERATURE

Fann, N. L., Nolte, C. G., Sarofim, M. C., Martinich, J., & Nassikas, N.J. (2021). Associations between simulated future changes in climate, air quality, and human health. JAMA Network Open, 4(1).

This analysis uses air quality surfaces (i.e., concentrations in response to changes in meteorology and emissions) and concentration-response functions employed by Fann et al. (2021) to quantify $PM_{2.5}$- and ozone-attributable premature mortality. Mortality is monetized using the value of statistical life (VSL). Two simulated air pollutant emissions inventories are considered as adaptation scenarios: a 2011 dataset that estimates unrestricted pollution burden from all sources as of that year, and a 2040 dataset that accounts for the implementation of a suite of regulatory policies on stationary and mobile emissions sources. Summaries of impacts by temperature bin degree in 2010 and 2090, the endpoints of socioeconomic modeling, and emissions inventory are included in **Figure B-1** below.

FIGURE B-1. AIR QUALITY IMPACTS BY TEMPERATURE BIN DEGREE

A. 2010 SOCIOECONOMICS

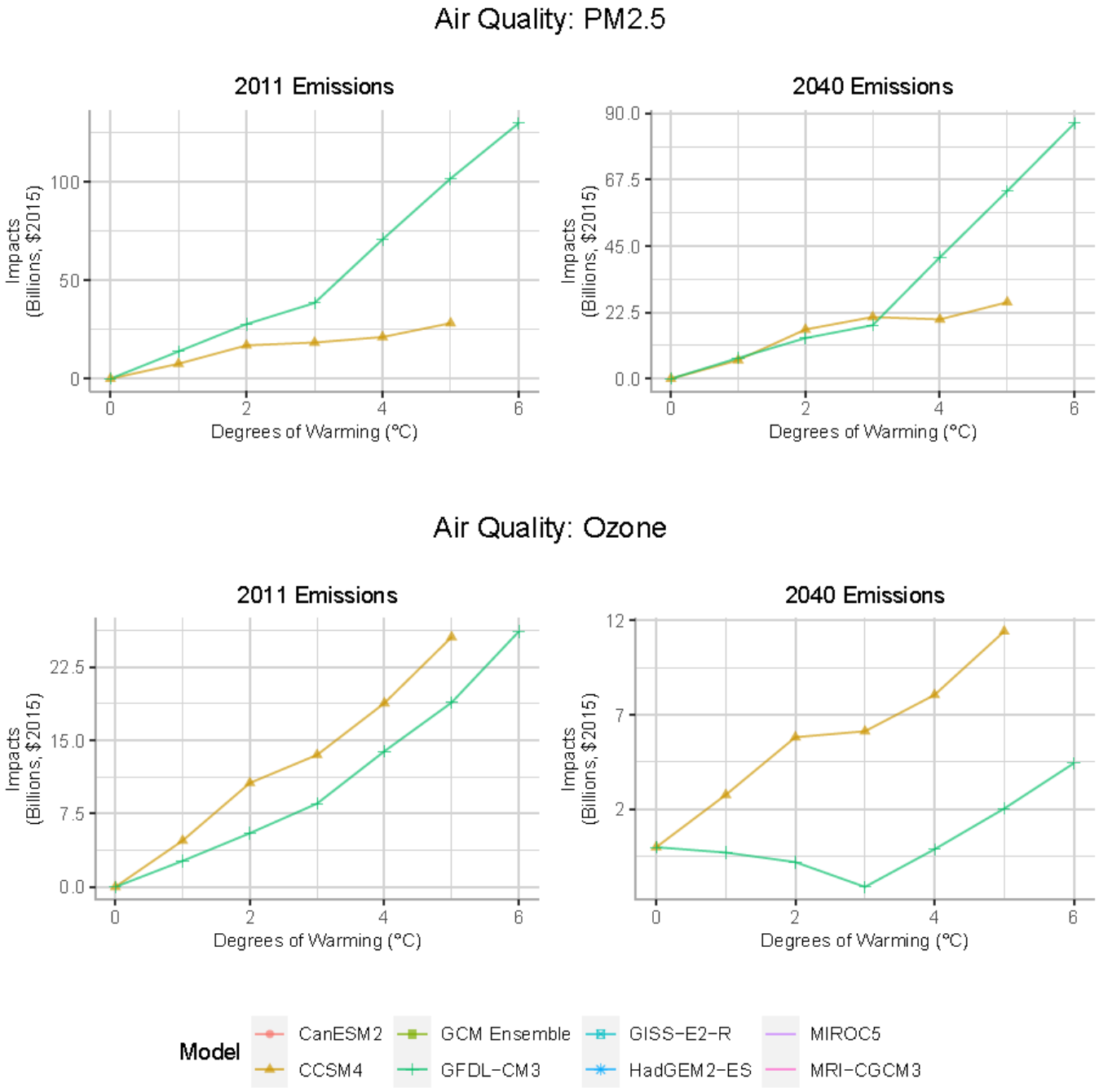

B. 2090 SOCIOECONOMICS

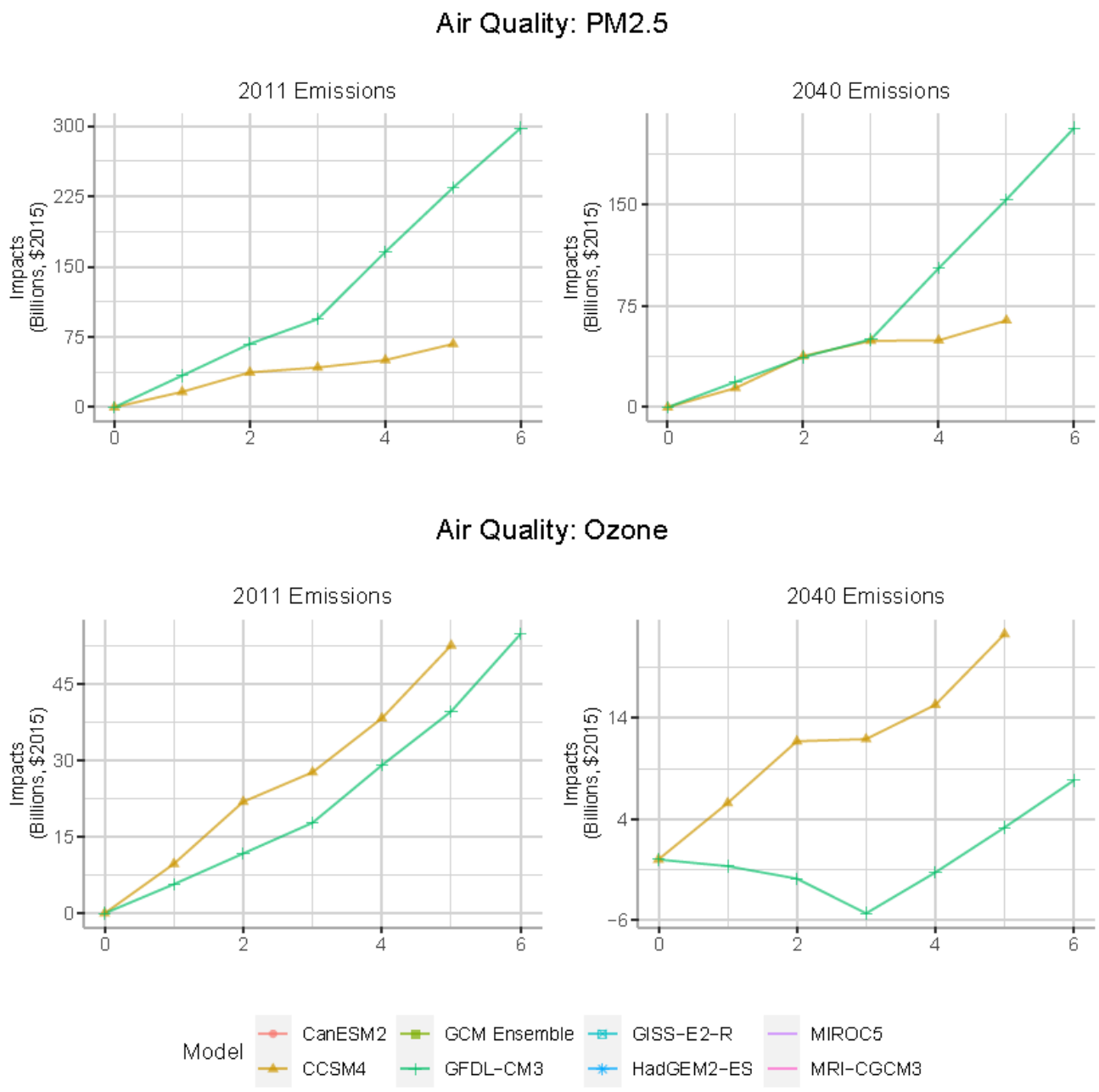

Processing steps

Processing steps are illustrated in **Figure B-2**. Data inputs from Fann et al. (2021) are compiled using U.S. EPA's Benefits Mapping and Analysis Program – Community Edition (BenMAP-CE) to generate results at the regional level. The original air quality data was provided by study authors with the dimension *era—GCM—36-km grid cell—pollutant (ozone/$PM_{2.5}$)—emissions inventory (2011/2040).* Data is available for four eras

(2030, 2050, 2075, 2095) and two climate models (CCSM4 and GFDL-CM3). Concentration-response functions employed by Fann et al. (2021) are based on risk model information for those age 30-99 for $PM_{2.5}$ and those age 0-99 for ozone. Within BenMAP-CE, impacts are aggregated to the regional level for each era, GCM, pollutant, and emissions inventory scenario. The original results provided already account for baseline incidence; therefore, no additional processing is needed to isolate climate impacts.

The third step divides total regional impacts by dynamic Integrated Climate and Land Use Scenarios, v2 (ICLUSv2) regional population to acquire per capita mortality estimates for each era. The calculations utilize total regional population anticipating alternative population inputs would be unlikely to contain age-stratified population projections. Next, era costs are assigned to the central year of the era (i.e., 2030, 2050, 2075, and 2095), and costs per era are transformed to annual costs by interpolating linearly between era impacts. Finally, yearly impacts for each pollutant impact type (ozone/$PM_{2.5}$) are averaged across the GCM-specific eleven-year windows around the first arrival times of integer degrees of warming relative to the baseline.

FIGURE B-2. AIR QUALITY PROCESSING FRAMEWORK

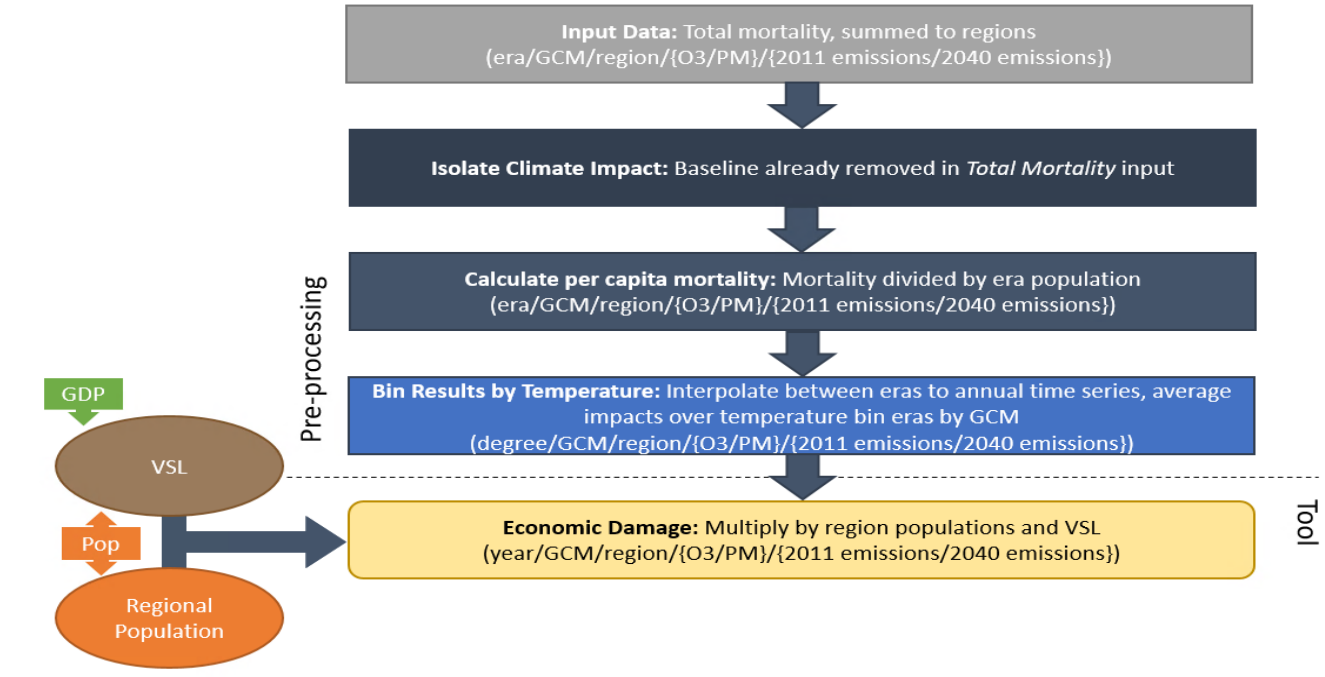

Final mortality estimates are produced by applying the per capita mortality rates to the input population scenario and GDP input-adjusted VSLs. VSL is adjusted for changes in GDP per capita using an income elasticity function[8]:

[8] This is a generic elasticity function that can be used in a time-series fashion, as used here, or for cross-sectional benefits transfers, as in the example in Masterman and Viscusi (2018), "The Income Elasticity of Global Values of a Statistical Life: Stated Preference Evidence", Journal of Benefit-Cost Analysis, 9(3):407-434. Note that the default elasticity used here is 0.4, consistent with current EPA policy but substantially lower than estimates provided in Masterman and Viscusi (2018).

$$VSL_t = VSL_{2010} \times \left(\frac{GDPcap_t}{GDPcap_{2010}}\right)^{0.4}$$

Limitations and Assumptions

- $PM_{2.5}$-attributable premature mortality is quantified for those age 30 and older, and this analysis assumes the impacts for those under 30 to be zero. Doing so underestimates the risk of premature mortality experienced by those under 30. Additionally, doing so assumes that age demographics remain proportional over the century.
- This analysis does not quantify morbidity effects associated with changes in $PM_{2.5}$ and ozone, which are likely to increase as temperature increases. Changes in air quality can provoke hospital admissions for respiratory diseases and worsen other conditions.
- For further discussion of the limitations and assumptions in the underlying sectoral modeling approach, see Fann et al. (2021).

Extreme Temperature

This sector addresses the impact of extreme temperature on premature mortality in 49 major U.S. cities. In the 2010 Census, the 49 cities accounted for 91.3 million of the total US population of 309.3 million, or nearly 30 percent.

UNDERLYING DATA SOURCES AND LITERATURE

Mills, D., Schwartz, J., Lee, M., Sarofim, M., Jones, R., Lawson, M., Duckworth, M., & Deck, L. (2014). Climate Change Impacts on Extreme Temperature Mortality in Select Metropolitan Areas in the United States. Climatic Change, 131, 83-95. Doi:10.1007/s10584-014-1154-8

Economic damages are based on extreme heat and cold mortality rates, monetized by applying the VSL. The VSL trajectory through the simulation period changes as a function of per capita income.

The underlying epidemiologic model includes runs with and without adaptation scenarios. The adaptation scenario does not reflect a benefit-cost calculation but an assumption that U.S. cities will gradually adapt to a hotter environment through physical acclimatization of their residents, infrastructure replacement with more heat suitable shading and air conditioning, and behavioral changes, so that the stressor-response will look like that of the current Dallas context.[9] The original estimates are provided for 49 cities. **Figure B-3** provides a summary of the results for heat and cold related mortality, for both adaptation scenarios and six GCMs at the endpoints of the socioeconomic scenarios; 2010 and 2090.

[9] The adaptation scenario was considered in Mills et al. (2015) and U.S. EPA (2017). More refined adaptation scenarios for this sector, including the costs and efficacy of increased air conditioning market penetration, are the subject of active and ongoing research. Some research has found the efficacy of cooling centers can be high in preventing extreme heat mortality, but surveys and current experience suggest that many residents are unwilling to use formal cooling centers. For at least some of the cities evaluated in Mills et al. (2015), the empirical data reflects the availability, if not the widespread use, of cooling centers to residents.

FIGURE B-3. EXTREME TEMPERATURE IMPACTS BY TEMPERATURE BIN DEGREE

A. 2010 SOCIOECONOMICS

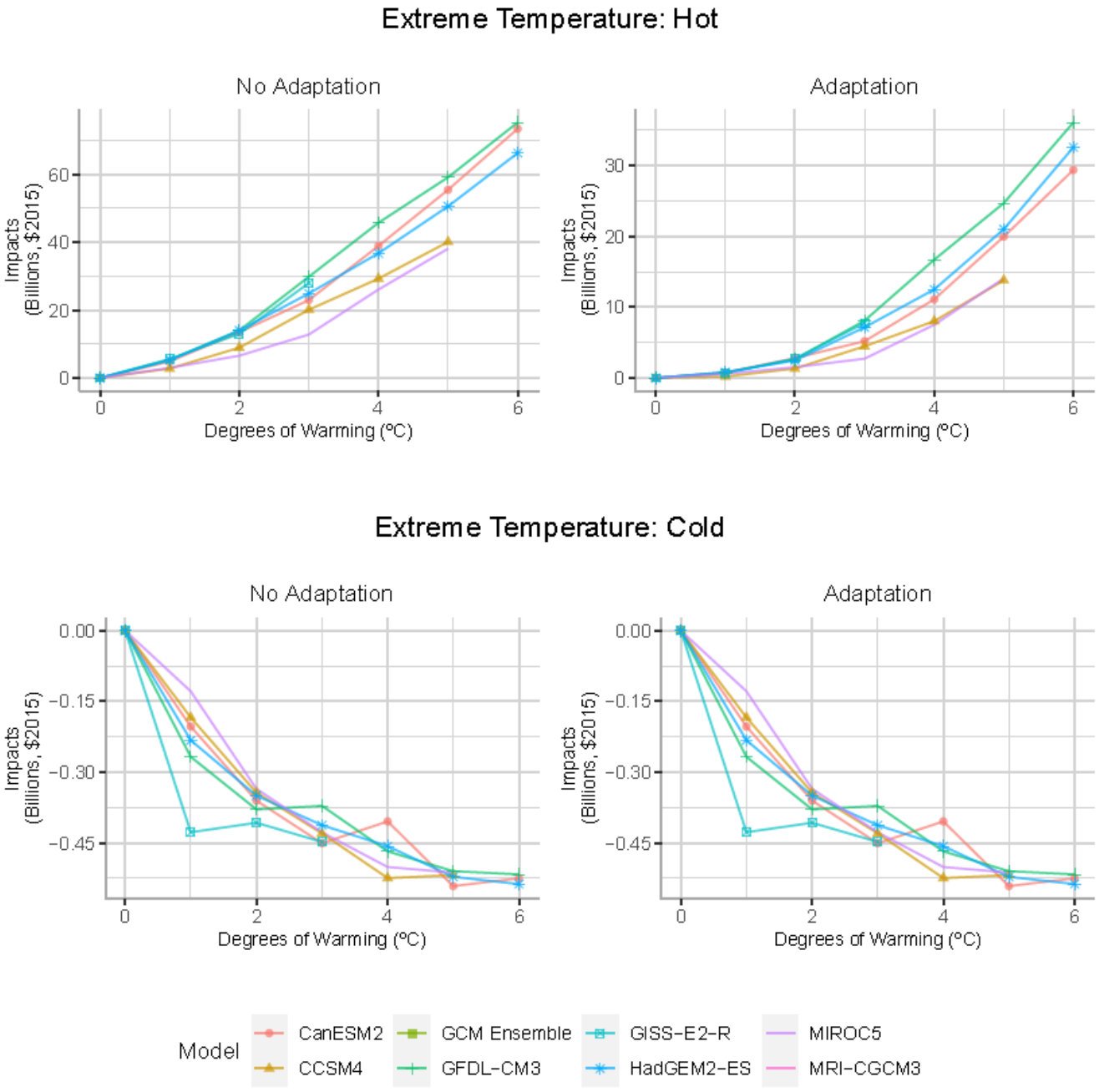

B. 2090 SOCIOECONOMICS

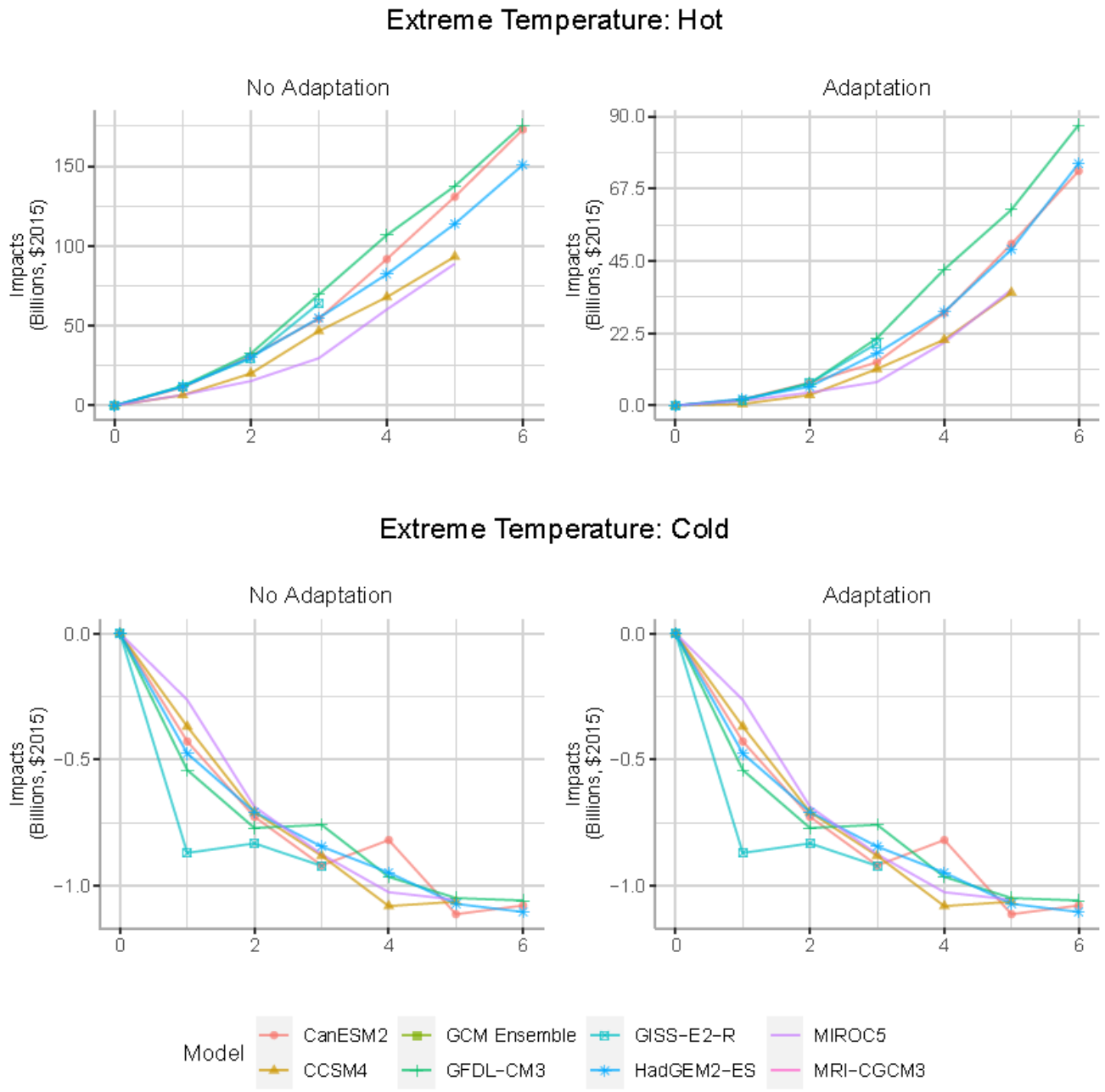

Processing steps

Processing steps are shown in **Figure B-4**. The original data was provided by the study authors with the dimension *degree – GCM – city – damage type (heat/cold mortality) – base population (2010/2090)*. The first processing step was to sum the city damages to regional damages. Next, the incremental impacts of climate change are isolated by subtracting the 0-degree bin mortality results from each warming bin.

The model was run under two constant population assumptions: 2010 and 2090 estimates from ICLUSv2 (EPA 2017; Bierwagen et al., 2010). In addition to having different total populations, these two scenarios vary in the distribution of population across modeled cities. In the third processing step, regional mortality in each scenario is divided by total population in each scenario to obtain a mortality per capita estimate for each population base. Both estimates, as well as an interpolation between the two, are available for impact estimations.

FIGURE B-4. EXTREME TEMPERATURE DATA PROCESSING FRAMEWORK

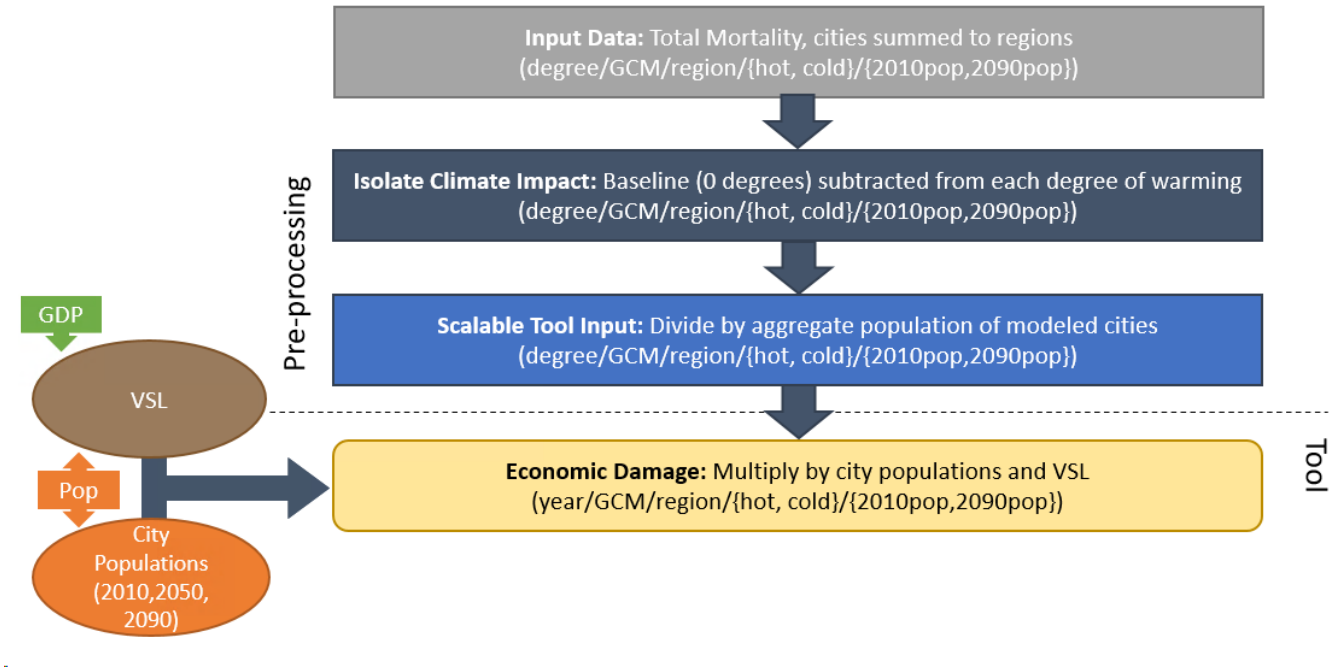

Final economic damage estimates are produced by applying the per capita mortality rates to the input population scenario and GDP input-adjusted VSLs. Regional population inputs are translated to city populations using factors derived from the ICLUSv2 population scenarios in 2010, 2050, and 2090, and interpolated for years in between. VSL scales relative to changes in GDP per capita to general impact estimates.

Limitations and Assumptions

- National per capita averages are based on the total population of modeled cities with heat and cold impacts. There are certain cities in the Southeast (Atlanta, Broward-Ft. Lauderdale, Miami, Orlando), Southern Plains (Austin, Dallas), and Southwest (Albuquerque, Los Angeles, Phoenix, San Diego) regions that are modeled for adaptation to heat but are not modeled for adaptation to extreme cold. It is assumed that these cities have minimal extreme cold damages, and therefore their populations are included in the denominator as part of the total population over which cold damages are averaged.

- This analysis only covers considers health impacts to individuals living in 49 cities within the contiguous U.S., and therefore omits a large majority of the population vulnerable to extreme temperatures.
- Cities that only experienced extreme cold in the historic period, notably those in the Northwest region, do not show an increase in extreme-temperature related mortality in this analysis. This result is an artifact of the methodology, which relies on observed temperature thresholds based on a historic period. With increased temperatures, it is likely that many of these Northwestern cities could experience heat-related mortality as well, which might be reflected if a different impact estimation methodology had been applied.
- For further discussion of the limitations and assumptions in the underlying sectoral model, please see Mills et al. (2014) and EPA (2017).

Labor

UNDERLYING DATA SOURCES AND LITERATURE

Neidell, M., Graff-Zivin, J., Sheahan, M., Willwerth, J., Fant, C., Sarofim, M., & Martinich, J. (2021). Temperature and work: Time allocated to work under varying climate and labor market conditions. PLoS ONE 16(8): e0254224. https://doi.org/10.1371/journal.pone.0254224

The labor sector addresses economic damages of changes in labor hours as a result of climate change. The analysis estimates changes in labor allocation, with both positive and negative responses of changes in hours worked in weather-exposed industries (e.g., agriculture, construction, manufacturing). The study finds the relationship between temperature and hours worked is not significant during recession periods, and therefore projected losses are adjusted to account for the probability of recession. Damages are based on a physical measure of average hours worked by workers in high risk industries, which is monetized in Neidell et al. (2021) by average wages across at-risk industries[10]. A summary of impacts by temperature bin degree at 2010 and 2090, the endpoints of socioeconomic modeling, is included in **Figure B-5**.

[10] Hourly wages are based on average wages across at-risk industries: agriculture, forestry, fishing, hunting, mining, construction, and manufacturing.

FIGURE B-5. LABOR IMPACTS BY TEMPERATURE BIN DEGREE

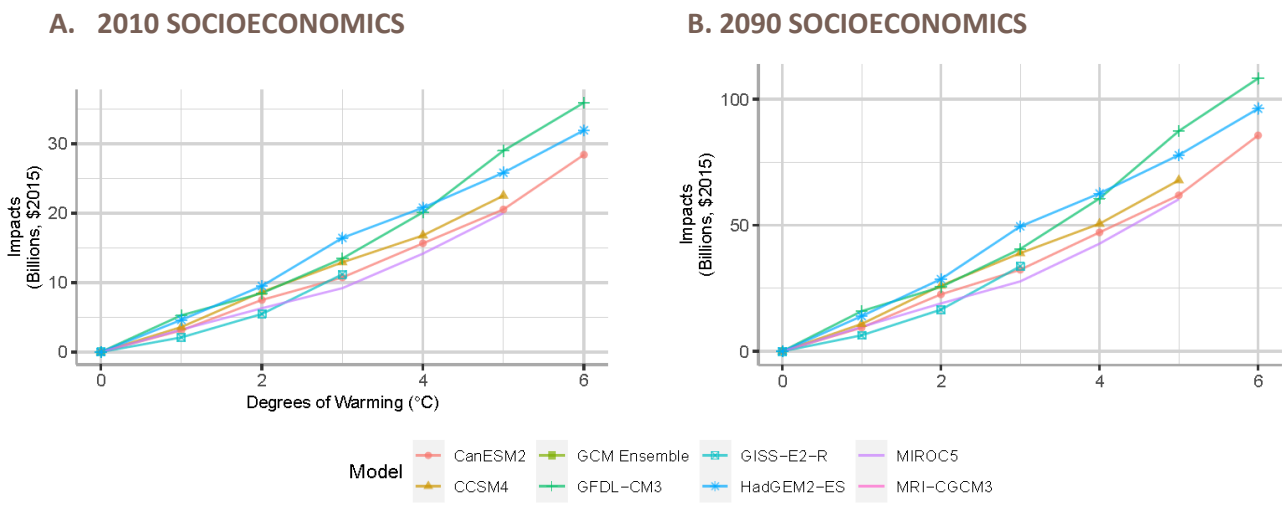

Processing steps

Processing steps are shown in **Figure B-6**. Forgone wages due to climate-induced temperature increase are calculated by combining an average hourly wage rate, high-risk worker population, and per high-risk worker hours lost. The original data includes forgone hours for each year, GCM, and region combination. In the first step, state-level data is summed to the NCA region level. The second step is bypassed; these results already account for baseline hours lost, so no additional processing is needed to isolate climate impacts. The third step divides these estimates by high-risk worker population to acquire per high-risk worker estimates. The population of high-risk workers varies by region but is assumed to remain constant over the course of the century. Per high-risk worker hours lost are stored as the underlying impact, and final economic damage estimates are produced by multiplying these rates by a regional population and an average wage.

FIGURE B-6. LABOR DATA PROCESSING FRAMEWORK

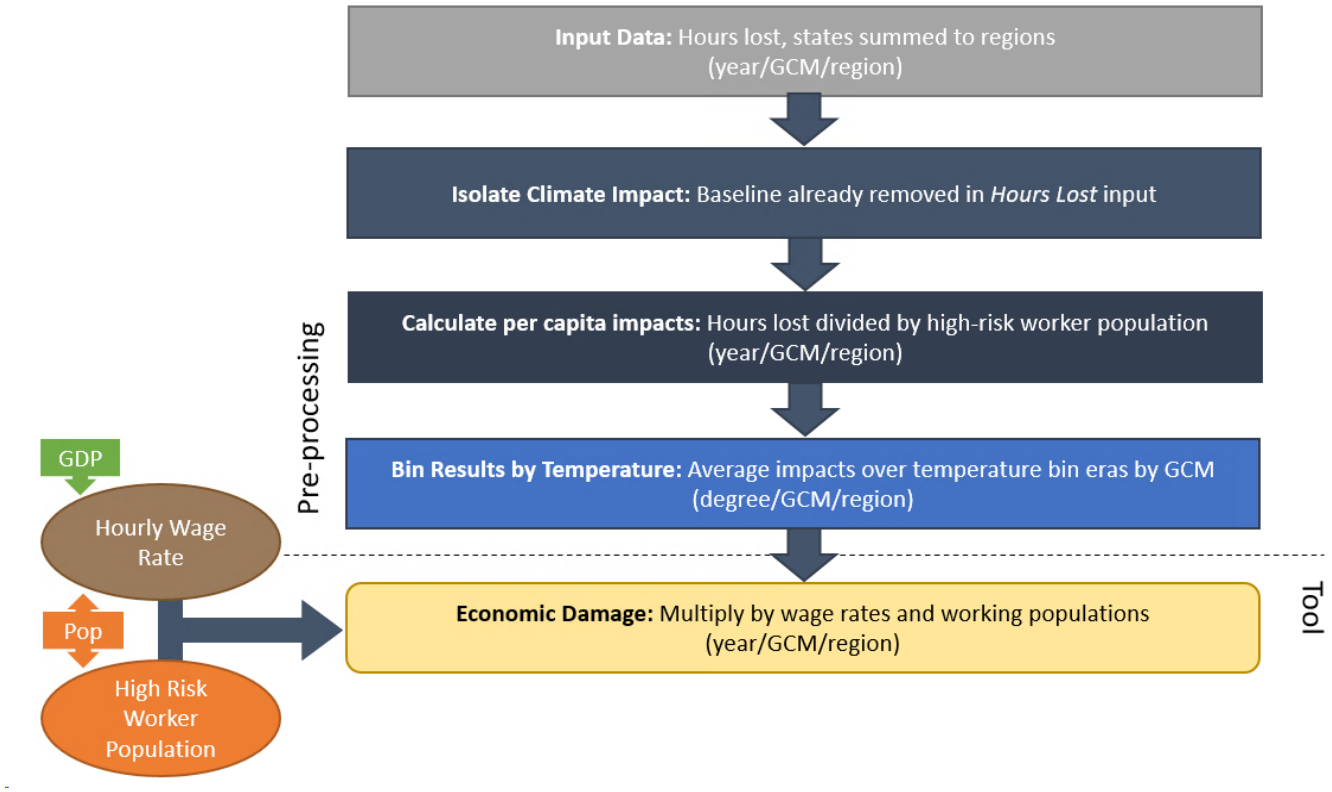

Limitations and Assumptions

- High risk worker population is assumed to remain constant over the course of the century.
- This analysis does not evaluate the potential for new adaptations (behavioral or technological) by workers or employers to mitigate the effects of extreme temperatures on labor allocation. Adaptations present in the baseline period upon which the econometric analysis is based are assumed to be part of the modeled response to future temperature changes, however, new adaptation behaviors or technology are not evaluated.
- For further discussion of the limitations and assumptions in the underlying sectoral model see Neidell et al. (2021).

Southwest Dust

This sectoral study estimates health burden and the economic value of that burden resulting from changes in fine and coarse airborne dust exposure due to climate change in the Southwest.

UNDERLYING DATA SOURCES AND LITERATURE

Achakulwisut, P., Anenberg, S. C., Neumann, J. E., Penn, S. L., Weiss, N., Crimmins, A., Fann, N., Martinich, J., Roman, H. A., & Mickley, L. J. (2019). Effects of increasing aridity on ambient dust and public health in the U.S. southwest under climate change. GeoHealth, 3(5), 127-144. Doi:10.1029/2019GH000187

Damages are based on the change in incidence of a range of morbidity and mortality outcomes, which are monetized using direct hospitalization costs, indirect loss of income from hospitalization, costs of emergency department visits, and (for premature mortality) the VSL.

Estimates of health costs are available by impact type: Emergency Department visits due to Asthma, Cardiovascular, Respiratory, Mortality, and Acute Myocardial Infarction. A summary of impacts by temperature bin degree in 2010 and 2090, the endpoints of socioeconomic modeling, is included in **Figure B-7**.

FIGURE B-7. SOUTHWEST DUST IMPACTS BY TEMPERATURE BIN DEGREE

A. 2010 SOCIOECONOMICS

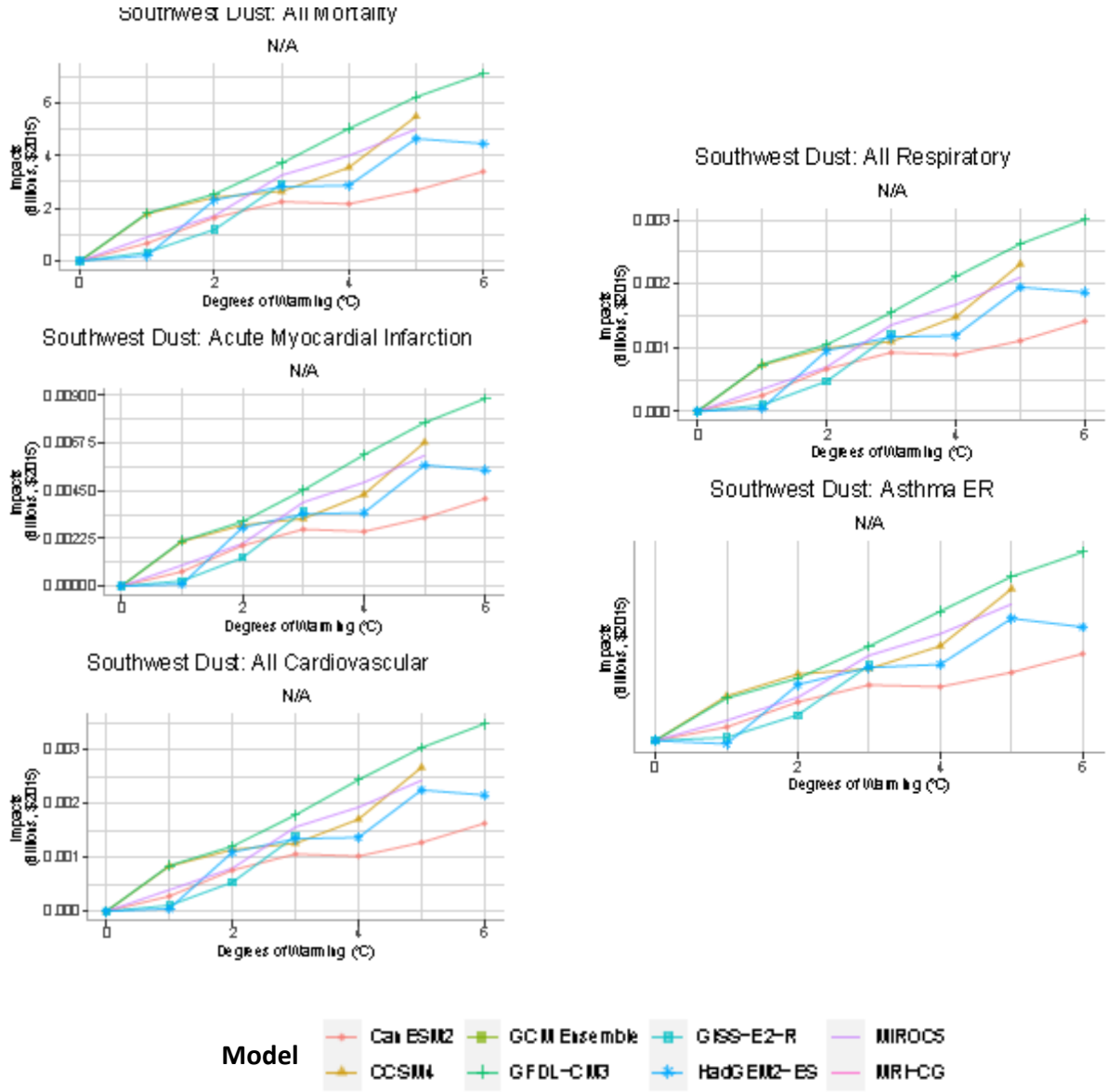

B. 2090 SOCIOECONOMICS

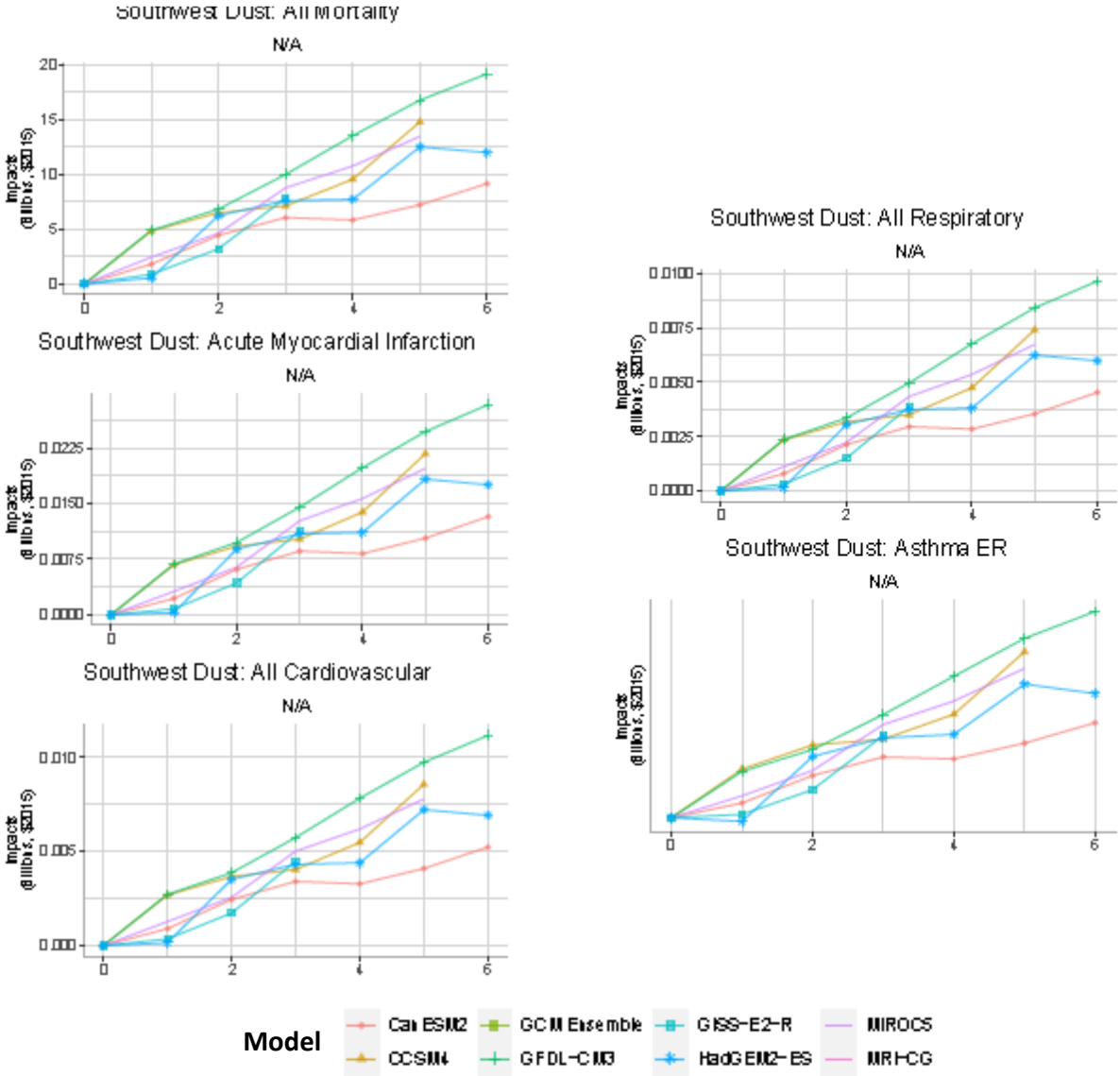

Processing steps

Processing steps are illustrated in **Figure B-8**. The health burden and costs incurred as a result of increased dust exposure due to climate change are calculated by combining average cost-of-illness and mortality costs, population, and average number of cases.

The original results already account for baseline incidence; therefore no additional processing is needed to isolate climate impacts. Original results are presented as increases in health impacts from baseline levels for affected populations — for example, cardiovascular disease impacts are considered only for people over 65. To calculate costs across all considered impacts, damages per capita are calculated for the total population by impact type; implicitly, damages for age groups not modeled are assumed to be zero. Per

capita estimates are calculated using total regional populations in 2010 and 2090. These damages are produced across integer degree, health impact, and GCM.

Both estimates (2010/2090), as well as an interpolation between the two, are available for impact estimation. Per capita estimates of health impacts are multiplied by regional population and average medical cost. Medical costs are variable across health impacts. For all mortality, the VSL is utilized, which scales relative to changes in GDP per capita. Final damages are calculated based off the temperature trajectory assigned in the tool.

FIGURE B-8. SOUTHWEST DATA PROCESSING FRAMEWORK

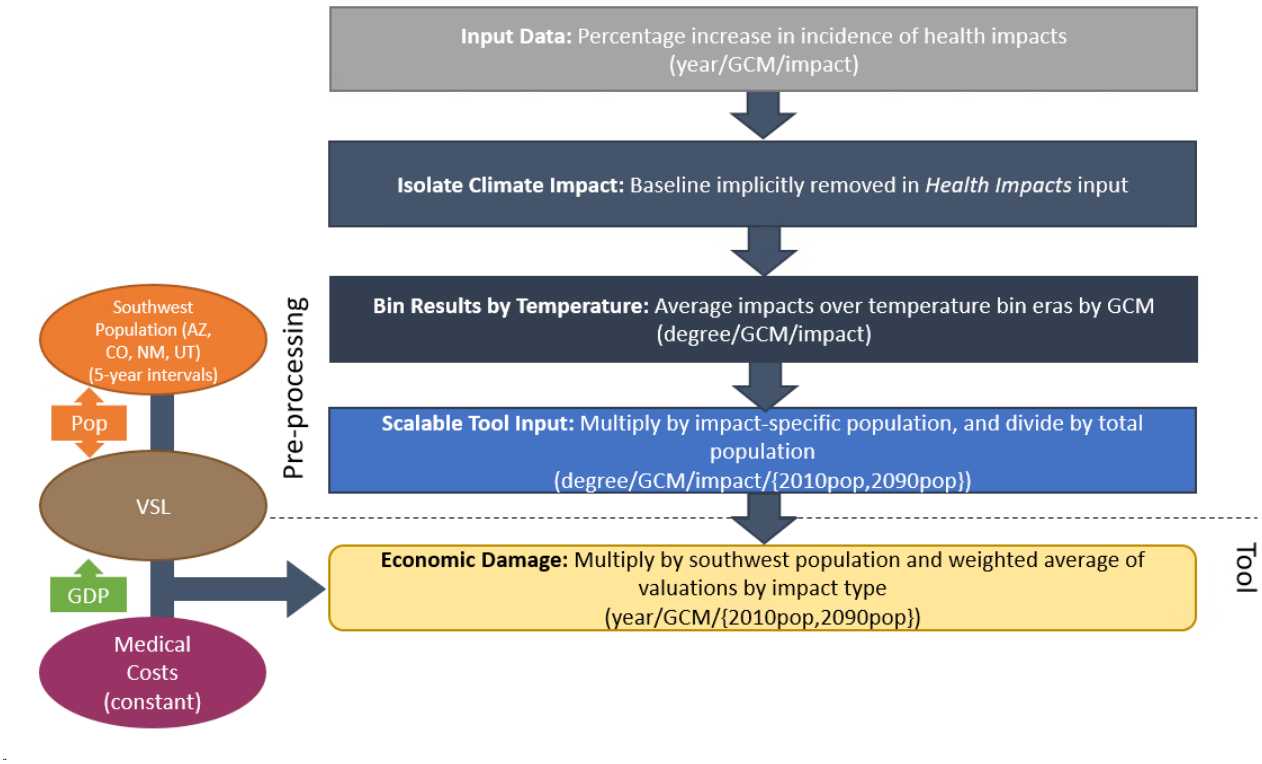

Limitations and Assumptions

- While dust exposures are known to be large in the southwestern U.S., this analysis does not consider health effects from coarse and fine dust in other regions of the U.S.
- This sector relies on population for a section of the Southwest region (Arizona, Colorado, New Mexico, Utah) to calculate damages across impact types. The scaling of damages by this population allows for custom inputs of socio-economic estimates but may introduce error if the age demographics of the population are not roughly constant over the simulation period.
- For further discussion of the limitations and assumptions in the underlying sectoral model, see Achakulwiset et al. (2019).

Valley Fever

This sectoral study estimates the health burden and economic value associated with climate change-related Valley fever incidence. Valley fever is a prevalent disease in the hot and dry Southwest region of the U.S. but is expected to expand in geographic scope with warming. Therefore, this analysis quantifies Valley fever impacts across the contiguous U.S., with most of the burden focused in the Southwest.

UNDERLYING DATA SOURCES AND LITERATURE

Gorris, M. E., Neumann, J. E., Kinney, P. L., Sheahan, M., & Sarofim, M. C. (2020). Economic Valuation of Coccidioidomycosis (Valley Fever) Projections in the United States in Response to Climate Change. Weather, Climate, and Society, 13(1), 107-123. Doi:10.1175/WCAS-D-20-0036.1

Impacts are based on the change in number of Valley fever cases and the probability of a range of morbidity outcomes, which are monetized using direct hospitalization costs, costs of emergency department visits, costs of physician visits, and indirect cost of lost productivity from hospitalization. Mortality is valued using the VSL. Summary of impacts by temperature bin degree in 2010 and 2090, the endpoints of socioeconomic modeling, are included in **Figure B-9**.

FIGURE B-9. VALLEY FEVER IMPACTS BY TEMPERATURE BIN DEGREE

A. 2010 SOCIOECONOMICS

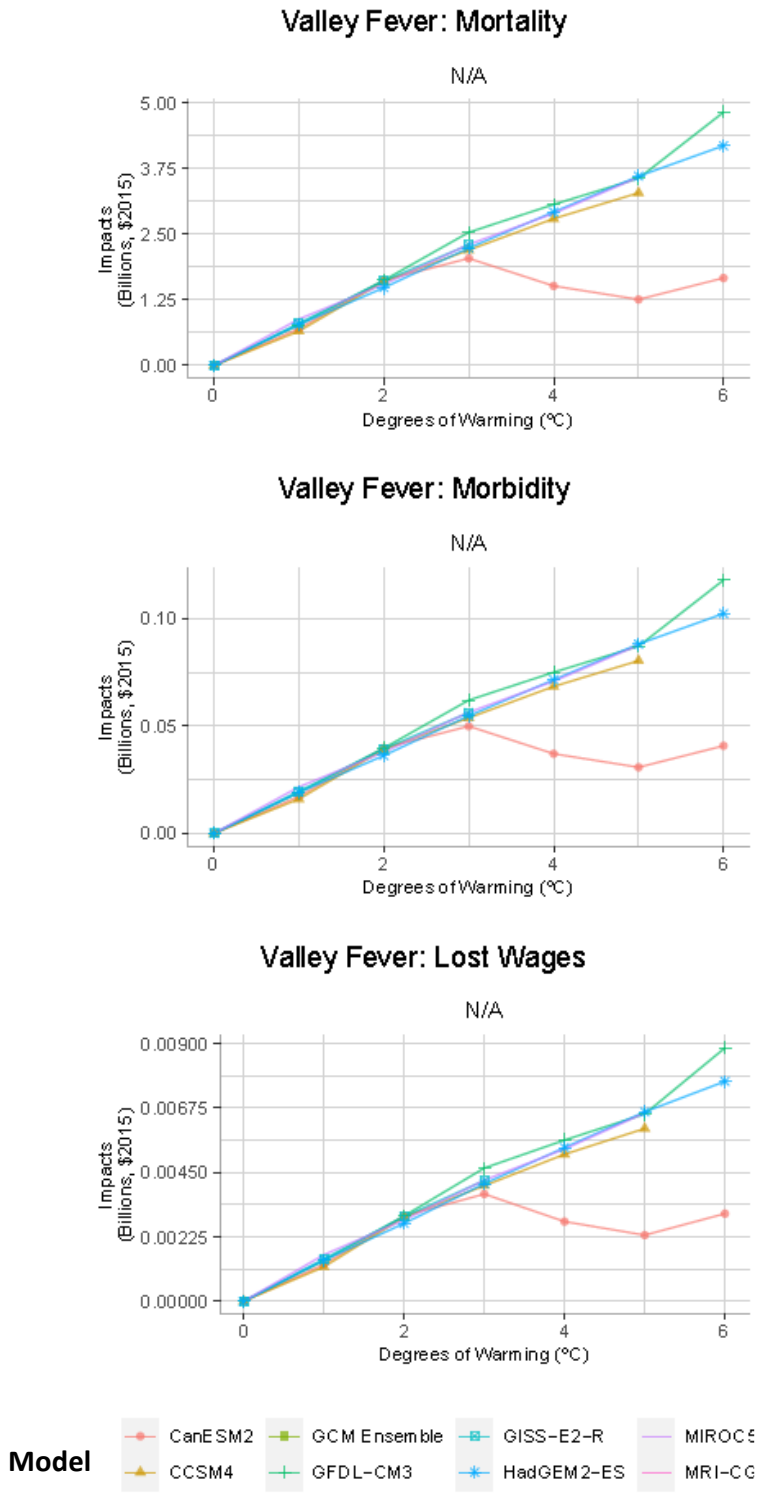

B. 2090 SOCIOECONOMICS

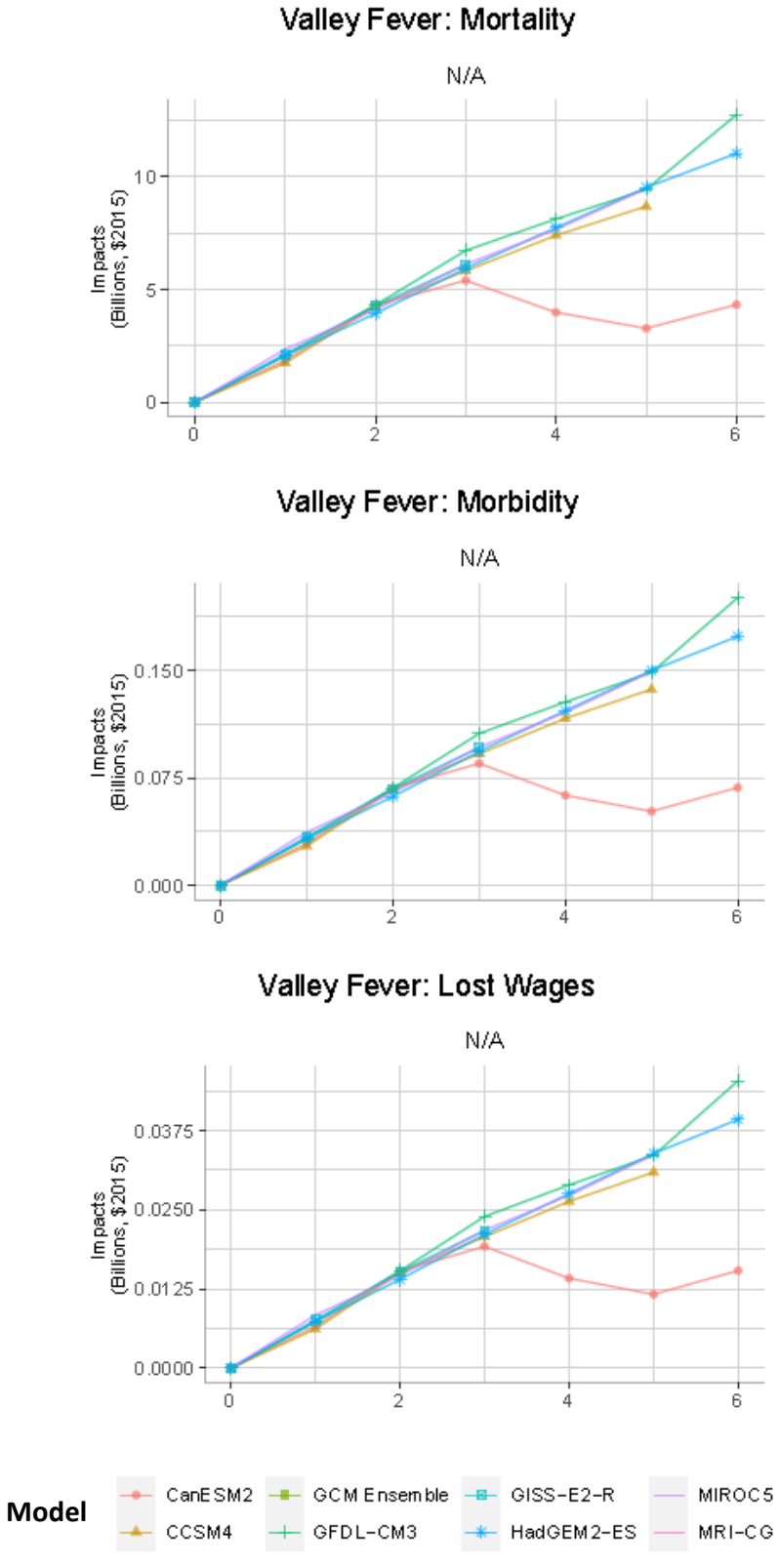

Processing steps

Processing steps are illustrated in **Figure B-10**. Projected Valley fever incidence at the county-level was provided by study authors for 10-year eras centered on 2030, 2050, 2070, and 2090, for six GCMs. In step 2, baseline incidence by county is subtracted from projected incidence for Southwest counties that met an endemicity threshold for Valley fever in the baseline period (112 Southwest counties out of 216). The modeled CIRA baseline based on LOCA weather data is used in place of the Precipitation-Elevation Regressions on Independent Slopes Model (PRISM) baseline from the underlying study. The PRISM baseline provides total regional incidence and does not line up temporally with the modeled CIRA baseline. The CIRA baseline for the period of 1995 (1986-2005) provides incidence by county and allows for comparison of impacts by degree across sectors. A baseline of zero is assumed for all other counties with projected incidence.[11] This includes counties in the Southwest that did not meet the endemicity threshold in the baseline period and counties outside of the Southwest region which, similarly, did not meet the endemicity threshold in the baseline period. The resulting county-level incidence identifies cases of Valley fever attributable to climate change.

Next, county-level impacts are summed to the regional level, resulting in a total count of Valley fever cases per region. In step 3, total impacts are divided by dynamic ICLUSv2 regional population to calculate a case per capita value for each era, GCM, and region. Finally, an annual time series is constructed by linearly interpolating between era values, and yearly impacts are temperature binned by GCM-specific eleven-year windows.

A range of morbidity and mortality outcomes of varying severity associated with Valley fever cases are valued to calculate a weighted average cost based on likelihood of outcome. Based on prior literature, morbidity outcomes are expected to occur in 96 percent of Valley fever cases. Valued morbidity impacts include direct hospitalization, emergency room visit with discharge, emergency room visit with hospitalization, and physician visit. Lost productivity costs associated hospitalizations are monetized using likelihood of outcome and wage rate. Finally, mortality is expected to occur in 4 percent of Valley fever cases and is valued using VSL. To generate impact estimates, cases per capita are multiplied by regional population and a weighted average valuation that accounts for likelihood and value of each outcome (the last step in Figure B-10 below).

[11] Note that climate-attributed excess cases are estimated by comparison of the modeled future climate to the model baseline, using the two-stage approach developed in the paper. Incidence is only calculated in counties that meet an endemicity threshold. Therefore there are two ways that cases can be attributed to climate change: 1. Endemicity thresholds are met in both the baseline and future climate, and so excess cases are the difference between the calculated incidence in future minus baseline; 2. Climate change causes a county to cross the endemicity threshold, in which all future cases are attributed to climate change. This approach is consistent with the current understanding of Valley fever incidence, which is that the fungus must first be established in the soil before a case attributed to exposure in the county can be inferred.

FIGURE B-10. VALLEY FEVER PROCESSING FRAMEWORK

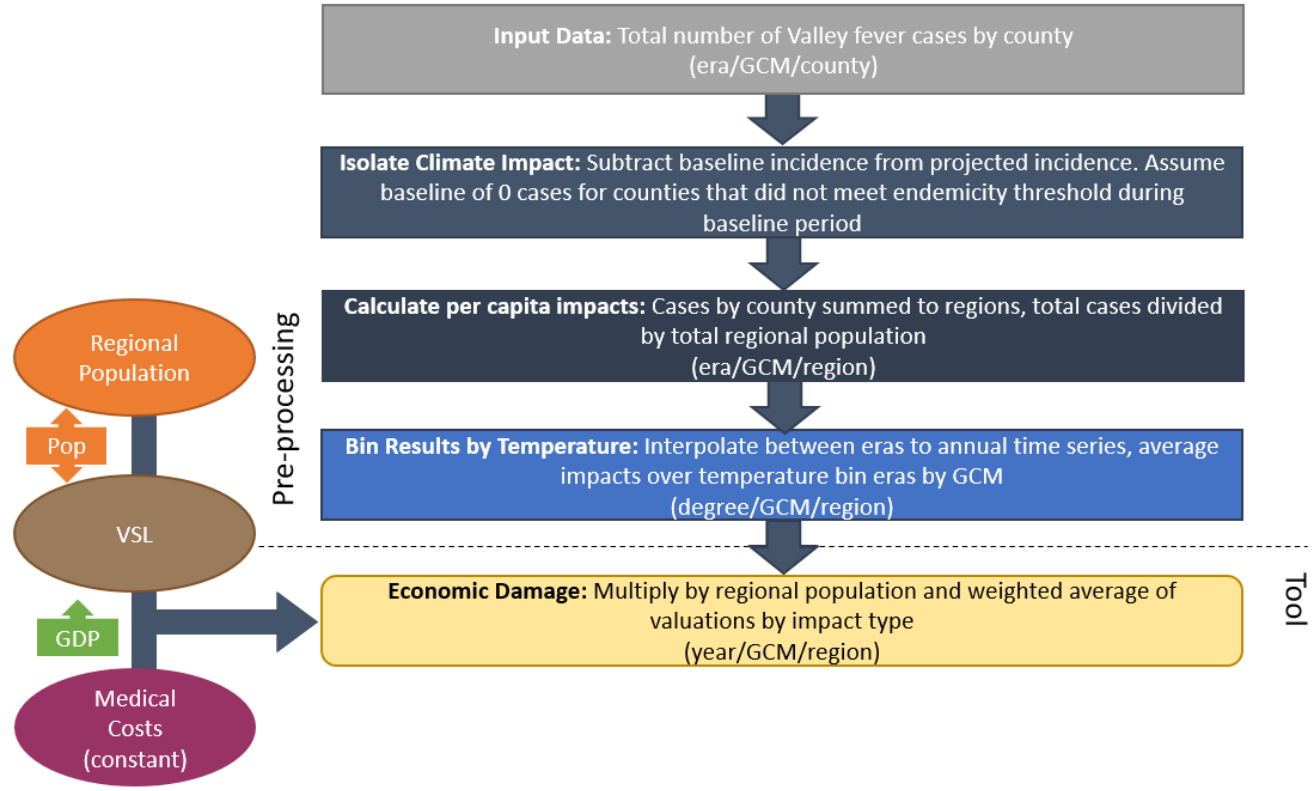

Limitations and Assumptions

- This analysis assumes a baseline of zero cases for counties that did not meet the endemicity threshold in the Southwest region during the baseline period as well as all counties with projected Valley fever cases outside of the Southwest region.
- For further discussion of the limitations and assumptions in the underlying sectoral model, see Gorris et al. (2020).

Wildfire

This sectoral study estimates health impacts from wildfire emissions and response costs from wildfire suppression. Neumann et al. (2021) models change in wildfire activity for the western region of CONUS. As such, response costs are limited to this area, but this study models health impacts of the particulate matter from western wildfires across the CONUS (as these emissions typically travel eastward across the continent).

UNDERLYING DATA SOURCES AND LITERATURE

Neumann, J. E., Amend, M., Anenberg, S., Kinney, P. L., Sarofim, M., Martinich, J., Lukens, J., Xu, J., & Roman, H. (2021). Estimating PM2.5-related premature mortality and morbidity associated with future wildfire emissions in the western US. Environmental Research Letters, 16(3). Doi:10.1088/1748-9326/abe82b

Health impacts are based on the change in incidence of a range of morbidity and mortality outcomes, which are monetized using direct hospitalization costs, costs of emergency department visits, lost productivity, and (for mortality) the VSL. Response costs are estimated based on average wildfire response costs per acre burned, by NCA region. Summaries of impacts by temperature bin degree in 2010 and 2090, the endpoints of socioeconomic modeling, are included in **Figure B-11** below.

FIGURE B-11. WILDFIRE IMPACTS BY TEMPERATURE BIN DEGREE

A. 2010 SOCIOECONOMICS

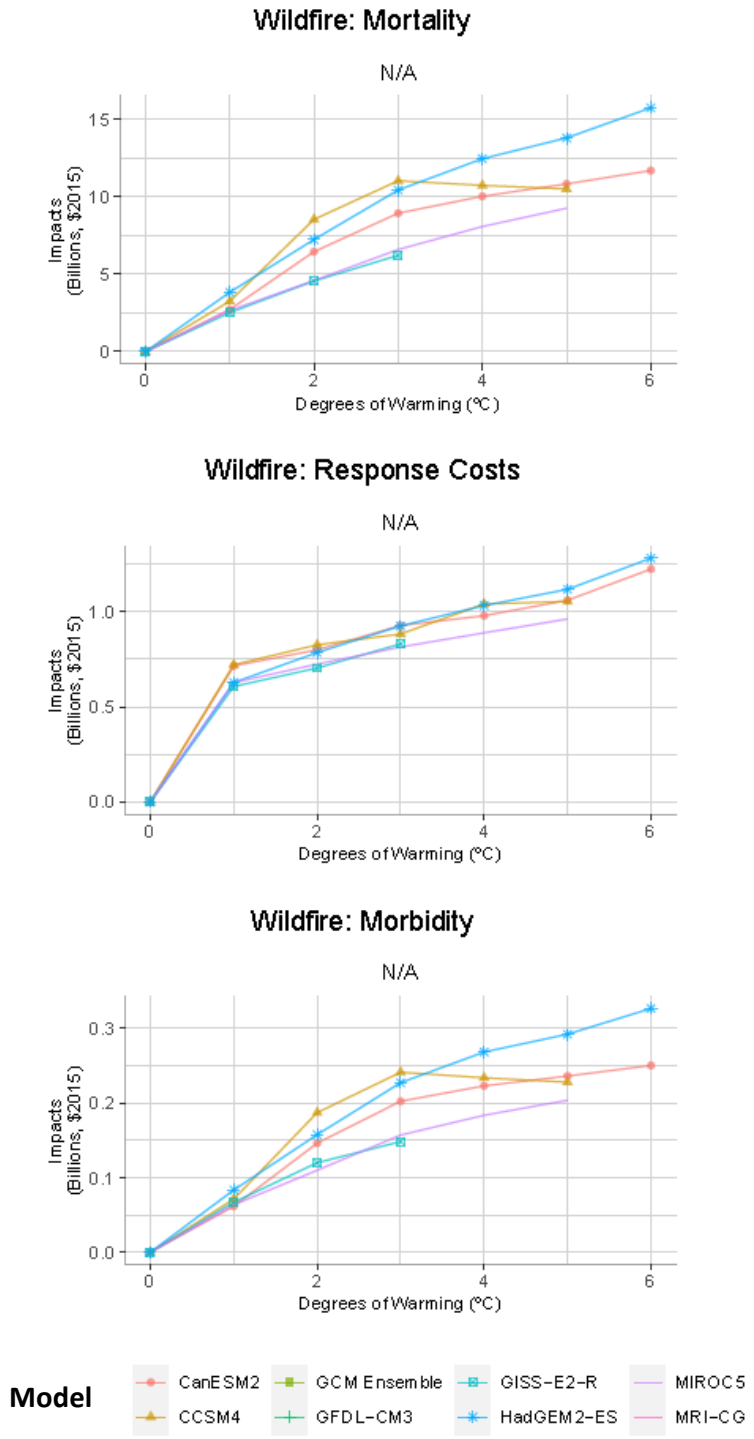

B. 2090 SOCIOECONOMICS

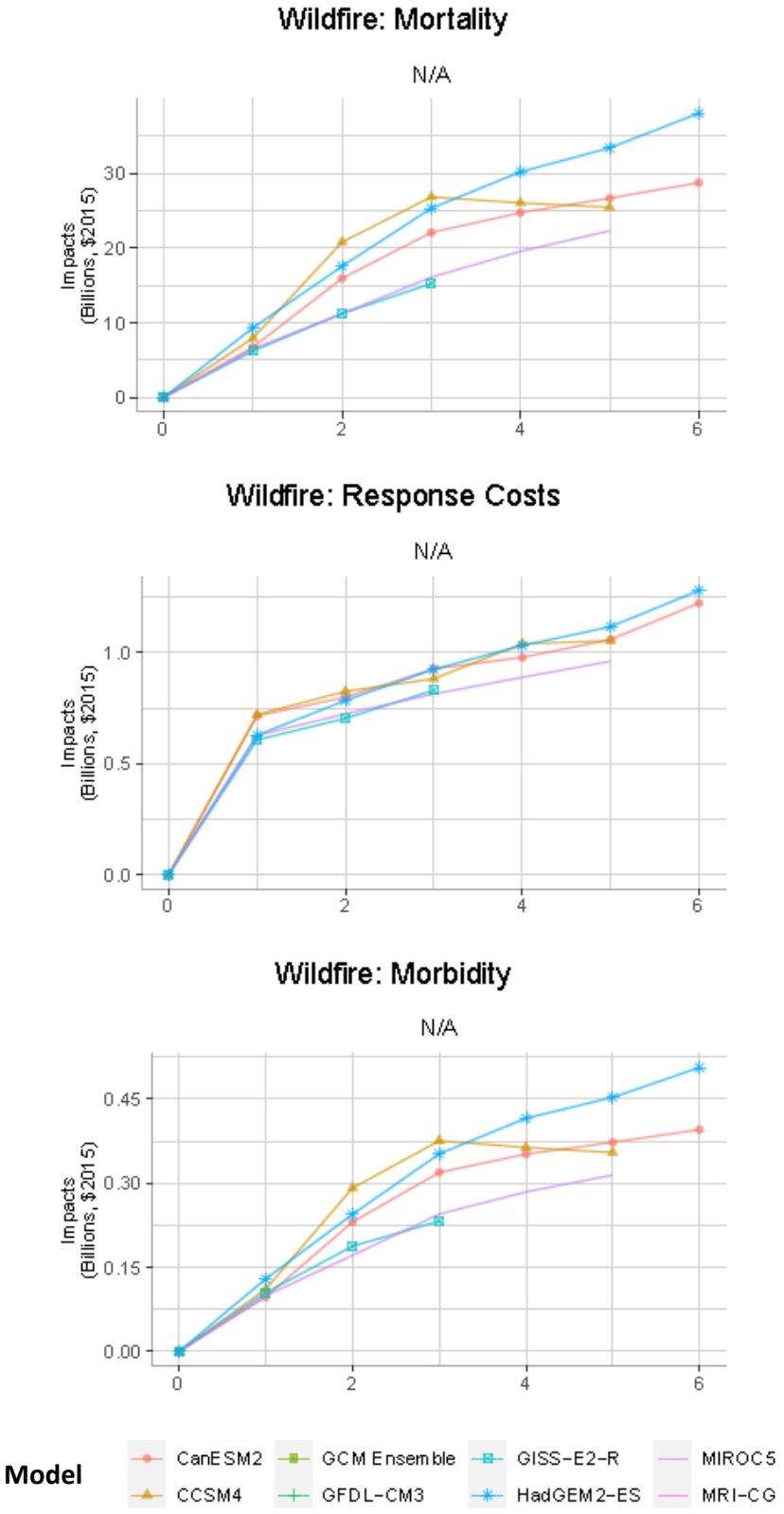

Processing steps

Processing steps are illustrated in **Figure B-12**. Data for each impact type (mortality, morbidity, and response costs) are each processed separately, and summed to estimate total cost across impact types.

Regional mortality incidence attributable to climate change-related changes in $PM_{2.5}$ concentrations resulting from wildfires is provided by study authors for two 10-year eras centered on 2050 and 2090 and five climate models. This analysis considers mortality estimated using a concentration-response function based on risk model information specific to those age 30 and older. A synthetic "no wildfires" mortality scenario that isolates the impact of projected climate (using the Localized Constructed Analogs, or LOCA data) on wildfires is subtracted from projected incidence to isolate the excess health burden associated with climate-induced changes in wildfire activity. This technique allows identification of air quality and health effects associated solely with wildfire. The climate change-related mortality incidence is divided by dynamic ICLUSv2 regional population for each era to calculate mortality per capita for each era/GCM/region scenario. Finally, an annual time series is constructed by linearly interpolating between era values, and yearly impacts are temperature binned by GCM-specific eleven-year windows.

Regional morbidity incidence and valuation was provided by study authors for the same 10-year eras centered on 2050 and 2090 and five climate models. This analysis sums valuation across a set of health endpoints to determine one value associated with all morbidity impacts, representing cost of illness and lost productivity for each era/GCM/region scenario.[12] Baseline valuation is subtracted from 2050 and 2090 projected valuation to isolate the impact of climate change on wildfire-related morbidity. Morbidity valuation is then divided by population, interpolated, and temperature binned as described above for mortality.

Acres burned with baseline implicitly accounted for was available from authors with the dimension *year—GCM—region,* excluding the Midwest, Northeast, and Southeast regions. Acres burned per region is averaged across the GCM-specific eleven-year windows around the first arrival times of integer degrees of warming relative to the baseline. Regional response costs per acre are inputted into the tool as a scalar multiplied by acres burned to calculate total impacts. Response costs per acre remain constant across the century.

Mortality incidence per capita is multiplied by total regional population and VSL to calculate total mortality valuation. Morbidity valuation per capita is multiplied by total regional population to calculate total morbidity valuation. Acres burned is multiplied by response costs per acre to calculate total response costs. The total cost for each impact type is summed to calculate total regional impacts.

[12] Full list of health endpoints includes: acute bronchitis, nonfatal acute myocardial infarction, asthma exacerbation (cough, wheeze, shortness of breath), asthma emergency room visits, cardiovascular hospital admissions, asthma hospital admissions, chronic lung disease hospital admissions (less asthma), respiratory hospital admissions, lower respiratory symptoms, upper respiratory symptoms, work loss days, and minor restricted activity days.

FIGURE B-12. WILDFIRE PROCESSING FRAMEWORK

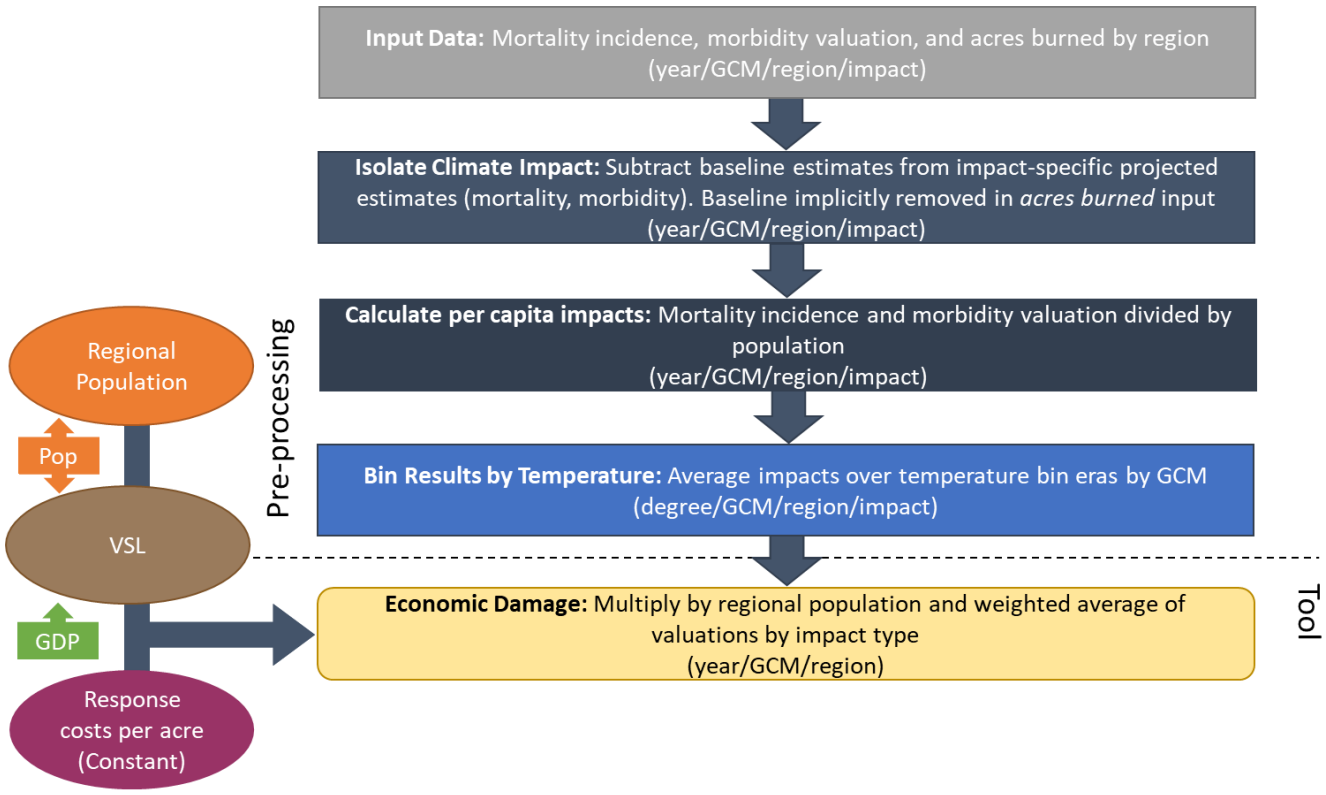

Limitations and Assumptions

- Mortality incidence is quantified for those age 30 and older, and this analysis assumes the impacts for those under 30 to be zero. Doing so underestimates the risk of premature mortality experienced by those under 30. Additionally, doing so assumes that age demographics remain proportional over the century.
- Similarly, the morbidity health endpoints included in this analysis are associated with various age distributions. Total valuation is divided by total regional population, assuming that the health burden outside of included age ranges is zero.
- For further discussion of the limitations and assumptions in the underlying sectoral model see Neumann et al. (2021).

B.3 Infrastructure Sectors Data Processing

Coastal Properties

This sector study estimates future property value damages as a result of sea level rise combined with storm surge attributed to climate change.

UNDERLYING DATA SOURCES AND LITERATURE

Neumann, J. E., Chinowsky, P., Helman, J., Black, M., Fant, C., Strzepek, K., & Martinich, J. (2021). Climate effects on US infrastructure: the economics of adaptation for rail, roads, and coastal development. Climatic Change. https://doi.org/10.1007/s10584-021-03179-w

Lorie, M., Neumann, J. E., Sarofim, M. C., Jones, R., Horton, R. M., Kopp, R. E., Fant, C., Wobus, C., Martinich, J., O'Grady, M., Gentile, L. E. (2020). Modeling coastal flood risk and adaptation response under future climate conditions. Climate Risk Management, 29. Doi:10.1016/j.crm.2020.100233

Damages are estimated for all real properties (land and structure) in all coastal counties that contain land with a hydraulic connection to the ocean and containing property that is within 20 m elevation above sea level for the year 2000. Property values for potentially vulnerable structures and land are "market adjusted" assessed values that reflect 2017 property values for 302 counties along the CONUS coast – see Neumann et al. (2021) for details. Within the model, real property values appreciate over the century by GDP per capita projections.

The underlying damage simulation model includes cost estimates for no adaptation and two adaptation scenarios (reactive and proactive), as defined in the underlying study. Under the no adaptation scenario, properties are abandoned once inundated. Reactive adaptation loosely reflects structural adaptation options that can be adopted without collective action (e.g., elevation of structures and land near structures), while proactive adaptation includes consideration of options that likely require collective action (such as beach nourishment and construction of seawalls).[13] The model conducts a series of benefit-cost calculations at the level of a 150m x 150m grid cell to assess where and when adaptation could be cost-effective in mitigating property damage due to sea level rise and storm surge. Summaries of impacts by integer degrees of warming in 2010 and 2090, the endpoints of socioeconomic modeling, and by adaptation scenario is included in **Figure B-13**.

[13] The underlying study (Neumann et al. 2021) outlines the logic for classifying measures as reactive or proactive. The general concept is that reactive measures are either responsive to events (without foresight about future events) or can be undertaken without coordinated action between individuals and governments. Elevation, for example, is modeled at the individual property level in response to highly localized hazards, not as a collective action of municipal governments to modify building codes.

FIGURE B-13. COASTAL PROPERTIES IMPACTS BY SLR SCENARIO OVER TIME

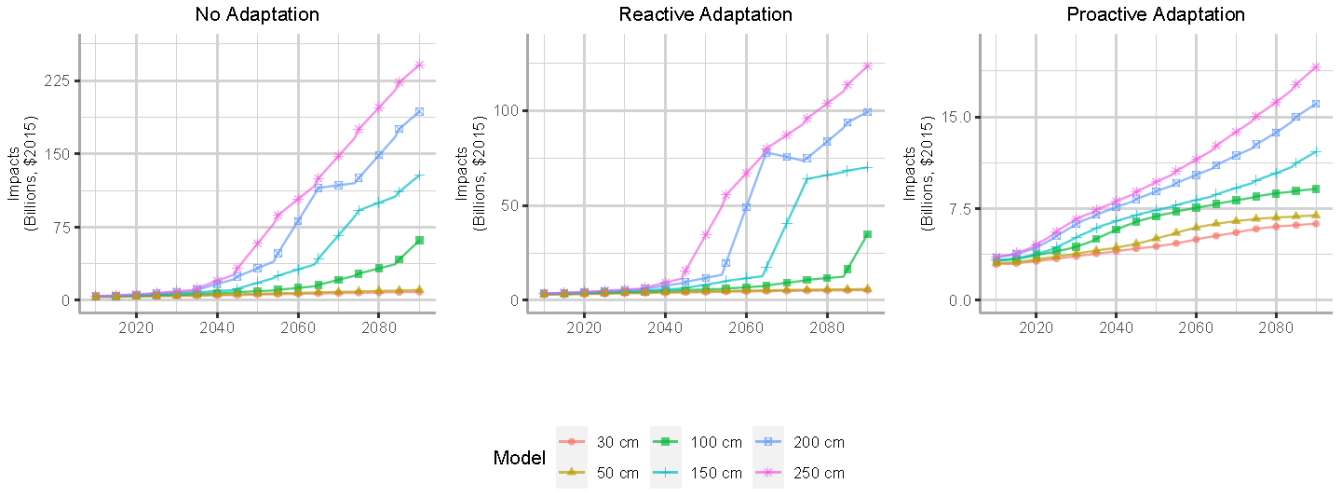

Processing steps

Processing steps are shown in **Figure B-14**. In step one, a trajectory of property damages that represent an 11-year rolling average of annual results from the underlying study are estimated for each sea level rise scenario, year, region, adaptation scenario, and for two static socioeconomic scenarios; 2010 and 2090. Residential and commercial properties, as well as energy infrastructure, are considered to calculate potential damages in the model. For this sector, the baseline is anchored at 2000, as the National Coastal Property Model (NCPM) starts with zero damages in this year. As with the temperature bin indexing, regional and local sea levels are mapped to GMSL based on the localized sea level rise projections from Sweet et al. (2017), which include effects such as land uplift or subsidence, oceanographic effects, and responses of the geoid and the lithosphere to shrinking land ice. When custom sea level rise scenarios are used in the Framework, the relationship between GMSL and regional sea levels, and ultimately regional impacts, are mapped implicitly based on the underlying models.

As noted in the main report text, SLR is estimated from a reduced complexity model that incorporates the time- and trajectory-dependent qualities of SLR response to temperature. That implies that damages should be estimated along the trajectory using both the sea level height and the year that the sea-level height is reached (and therefore, that year's implicit socioeconomics). Damages for any year therefore use the 11-year rolling average damages for each sea level rise scenario, and the input sea level rise trajectory, and a damage trajectory is interpolated between the two underlying sea level rise scenarios that have sea level rise heights closest to the input scenario in any given year. For example, if the SLR trajectory reaches 175 cm in 2080, the damage estimate would fall between the 150cm and 200cm scenarios.

Because of the decision-tree structure of the NCPM, population and GDP cannot be disentangled as drivers of impacts. A linear interpolation between impact estimates associated with runs of the NCPM where socioeconomics are held constant in 2010 and 2090 is used to model changes in socioeconomic drivers for this sector.

FIGURE B-14. COASTAL PROPERTIES DATA PROCESSING FRAMEWORK

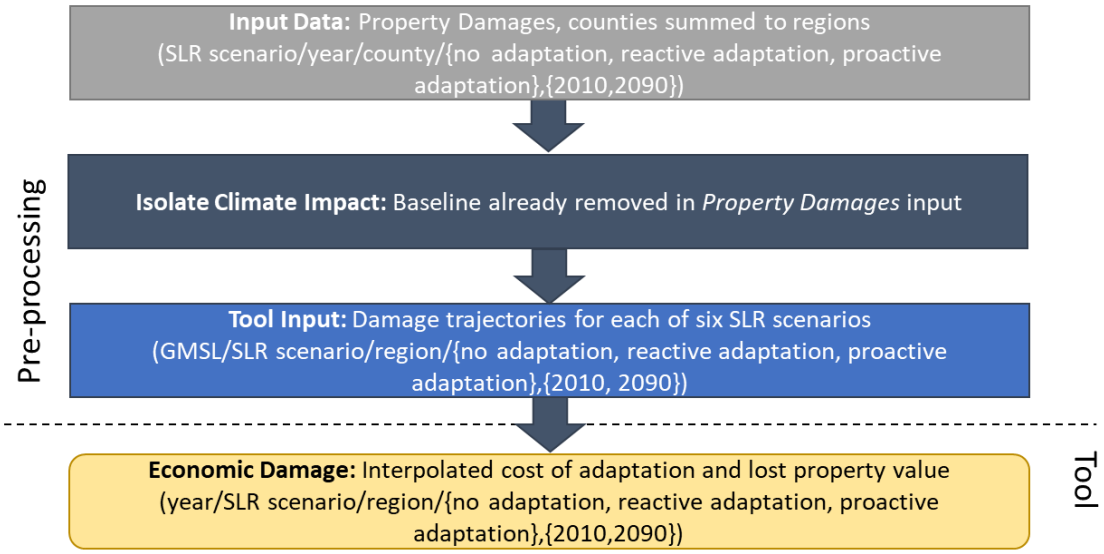

Limitations and Assumptions

- Damages are limited to land and structures within the study domain (i.e., flooding impacts to structures inland of 20m elevation are not quantified), and exclude the value of public infrastructure, which was not considered in the underlying sectoral study.
- Adaptation response decisions in the coastal zone are not typically made with strict cost-benefit decision rules, particularly at the local level. Other factors may include local zoning bylaws, future land use plans, the presence of development-supporting infrastructure, or proximity to sites with high cultural value. However, the analytical framework of this coastal property model provides a simple, benefit-cost decision framework that can be consistently applied for regional and national-scale analysis.
- The underlying study does not consider the effects of climate on storm surge activity (although impacts on wind damage are considered in a separate sector study included in the tool). The only non-climate change driven change to coastline considered was an increase in land and existing structure value over time.
- For further discussion of the limitations and assumptions in the underlying sectoral model see Neumann et al. (2021), Lorie et al. (2020), and USEPA (2017).

High Tide Flooding and Traffic

This sector study estimates the cost of delays to passenger and freight traffic on coastal roads that experience flooding due to combinations of high tides and sea level rise, and costs of adaptation in the form of infrastructure improvements.

UNDERLYING DATA SOURCES AND LITERATURE

Fant, C., Jacobs, J. M., Chinowsky, P., Sweet, W., Weiss, N., Martinich, J. & Neumann, J. E. (2021). Mere nuisance or growing threat? The physical and economic impact of high tide flooding on US road networks. Journal of Infrastructure Systems. doi: 10.1061/(ASCE)IS.1943-555X.0000652

Delay damages are in terms of passenger and freight vehicle-hours. These are monetized based on the value of travel time savings (VTTS) for passenger traffic, and the National Cooperative Highway Research Program's (NCHRP) inputs for cost of delay for freight traffic. Infrastructure improvements include building sea walls or elevating the elevation of the roadway surface. Infrastructure improvement costs include estimates of material, labor, and construction delays.

This sector considers three adaptation scenarios: no adaptation, reasonably anticipated adaptation, and direct adaptation. These adaptation scenarios differ from scenarios modeled for other infrastructure sectors. The no adaptation, reactive adaptation, and proactive adaptation scenarios of other infrastructure sectors are based on infrastructure development for an unchanging, current, or future climate in a given model time step. For this sector, the no adaptation scenario estimates costs of delays associated with flooding of roadways with the assumption that drivers do not re-route and instead wait until the roadway is clear to travel. The reasonably anticipated adaptation scenario assumes drivers re-route to avoid flooded roadways, with only slight delay due to increased travel time. This scenario also includes ancillary protection; in cases where flooded roadways are near properties that would be protected by sea walls or beach nourishment, this scenario assumes those roadways would also be protected and thus no longer flood.[14] In the direct adaptation scenario, where delay costs are high enough, roadways are either protected from flooding through the construction of a sea wall or elevation of the road profile. **Figure B-15** provides a summary of results by integer degree of warming and adaptation scenario in 2010 and 2090, the endpoints of socioeconomic modeling, and representing the static runs for each SLR scenario.

FIGURE B-15. HIGH TIDE FLOODING AND TRAFFIC IMPACTS BY INTEGER DEGREE OF WARMING

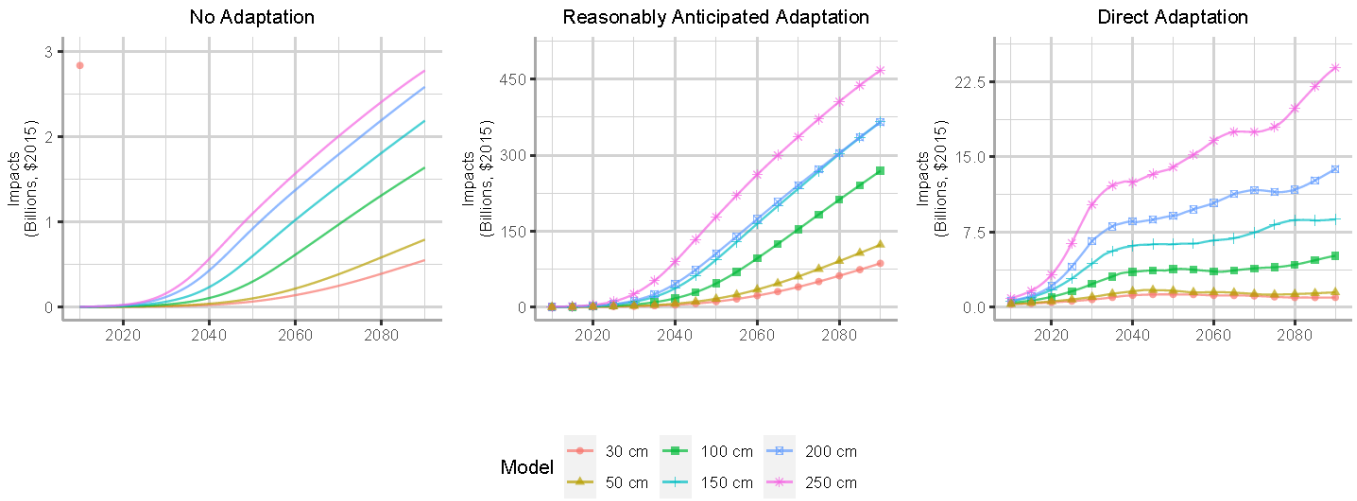

[14] Note that the including of ancillary protection of properties with sea walls in the "reasonably anticipated" category, consistent with the underlying Fant et al. (2021) study, may seem inconsistent with the classification of sea walls as "proactive" adaptation in the coastal properties sector. As outlined in the Fant et al. (2021) high-tide flooding paper, however, the impact of this potential inconsistency is slight - Figure 3 and accompanying text in that paper notes that alternative routing reduces the no adaptation impacts by 77%, while the marginal additional impact of ancillary sea wall protection increases the total to an 80% reduction.

Processing steps

Processing steps are seen in **Figure B-16**. In step one, damages at the county level are aggregated to the regional level. These damages are available for all SLR scenario, year, and adaptation scenario combinations for both the 2010 and 2090 static socioeconomic runs.

Similar to the Coastal Properties sector, this sector "zeroes out" in 2000, and thus has no baseline for which to adjust, and also relies on an interpolated damage estimate technique. Damages for any year use the 11-year rolling average damages for each sea level rise scenario, and the input sea level rise trajectory, and a damage trajectory is interpolated between the two underlying sea level rise scenarios that have sea level rise heights closest to the input scenario in any given year. For example, if the SLR trajectory reaches 175 cm in 2080, the damage estimate would fall between the 150cm and 200cm scenarios.

FIGURE B-16. HIGH TIDE FLOODING AND TRAFFIC DATA PROCESSING FRAMEWORK

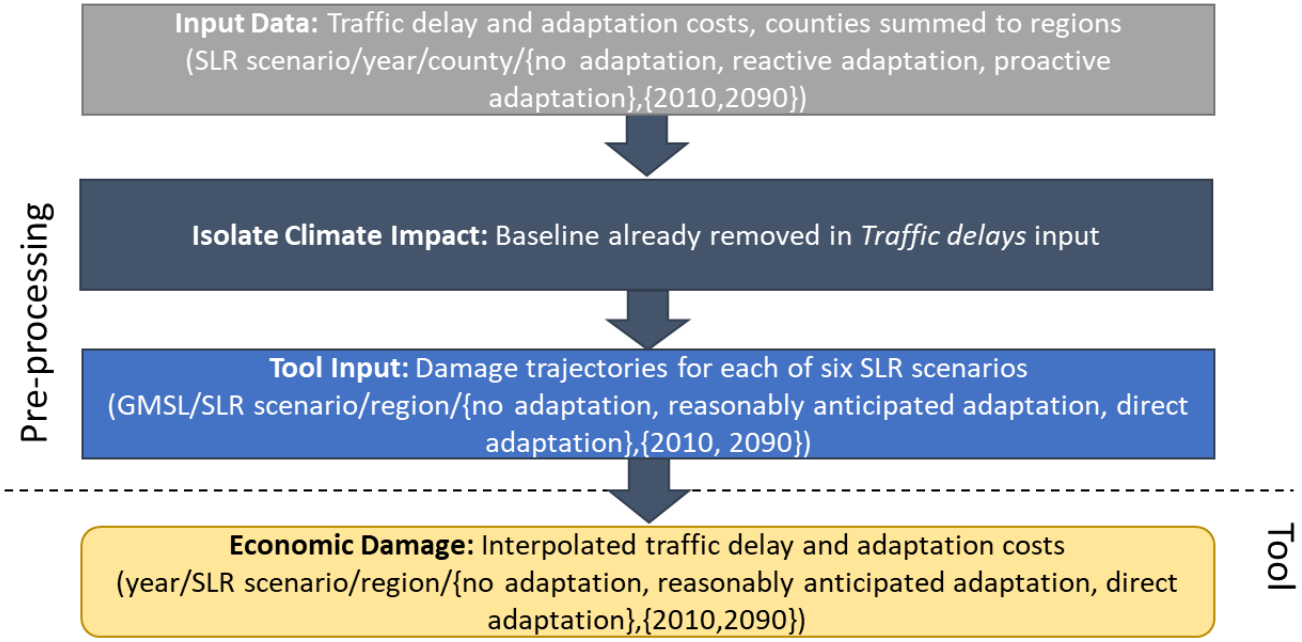

Limitations and Assumptions

- The underlying sectoral analysis is limited to road segments within the flood extent for the current minor flood level. This extent is expected to migrate further inland as sea levels rise. This analysis also omits consideration of impacts to underground roads.
- Flooding as a result of rainfall or riverine flooding is not modeled and may exacerbate flood events or durations in the coastal zone if they occur simultaneously.
- Many direct adaptation options (e.g., hydrologic infrastructure) are not considered.
- The economic cost per hour of delay per passenger or freight vehicle is assumed to be constant over the century.
- For further discussion of the limitations and assumptions in the underlying sectoral model see Fant et al. (2021).

Rail

This analysis estimates repair, equipment, and delay costs to rail infrastructure due to rail track buckling or the risk of buckling associated with elevated temperatures.

Damages are based on costs of repair, including equipment and labor, and delay costs. These costs are then scaled using total track miles in each region of CONUS.

UNDERLYING DATA SOURCES AND LITERATURE

Neumann, J. E., Chinowsky, P., Helman, J., Black, M., Fant, C., Strzepek, K., & Martinich, J. (2021). Climate effects on US infrastructure: the economics of adaptation for rail, roads, and coastal development. Climatic Change. https://doi.org/10.1007/s10584-021-03179-w

Chinowsky, P., Helman, J., Gulati, S., Neumann, J., & Martinich, J. (2019). Impacts of climate change on operation of the US rail network. Transport Policy, 75, 183-191. Doi:10.1016/j.tranpol.2017.05.007

The analysis is completed for each of three adaptation scenarios: no adaptation, proactive adaptation, and reactive adaptation. The no adaptation scenario incorporates no speed restrictions but results in a higher risk of track buckling associated with continued use of trains during high temperature events. Track buckling events require repair that create delays. The reactive scenario considers reduced train speeds at higher temperatures to reduce likelihood of track buckling. The proactive scenario includes installation of temperature sensors to monitor probabilities of track buckling and modify train speeds as necessary (and therefore prevent delays associated with their unexpected need for repair). A summary of results by temperature bin degree and adaptation scenario in 2010 and 2090, the endpoints of socioeconomic modeling, is included in **Figure B-17**.

FIGURE B-17. RAIL IMPACTS BY TEMPERATURE BIN DEGREE

A. 2010 SOCIOECONOMICS

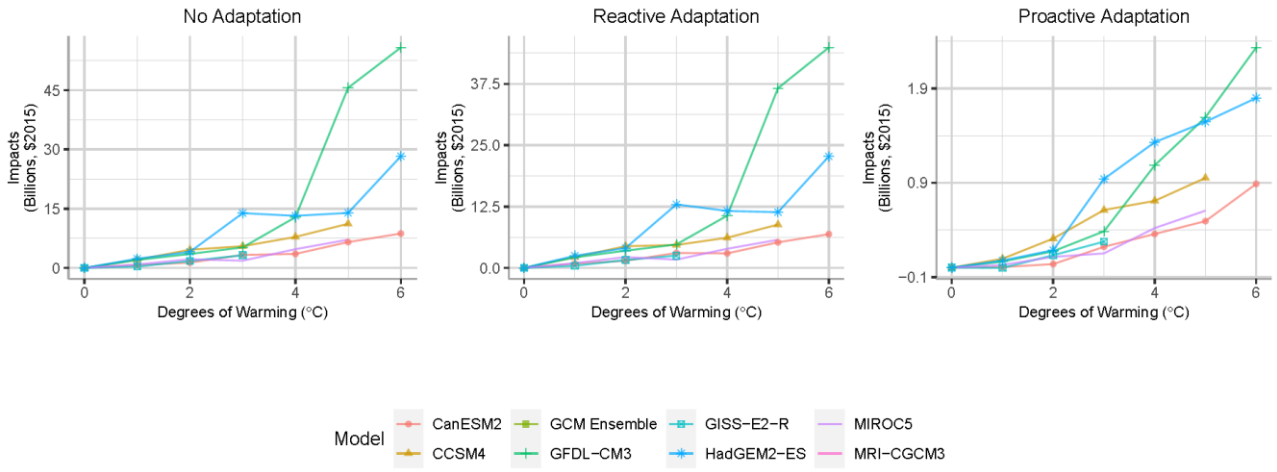

B. 2090 SOCIOECONOMICS

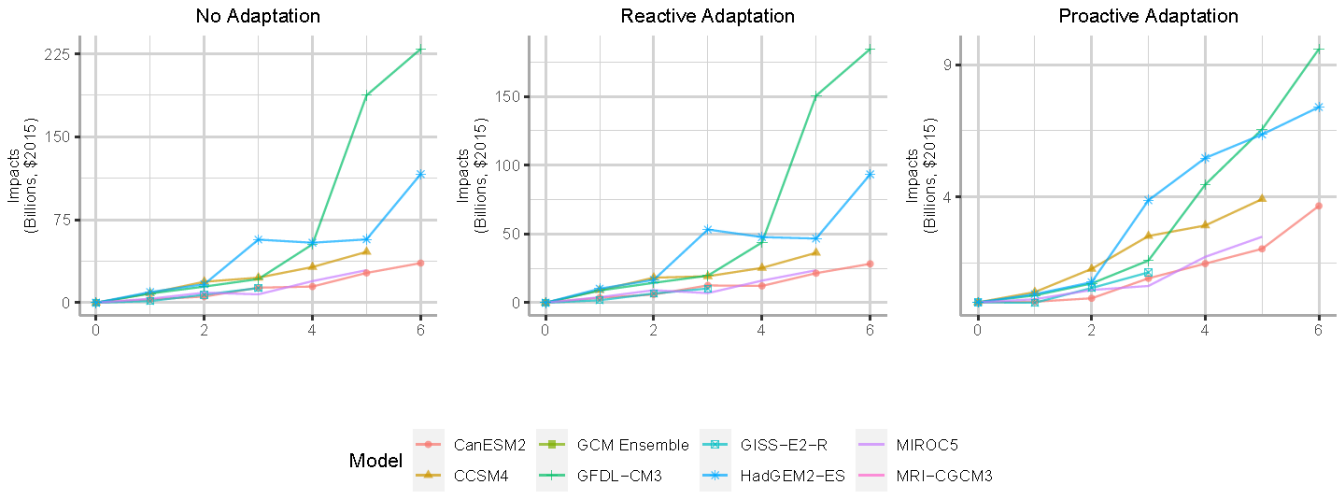

Processing steps

Processing steps are shown in **Figure B-18**. In step one, the impact model for this sector is run at the Climatic Research Unit (CRU) grid cell level, and damages are aggregated to the NCA region level. This impact model assumes that the spatial extent and distribution of rail infrastructure remains constant across the 21st century. In step two, baseline costs associated with delays and costs under a control climate scenario are subtracted for all adaptation scenarios. Thus, damages presented are due to climate change.

Annual damages are then temperature binned. Total damages are then divided by total miles of rail within a region to produce damages per mile.

Damages per mile are scaled with the number of rail miles in a region as well as a socioeconomic growth scalar, with 2010 as the base year. The model assumes rail traffic increases linearly with GDP growth for freight traffic, and linearly with population growth for passenger traffic. Freight traffic represents 96

percent of rail traffic, and passenger traffic the remaining 4 percent. This analysis assumes that rail traffic can be modified with custom GDP and/or population projections.

FIGURE B-18. RAIL DATA PROCESSING FRAMEWORK

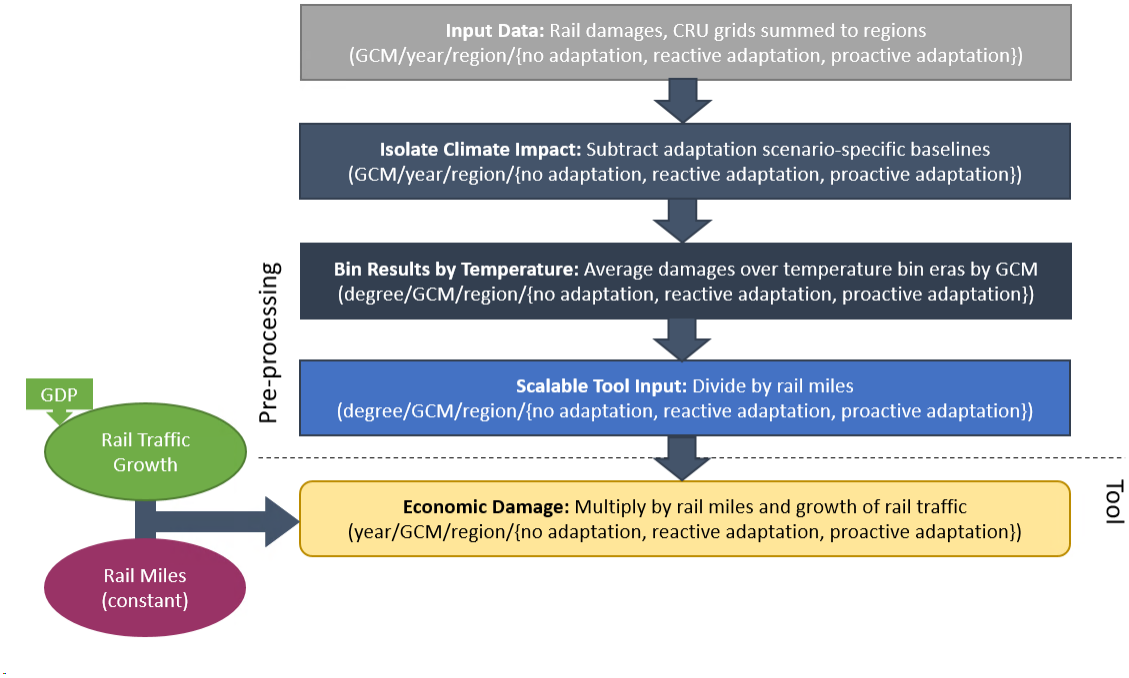

Limitations and Assumptions

- The model assumes the number of rail miles is fixed and does not grow over time, though rail traffic over the existing rail network grows with a weighted average of population growth (for the passenger rail component) and economic growth (for the much larger freight rail component).
- Equipment, labor, and repair supply costs are assumed to remain constant.
- For further discussion of the limitations and assumptions in the underlying sectoral model see Neumann et al. (2021), Chinowksy et al. (2017), and EPA (2017).

Roads

This sector study estimates the cost of road repair, user costs (vehicle damage), and road delays due to changes in road surface quality as a result of climate change (specifically changes in temperature, precipitation, and flooding).

Damages are based on the cost of repairs and delays associated with

UNDERLYING DATA SOURCES AND LITERATURE

Neumann, J. E., Chinowsky, P., Helman, J., Black, M., Fant, C., Strzepek, K., & Martinich, J. (2021). Climate effects on US infrastructure: the economics of adaptation for rail, roads, and coastal development. Climatic Change. https://doi.org/10.1007/s10584-021-03179-w

Neumann, J. E., Price, J., Chinowsky, P., Wright, L., Ludwig, L., Streeter, R., Jones, R., Smith, J. B., Perkins, W., Jantarasami, L., & Martinich, J. (2014). Climate change risks to US infrastructure: impacts on roads, bridges, coastal development, and urban drainage. Climatic Change, 131, 97-109. Doi:10.1007/s10584-013-1037-4

either deteriorated road surfaces or road shutdowns to complete repairs, and delays are scaled by current period traffic, which in turn is adjusted for future changes in population (described further below). The per mile impacts are then multiplied by total regional road miles, and adjusted to reflect the likelihood of delay mitigation as proxied by an index of road density in each ½ degree by ½ degree grid cell, to produce a total damage estimate in a region.

Similar to the rail and coastal properties studies, the analysis models three adaptation scenarios: no adaptation, proactive adaptation, and reactive adaptation. In the no adaptation scenario, repairs to roads are limited to historic repair budgets; damages in this scenario are based on the cost of repairs to road surfaces, damage to vehicles associated with incompletely maintained roads, and delays associated with repairs to road surfaces or speed limitations attributed to poorly maintained roads.[15] Under the reactive adaptation scenario, repair budgets are increased to repair all damages in a given year to re-establish the pre-repair level of service. In the proactive scenario, roads are pre-emptively strengthened to prevent damage with consideration of future climate changes in the design and materials used for repair. Under the reactive and proactive adaptation scenarios, damages are based on the cost of repairs to road surfaces and the delays associated with repairs or speed limitations due to poorly maintained roads. The model considers three types of environmental stressors: temperature, precipitation, and flooding. Damages differ by road surface; road surfaces are either unpaved, paved, or gravel. This impact model runs at the quarter-degree grid cell level, and each grid cell is assigned adaptation-scenario specific budget for repairs. **Figure B-19** provides a summary of results by temperature bin degree and adaptation scenario in 2010 and 2090 (the endpoints of socioeconomic modeling). Note that the proactive adaptation results generally reflect a much lower damage estimate overall than no adaptation or reactive costs, but that in some scenarios the timing of those costs may be accelerated (and actually be triggered by relatively modest levels of warming) because of optimization of the capital cost of resilience investments and the high payoff to these investments in terms of avoiding future repairs and delays.

[15] The budget constraint in the no adaptation scenario can be thought of as a resilience threshold. For small amounts of warming, roads and their maintenance systems are adequate to meet increased stress. Once that resilience threshold is exceeded, costs increase quickly as road damage occurs.

FIGURE B-19. ROADS IMPACTS BY TEMPERATURE BIN DEGREE

A. 2010 SOCIOECONOMICS

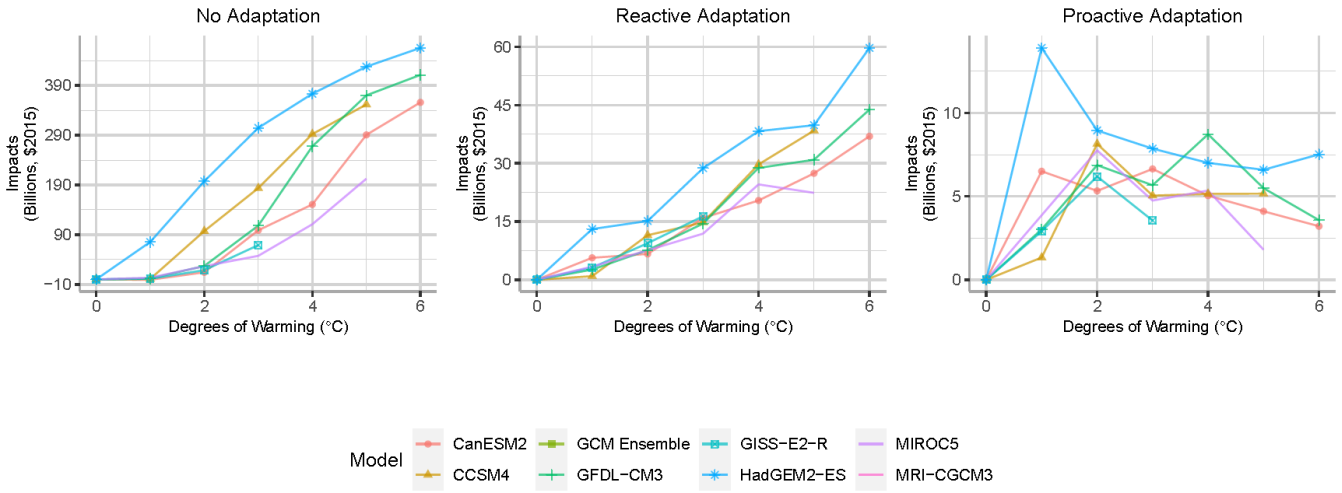

B. 2090 SOCIOECONOMICS

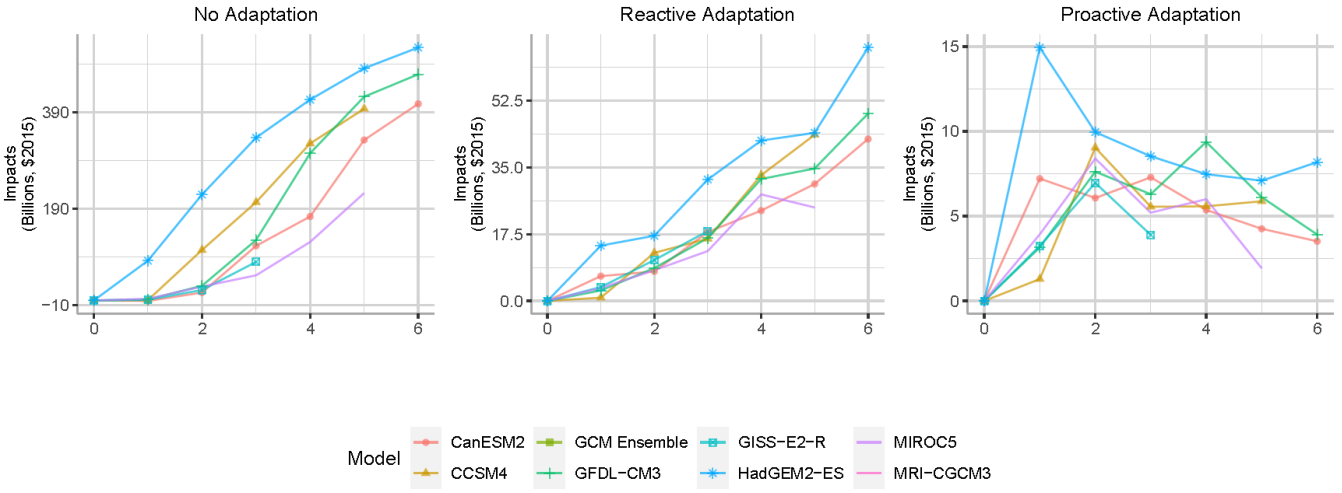

Processing steps

Processing steps are seen in **Figure B-20**. In step one, damages at the quarter-degree grid cell level are aggregated to the regional level. These damages are available for all GCM, year, and adaptation scenario combinations.

Baseline damages are then subtracted from projected damages for each GCM to arrive at damages associated with climate change from the baseline period for each adaptation scenario. Damages associated with climate change from the baseline period are then temperature binned — temperature binned damages are average annual damages from eleven-year windows around first arrival times of integer degrees of warming from the baseline period for each GCM. Total damages are then divided by total miles of road within a region to produce damages in terms of dollars per mile.

Damages per mile are scaled using total regional road miles. To account for additional repair due to increased traffic on damaged roads, a population-dependent scalar is applied to damage trajectories. This scalar is based on the percent increase in damages across the century when the underlying model is run with population growth compared to a run with static population. Impact estimates are calculated using temperature binned damages multiplied by road miles and adjusted based on changes in road traffic. Note that because repair under the proactive scenario strengthens road surfaces pre-emptively, before damage occurs and with a planned road closure, delay times under the proactive adaptation scenario are approximately half the projected delays for no adaptation and reactive adaptation– see Neumann et al. (2021) for details.

FIGURE B-20. ROADS DATA PROCESSING FRAMEWORK

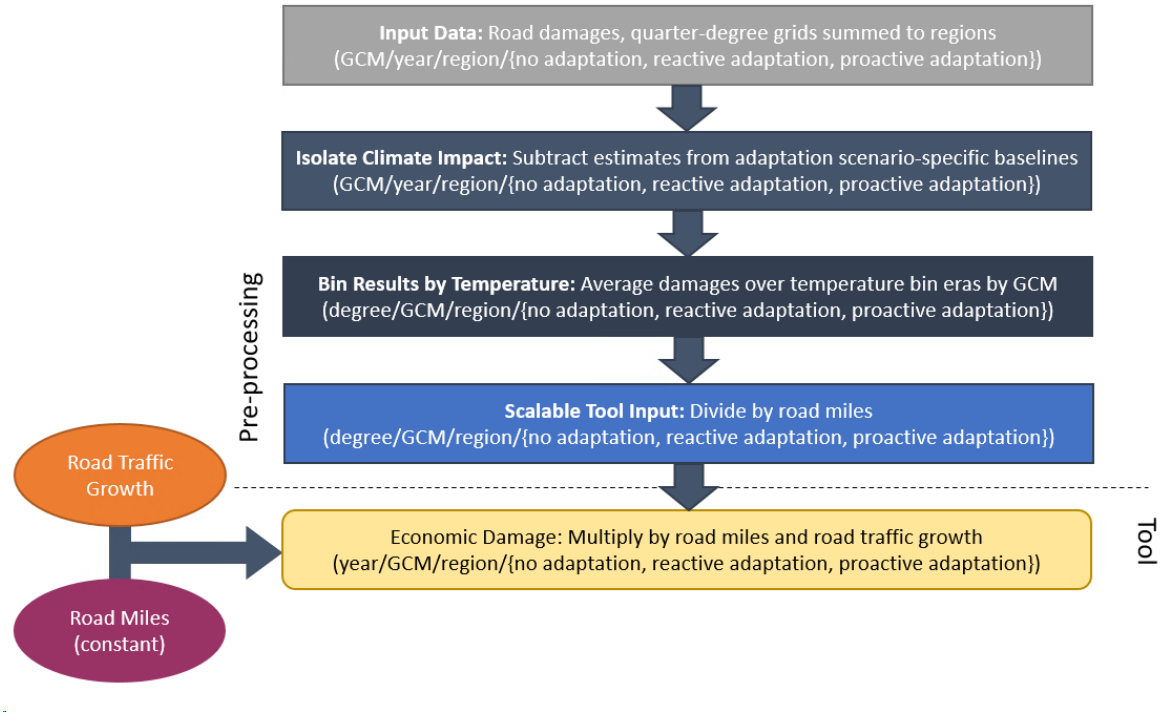

Limitations and Assumptions

- The model assumes a fixed capital and maintenance expense budget, which is usually exhausted at some point under the no-adaptation scenario. This time dependency of the no adaptation scenario is difficult to eliminate in the data processing steps, which could bias the estimate up or down, depending on the speed of warming relative to the underlying scenarios. This bias is expected to be relatively small and the use of GCM average results minimizes this potential bias.
- Damages to vehicles associated with incompletely maintained roads are modeled only in the no adaptation scenario; the model assumes roads are completed repaired and thus vehicles receive no damage under the reactive and proactive adaptation scenarios.
- For further discussion of the limitations and assumptions in the underlying sectoral model see Neumann et al. (2021), Neumann et al. (2014), and EPA (2017).

Asphalt Roads

This sector study estimates the cost of asphalt road maintenance associated with climate change. Unlike the CIRA roads sector, this sector does not model any adaptation scenarios.

UNDERLYING DATA SOURCES AND LITERATURE

Underwood, B. S., Guido, Z., Gudipudi, P., & Feinberg, Y. (2017). Increased costs to US pavement infrastructure from future temperature rise. Nature Climate Change, 7, 704-707. Doi:10.1038/nclimate3390

Future impacts are quantified by comparing historical asphalt grades (values associating pavement temperature and performance) and those associated with future climate projections. This analysis includes four roadway types: interstates, national routes, state routes, and local roads. Impacts are based on the cost of maintaining the standard practice of material selection for asphalt road maintenance rather than employing proactive pavement adaptation. Costs per lane mile are multiplied by total regional asphalt lane miles to produce a total damage estimate in a region. A summary of results by temperature bin is included in **Figure B-21** below. Note that asphalt lane miles are constant throughout the century, therefore only one set of impacts is shown in the figure.

FIGURE B-21. ASPHALT ROADS IMPACTS BY TEMPERATURE BIN DEGREE

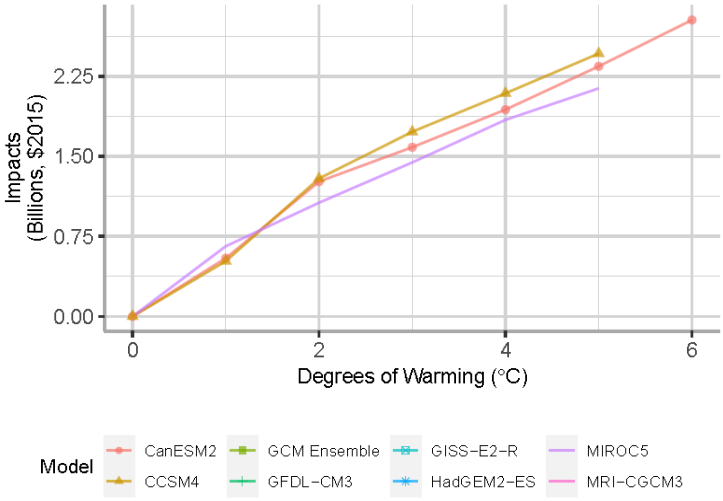

Climate Data Processing

This study was not part of the CIRA project and relies on different climate data that needed to be processed for this sector to be included in the Framework. Underwood et al. (2017) select 19 climate models from CMIP5, three of which (CanESM2, CCSM4, and MIROC5) overlap with the CIRA suite of GCMs, from the archives of the Climate Analytics Group. Although this study used the same GCMs, the bias correction and downscaling processes used by Climate Analytics Group differed from those used in the LOCA climate dataset; therefore, new temperature bins are defined for the relevant new climate scenarios. RCP8.5 results are used for consistency with CIRA sectors. Maximum and minimum daily temperature data for these three GCMs were processed in the 30-year periods employed by the study to determine future annual temperatures associated with the era-level GCM-specific asphalt road damage estimates available

from the study. The CONUS baseline mean temperature was calculated from downscaled LOCA data that matches the CIRA baseline period of 1986-2005, rather than the 1966-1995 U.S. Historical Climatology Network (USHCN) baseline data employed by Underwood et al. (2017). The USHCN baseline data is available by station location and aggregating to CONUS may introduce error relative to the underlying methodology. The LOCA data serves as the best available proxy for USHCN station data while also allowing for comparison by degree across sectors, which use the same baseline. The LOCA baseline mean temperature was subtracted from yearly projected temperature to identify GCM-specific integer degree arrival years that were used for temperature binning.

Processing steps

Processing steps are seen in **Figure B-22**. In step one, total undiscounted costs and total lane miles by weather station are aggregated to the regional level. These impacts are available for all GCMs and regions for three eras: 2010 (2010-2039), 2040 (2040-2069), and 2070 (2070-2099), as well as a baseline era, which are assigned to 1995 (1986-2005). Total costs, which refer to the sum of impacts over each 30-year era, are divided by 30 to reflect an annual cost.

Baseline impacts are then subtracted from projected impacts for each GCM to arrive at maintenance costs associated with climate change for each era. Total costs attributable to climate change are divided by total lane miles per region, resulting in a cost per lane mile for each era and GCM scenario. Next, era costs are assigned to the central year of the era (i.e., 2025, 2055, and 2085), and costs per era are transformed to annual costs by interpolating linearly between era impacts. Finally, costs per lane mile are binned in GCM-specific eleven-year windows around the first arrival times of integer degrees of warming relative to the baseline. Costs per lane mile are scaled using total regional lane miles. Final impact estimates are calculated based on regional lane miles and temperature-binned damages per road mile.

FIGURE B-22. ASPHALT ROADS DATA PROCESSING FRAMEWORK

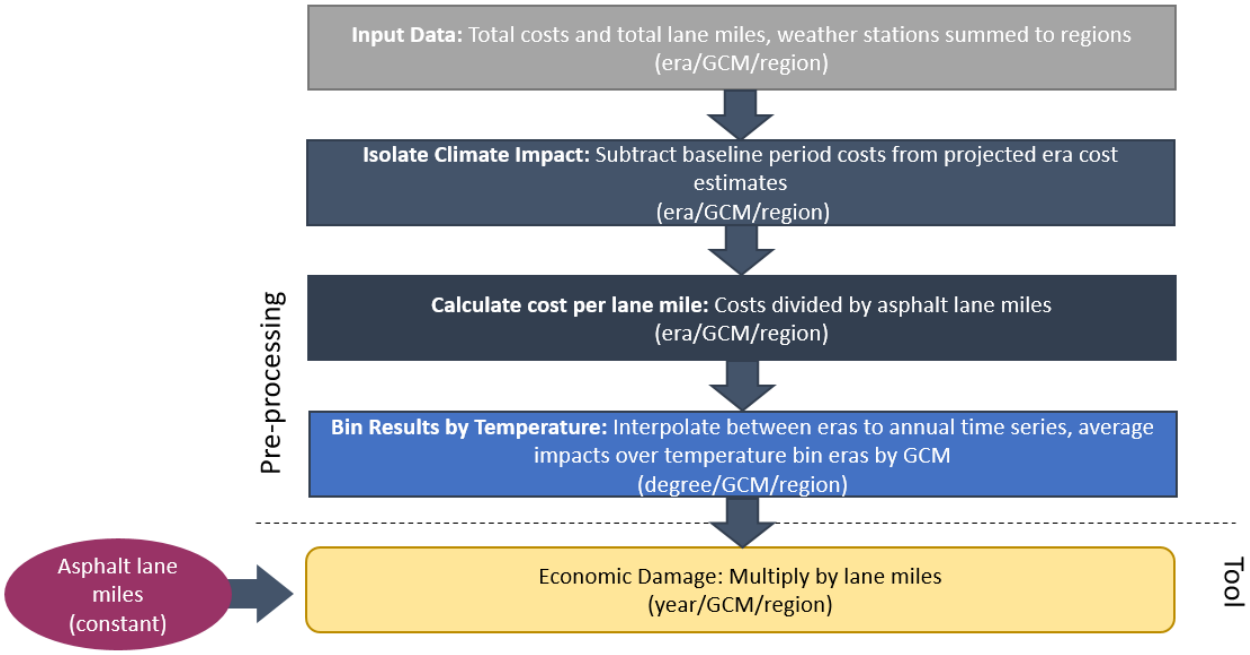

Limitations and Assumptions

- The underlying study uses a different set of climate projections (Climate Analytics Group) from most of the sectors that use LOCA, and a different baseline. While using a difference from the baseline and adjusting temperature arrival times is an attempt to correct any bias introduced, it is possible that these different climate projections and differences in the baseline create inconsistencies between this non-CIRA sector and other CIRA sectors.
- The underlying study includes a suite of 19 climate models, three of which are part of the CIRA suite of GCMs (CanESM2, CCSM4, and MIROC5). These three models reach warmer temperatures more quickly than the average across all 19 models in Underwood et al. (2017), and thus result in a higher average estimate of damages compared to the results presented in the paper. However, compared to the full suite of 38 CMIP5 GCMs, the three models are relatively close to the median temperature change values in 2090.
- The model references, but does not quantify, impacts of a proactive adaptation scenario. Therefore, uncertainty exists in how the modeled maintenance costs may be reduced as a result of adaptive actions or technologies.
- For further discussion of the limitations and assumptions in the underlying sectoral model see Underwood et al. (2017).

Urban Drainage

This sector study estimates the costs of proactive adaptation for urban drainage systems in 100 major coastal and non-coastal cities of the contiguous U.S. to meet future demands of increased runoff associated with more intense rainfall under climate change.

UNDERLYING DATA SOURCES AND LITERATURE

Price, J., Wright, L., Fant, C., & Strzepek, K. (2014). Calibrated Methodology for Assessing Climate Change Adaptation Costs for Urban Drainage Systems. Urban Water Journal, 13 (4), 331-344. Doi:10.1080/1573062X.2014.991740

Adaptive actions focus on the use of best management practices to limit the quantity of runoff entering stormwater systems and maintain current level of service (i.e., proactive adaptation to avoid damages), instead of expanding formal drainage networks of basins and conveyance systems. These best management practices generally include temporary storage above or below ground (e.g., bioswales, retention ponds), or infiltration (e.g., permeable pavement), and are based on EPA guidelines and construction cost estimates (see Price et al., 2014 for additional details).

Specifically, the analysis uses a reduced-form approach for projecting changes in flood depth and the associated costs of flood prevention under future climate scenarios, based an approach derived from EPA's Storm Water Management Model (SWMM). The approach assumes that the systems are able to manage runoff associated with historical climate conditions and estimates the costs of implementing the adaptation measures necessary to manage increased runoff due to climate change. Impacts are estimated in units of average adaptation costs per square mile for a total of 100 cities across the contiguous U.S. for three categories of 24-hour storm events (those with precipitation intensities occurring every 10, 25, and 50 years—metrics commonly used in infrastructure planning) and four future eras periods: 2030 (2020-2039), 2050 (2040-2059), 2070 (2060-2079), and 2090 (2080-2099). A summary of results by temperature bin degree is included in **Figure B-23** below. Note that urban drainage impacts by degree are constant throughout the century, therefore only one set of impacts is shown in the figure.

FIGURE B-23. URBAN DRAINAGE IMPACTS BY TEMPERATURE BIN DEGREE

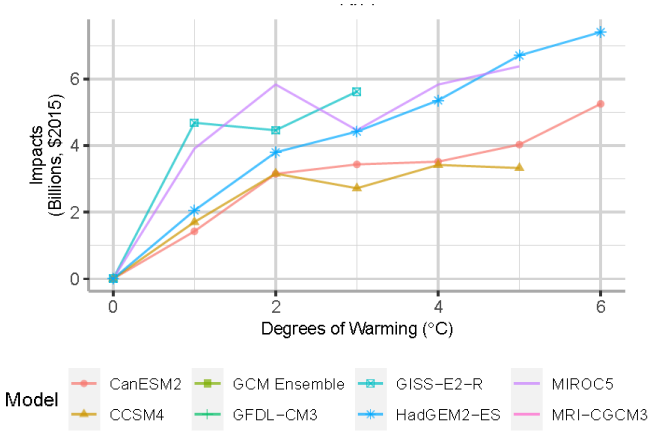

Processing steps

Processing steps are seen in **Figure B-24**. First, the adaptation costs per square mile (weighted by area) for the 50-year storm for each GCM, city, scenario, and era combination, are aggregated to the regions used in NCA4 (and the Temperature Binning Tool).[16] Unlike most other underlying studies, the Urban Drainage study does not produce an annual time series of results, due in part to the impact of extreme events which are not well-characterized at an annual scale. The binning process requires an annual time series from which the 11-year windows of damages corresponding to each integer degree arrival by GCM can be pulled; therefore, linear interpolation is used to create an annual time series of values for each GCM, scenario, and region combination for the period 1995-2099, using the known damage values at each of the four eras. Values are extrapolated for 2090-2099 using the linear trend observed between the 2070 and 2090 eras, and values for years prior to 2030 are estimated by using 1995 as a baseline year; i.e., impacts are assumed to be zero in 1995 and results are interpolated linearly between 1995 and 2030. Finally, impacts are binned by integer degrees of warming for each GCM, scenario, and region combination. No physical or economic scaling is required since analytic results are scaled to the NCA region level in Step 2.

FIGURE B-24. URBAN DRAINAGE DATA PROCESSING FRAMEWORK

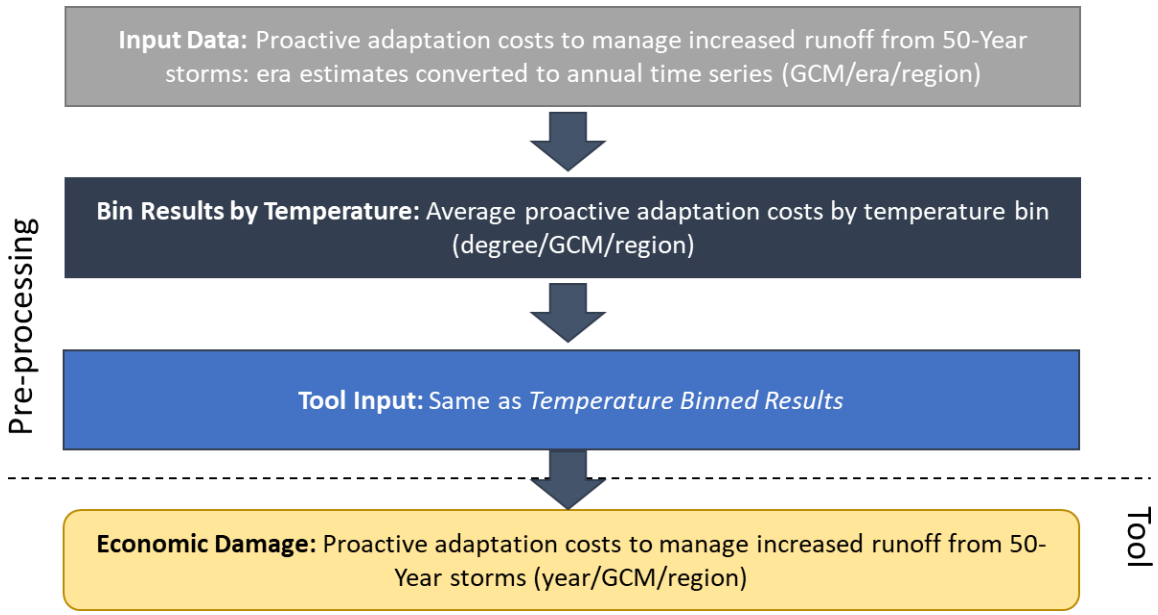

Limitations and Assumptions

- The underlying analysis assumes that the systems are able to manage runoff associated with historical climate conditions and estimates the costs of implementing the adaptation measures necessary to manage increased runoff due to climate change.

[16] For example, for a region with 2 cities, each with an area of 100 square miles, each city's area is divided by the sum of the areas, resulting in a proportion value of 0.5 for each city. This proportion value is then multiplied by each calculation of per-square-mile adaptation costs (calculated by storm, scenario, and year) to produce a weighted average adaptation cost per square mile. Note that the intensity/size of the 50-year storm varies with GCM, city, scenario, and era. The method yields changes in the absolute size of the storm over time and space, rather than the change in the frequency of the base period 50-year storm event.

- Inclusion of all U.S. cities with stormwater conveyance systems would provide a more comprehensive characterization of future impacts. The underlying study is limited to 100 major U.S. cities. Therefore the current estimates included for this sector represent underestimates of potential damages.
- For further discussion of the limitations and assumptions in the underlying sectoral model see Neumann et al. (2014), Price et al. (2014), and EPA (2017).

Inland Flooding

This sector study estimates the impact of riverine flooding attributable to climate change on property value.

UNDERLYING DATA SOURCES AND LITERATURE

Wobus, C.W., Porter, J., Lorie, M., Martinich, J., & Bash, R. (2021). Climate change, riverine flood risk and adaptation for the conterminous United States. Environmental Research Letters. doi: 10.1088/1748-9326/ac1bd7.

Wobus, C.W., Zheng, P., Stein, J., Lay, C., Mahoney, C., Lorie, M., Mills, D., Spies, R., Szafranski, B., & Martinich, J. (2019). Projecting Changes in Expected Annual Damages From Riverine Flooding in the United States. Earth's Future, 7(5), 516-527. Doi:10.1029/2018EF001119

The analysis uses change in expected annual damage (EAD) from flooding at each property in the United States under different temperature scenarios to value riverine flood impacts. The underlying data considers flooding for return intervals of two years through 500 years. Study authors calculate a frequency-loss curve for each property and integrate under the curve between flood frequencies of 0.0001 and 0.10 to calculate the EAD. The data excludes flooding events associated with urban drainage, quantifying only riverine floods instead. As a result, this sector does not account for all flooding events in cities and other urban areas; pluvial floods (associated with localized high rainfall events) are assessed in the *Urban Drainage* sector. The method applied estimates the baseline annual EAD using current structure characteristics (e.g., ground level floor elevation[17], replacement cost, market value), the flood depths associated with baseline conditions for varying return periods[18], and depth-damage functions available from FEMA's HAZUS documentation.[19] The underlying study model provides estimates of projected property damage at multiple spatial scales – for this work, results were provided at the Census block group level; properties were grouped by Census block group and EAD values summed under baseline and future climate scenarios. Property values are held constant over the course of the century, and impacts are projected under a "no adaptation" scenario.

[17] These characteristics were made available to the study team by the First Street Foundation. Details of the dataset are provided in: First Street Foundation, 2020a. The First National Flood Risk Assessment: Defining America's Growing Risk. Available at https://assets.firststreet.org/uploads/2020/06/first_street_foundation__first_national_flood_risk_assessment.pdf

[18] Details of the "current climate" baseline flood risk modeling can be found in First Street Foundation, 2020b. First Street Foundation Flood Model: Technical Methodology Document. Available: https://assets.firststreet.org/uploads/2020/06/FSF_Flood_Model_Technical_Documentation.pdf

[19] FEMA, undated. Multi-hazard Loss Estimate Methodology: Flood Model Technical Manual. https://www.fema.gov/sites/default/files/2020-09/fema_hazus_flood-model_technical-manual_2.1.pdf

Figure B-25 provides a summary of national impacts by integer degrees of warming for an averaged GCM ensemble at the endpoints of the socioeconomic scenarios; 2010 and 2090.

FIGURE B-25. INLAND FLOODING IMPACTS BY TEMPERATURE BIN DEGREE

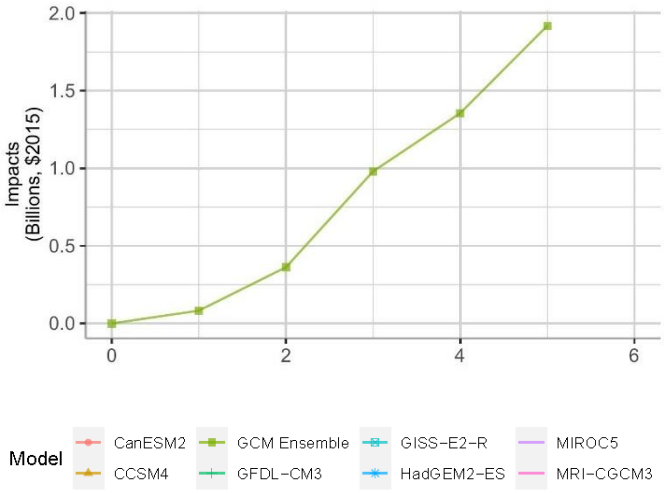

Processing steps

Processing steps are shown in **Figure B-26.** Study authors provided impacts by degree by Census block group, as well as baseline EAD for the period 2001-2020. Impacts are averaged for one "GCM Ensemble", which includes fourteen models: ACCESS1-0, CanESM2, CESM1-CAM5, CMCC-CM, CSIRO-Mk3-6-0, FGOALS-g2, GFDL-CM3, HadGEM2-AO, HadGEM2-CC, HadGEM2-ES, IPSL-CM5B-MR, MIROC-ESM-CHEM, MIROC-ESM, and NorESM1-M. In the underlying study, authors use the projected hydrology for each climate model to extract an annual maximum flow timeseries for a 20-year window centered on the year that the model reaches temperature thresholds of 1°C through 5°C above the 2001-2020 baseline.

The first processing step was to sum block group damages to regional damages. Next, the baseline EAD was subtracted from projected EAD by degree to isolate impacts attributable to climate change. Finally, values were adjusted from 2020 dollars to 2015 dollars.

FIGURE B-26. INLAND FLOODING DATA PROCESSING FRAMEWORK

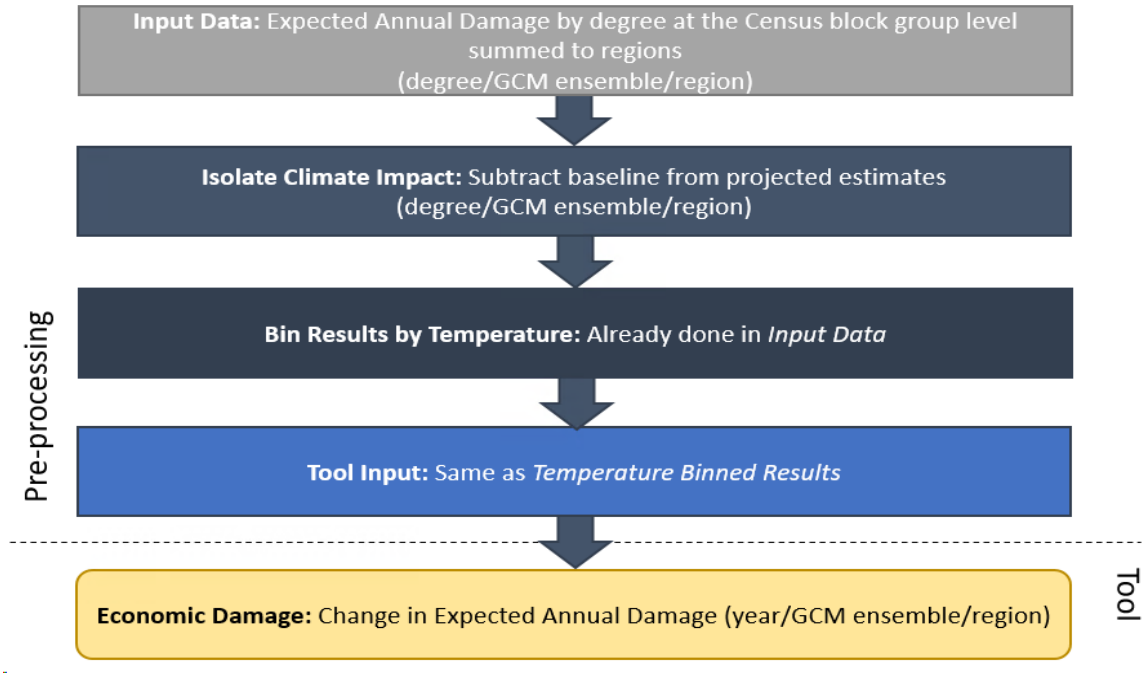

Limitations and Assumptions

- The analysis does not evaluate the potential for adaptation measures to mitigate flood risk at the property or community levels.
- The analysis does not account for changes in population and development within flood risk zones. Without a reasonable method to predict future floodplain development or policies governing development, these factors are held constant.
- This analysis relates increases in CONUS temperatures to changes in economic impacts of riverine floods. While climate science indicates that warming temperatures accelerate the hydrologic cycle, which in turn increase river flows, changes in near-surface temperatures do not necessarily characterize local or regional precipitation changes, or river flows, with a consistent signal. Local precipitation changes may also be correlated with other drivers that are not necessarily well correlated with CONUS or regional scale temperature changes, e.g., the El Nino Southern Oscillation (ENSO). The study used here, however (Wobus et al., 2021) finds a monotonic trend of increases in the economic impact of floods at the regional scale (aggregated from the property level) as regional scale temperatures rise, supporting the relationship between U.S. regional temperature changes and flood impacts.
- For further discussion of the limitations and assumptions in the underlying sectoral model see Wobus et al. (2021) and Wobus et al. (2019).

Hurricane Wind Damage

UNDERLYING DATA SOURCES AND LITERATURE

Dinan, T., (2017). Projected increases in hurricane damage in the United States: the role of climate change and coastal development. Ecol. Econ. 138: 186–198. https://doi.org/10.1016/j.ecolecon.2017.03.03.

Congressional Budget Office (CBO). (2016). Potential Increases in Hurricane Damages in the United States: Implications for the Federal Budget. Washington, DC. June 2016

Marsooli, R. Lin, N., Emanuel, K., Feng, K. (2019). Climate change exacerbates hurricane flood hazards along US Atlantic and Gulf Coasts in spatially varying patterns. Nature Communications. https://doi.org/10.1038/s41467-019-11755-z

This sector study estimates the impact of changes in the frequency of hurricane strength wind damage to coastal properties. The results are primarily based on analysis by Dinan (2017), which projects hurricane damage from both wind and storm surge to properties in the Gulf and Atlantic coast states using a proprietary model developed by the firm Risk Management Solutions (RMS). Dinan (2017) projected changes in future hurricane frequency by hurricane category (Saffir-Simpson scale of Category 1 to Category 5) using a Monte Carlo aggregation of results from Emanuel (2013) for RCP8.5 and Knutson (2013) for RCP4.5.[20] The hurricane projections used in Dinan (2017) do not readily convert to an impact-by-degree warming indexing, so as part of processing this analysis instead relies on results from more recent Marsooli et al. (2019) study which provides change in return periods, maximum wind speed, and Category 5 storm frequency for the a late century period using an updated version of the Emanuel (2013) model, to project future hurricane activity by degree of warming for a set of GCMs. Further, because the detailed spatial and climate stressor specific results are not publicly accessible, we worked with Dinan, RMS, and other publicly available data to generate an estimate of damages attributable to climate change induced changes in wind damage to properties. Results by degree of warming are shown in **Figure B-27** below.

[20] See Emanuel, K., 2013. Downscaling CMIP5 climate models shows increased tropical cyclone activity over the 21st century. Proc. Natl. Acad. Sci. 110 (30), 12219–12224, and Knutson, T., et al., 2013. Dynamical downscaling projections of twenty-first-century Atlantic hurricane activity: CMIP3 and CMIP5 model-based scenarios. J. Clim. 26 (17), 6591–6617.

FIGURE B-27. HURRICANE WIND DAMAGE IMPACTS BY TEMPERATURE BIN DEGREE BY GCM

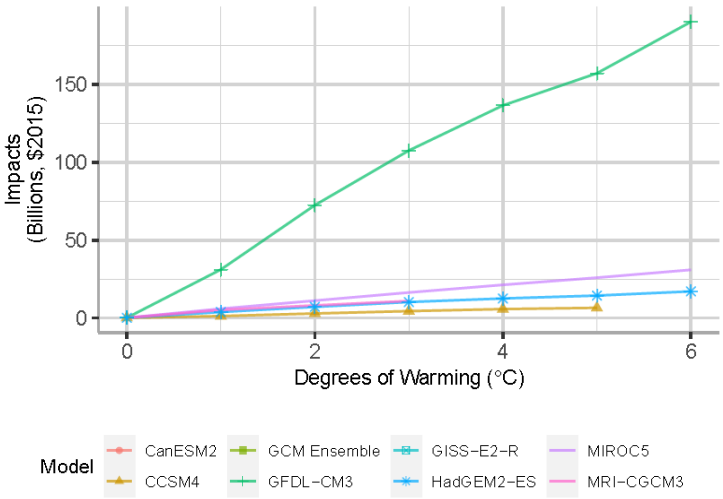

Processing steps

Three data processing steps are used to develop estimates suitable for use in FrEDI: 1. Estimating baseline expected annual wind damage to exposed properties; 2. Projecting changes in wind profile as a result of climate change; 3. Estimating economic damage from the change in wind profile from baseline to future periods.

Baseline wind damage is calculated by parsing Dinan's total hurricane damage by state, reported in CBO (2016), into wind and storm surge components by state, using data on the ratio of wind to storm surge damage by state provided by the author (with permission from RMS). Wind damages by state are then allocated to the county scale by using weights derived from the National Coastal Property Model for county-level storm surge damage attributed to hurricanes in the year 2000 (base year with no SLR). This allocation method assumes that storm surge and wind damage are correlated but exclude some non-coastal inland counties which might be expected to incur wind damage (albeit with significant decay of wind speed relative to coastal counties).

Wind profile changes are projected using estimates reported in Marsooli et al. (2019), which provides gridded estimates of the max wind speed and frequency of the 90th percentile event from an ensemble of simulated tropical cyclones for the Gulf and Atlantic Coasts for both the baseline of 1980–2005 to the future period of 2070–2095. The grid-cell results are spatially reaggregated to coastal counties. Future damages are projected using ratios of future damage to baseline damage for each coastal county that employ a logistic function proposed by Emanuel et al. (2012) for the baseline and each of six GCMs evaluated in Marsooli et al. (2019). These ratios are then applied to the baseline damage estimated above, and baseline damages are subtracted to estimate future damages attributed to climate change. Damages by degree aggregated at the region level are estimated as a linear function of warming for each of the relevant GCMs. B-The results indicate good agreement for four of the five models, with the fifth (GFDL) showing much higher damages than the other four. We considered applying skill weighting of the GCMs

using weights provided in Marsooli et al. (2019) – the results using skill-weighting down-weight GFDL relative to other models, reducing the mean damages across all GCMs by about one-third – but the skill weights were calculated for wind speed rather than damage (damage is a non-linear logistic function of wind speed, capped at the high end by total structure value). The non-skill weighted results are used here for consistency with other sectoral analyses.

FIGURE B-28. HURRICANE WIND DAMAGE IMPACT PROCESSING FRAMEWORK

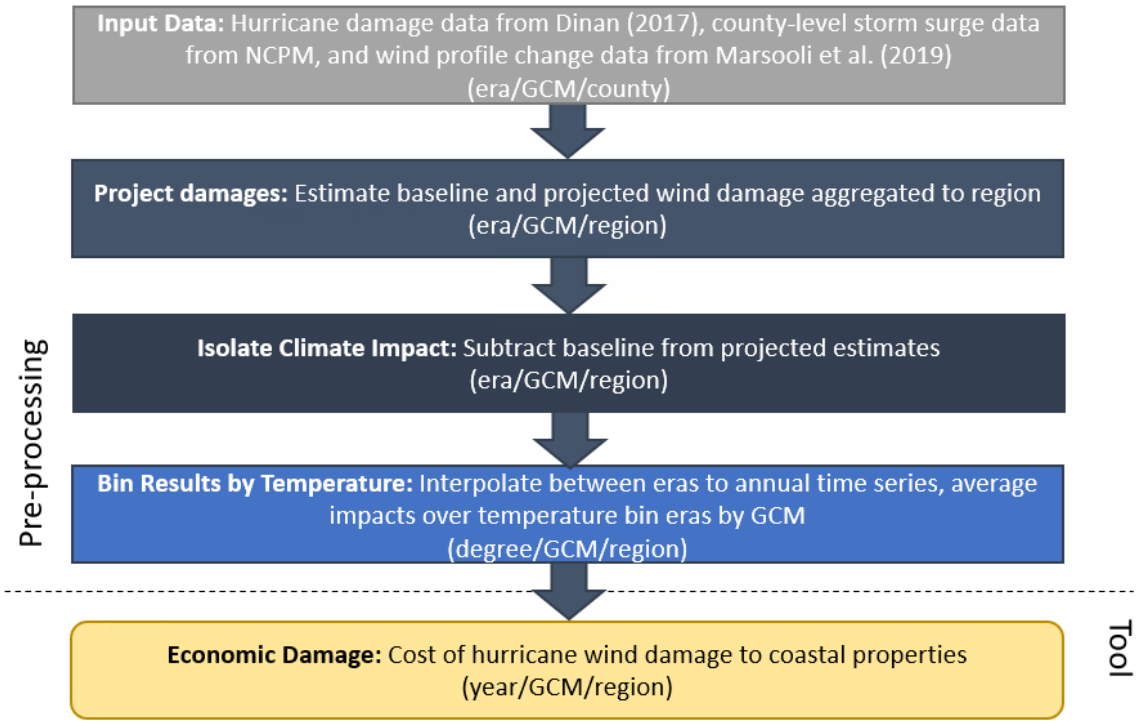

Limitations and Assumptions

- Hurricanes are relatively rare extreme events and are observed infrequently, which both limits the observed damage data on which estimates can be based and complicates estimates of projected hurricane activity. The Marsooli et al. (2019) study used here employs a well-regarded model of projected hurricane activity which provides results needed to estimate projected damages on a spatially disaggregated basis, but other models could yield different results.
- The underlying economic impact study relies on a proprietary model of hurricane wind and storm surge damages; the detailed county and scenario specific results from the model are not available for use in the Framework. The published results are therefore disaggregated from publicly available total estimates into storm surge and wind using storm surge estimates from the Coastal Properties sector. This procedure ensures that damage estimates are not double-counted, but introduces error and uncertainty in the estimates used here.
- Results from the underlying study were made available only at the state level, but analyses of projected storm surge damages are at the county level, and estimates of future hurricane activity

are at a grid cell level. Adjustments made for spatial mismatches also introduce error and uncertainty in the estimates used here.

- This analysis interpolates linearly between the baseline period and late century (2070-2095) projection with no intermediate damage estimates, so mid-century values are less precise than other sectors.
- For further discussion of the limitations and assumptions in the underlying sectoral model see Dinan et al. (2017) and Marsooli et al. (2019).

B.4 Water Resources Sectors Data Processing

Water Quality

This analysis estimates damages in terms of the change in willingness to pay to avoid changes in water quality. This analysis estimates climate change effects on water quality at the eight-digit HUC scale of the contiguous U.S. using the Hydrologic and Water Quality System (HAWQS) biophysical model. Note that the damages estimated for this sector only cover the change in value of recreation opportunities and do not include the value of health effects or other amenities associated with clean water.

UNDERLYING DATA SOURCES AND LITERATURE

Fant, C., Srinivasan, R., Boehlert, B., Rennels, L., Chapra, S. C., Strzepek, K. M., Corona, J., Allen, A., & Martinich, J. (2017). Climate change impacts on US water quality using two models: HAWQS and US Basins. Water, 9(2), 118. Doi:10.3390/w9020118

Boehlert, B., Strzepek, K. M., Chapra, S. C., Fant, C., Gebretsadik, Y., Lickley, M., Swanson, R., McCluskey, A., Neumann, J., & Martinich, J. (2015). Climate change impacts and greenhouse gas mitigation effects on US water quality. Journal of Advances in Modeling Earth Systems, 7, 1326-1338. Doi:10.1002/2014MS000400

Yen, H., Daggupati, P., White, M. J., Srinivasan, R., Gossel, A., Wells, D., & Arnold, J. G. (2016). Application of large-scale, multi-resolution watershed modeling framework using the hydrologic and water quality system (HAWQS). Water, 8(4), 164. Doi:10.3390/w8040164

HAWQS advances the functionality of the widely used and accepted Soil and Water Assessment Tool (SWAT), providing a platform for water quality modeling, primarily by minimizing the necessary initialization time. Originally developed by the U.S. Department of Agriculture (USDA), SWAT has been the core simulation tool for numerous U.S. national and international assessments of soil and water resources. The use of HAWQS over SWAT improves the ease of application to national scale analyses while still simulating a large array of watershed processes for a defined period of record.

The HAWQS model follows a broad modeling sequence: (1) the landscape phase, where the primary processes are climate, soil water balance, nutrient and sediment transport and fate, land cover, plant growth, farm management, and (2) the main channel phase, where the main processes are river routing, and sediment and nutrient transport through the rivers and reservoirs.

The HAWQS model projects changes in water quality parameters and simulated changes in river flow for five climate models under RCP8.5 and RCP4.5. These projections include future municipal wastewater treatment plant loadings (point source) scaled to account for population growth. Changes in overall water quality are estimated using changes in a Climate-oriented Water Quality Index (CWQI), a metric that combines multiple pollutant and water quality measures. Four water quality parameters (water temperature, dissolved oxygen, total nitrogen, and total phosphorus) are aggregated from the eight-digit HUC level to the Level-III Ecoregions, weighted by area.[21] Finally, a relationship between changes in the

[21] Designed to serve as a spatial framework for environmental resource management, ecoregions denote areas within which ecosystems (and the type, quality, and quantity of environmental resources) are generally similar. Ecoregions were originally created to support the development of regional biological criteria and water quality standards, and to set management goals for nonpoint source pollution.

CWQI and changes in the willingness to pay for improving water quality is used to estimate the economic implications of projected water quality changes. For more information on the approach and results for the water quality sector, please refer to Fant et al. (2017), Boehlert et al. (2015), and Yen et al. (2016). Specifically, impacts are estimated as per capita change in the willingness to pay to improve water quality for two future eras: 2050 (2040-2059) and 2090 (2080-2099). A summary of results by temperature bin degree in 2010 and 2090 (the endpoints of socioeconomic modeling) is included in **Figure B-29** below.

FIGURE B-29. WATER QUALITY IMPACTS BY TEMPERATURE BIN DEGREE

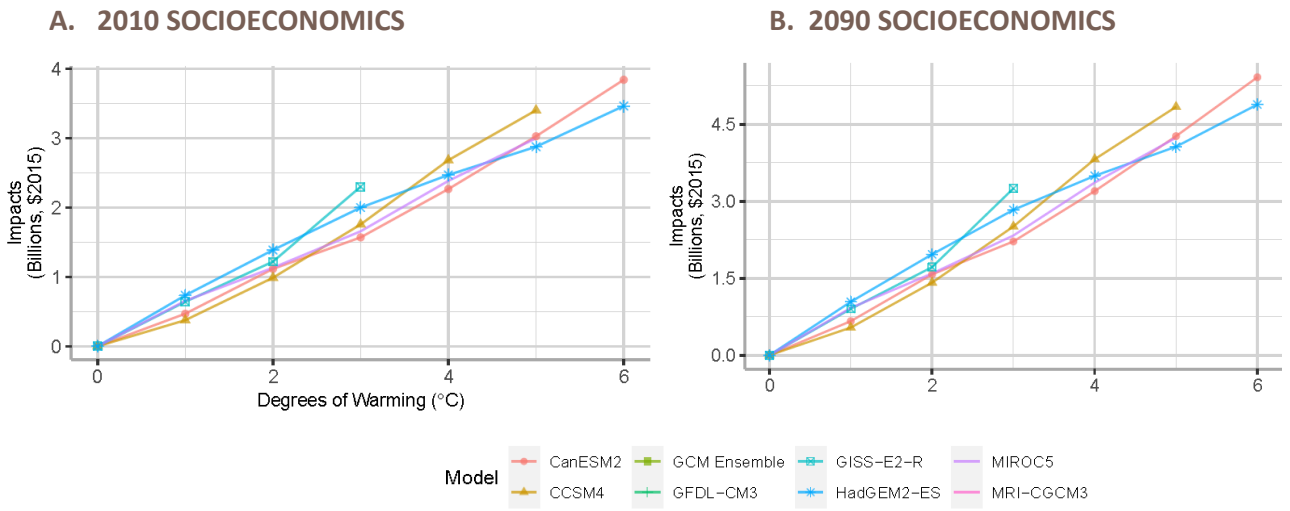

Processing steps

Processing steps are seen in **Figure B-30**. The per capita willingness to pay for each EPA Level 3 Ecoregion, GCM, and era combinations are first aggregated to the state-level and then to the regions used in NCA4 (and the Temperature Binning Tool). These climate change impacts are relative to a "control" scenario (one with socioeconomic growth and historical climate) to isolate the climate change impacts from the impacts of socioeconomic growth. Like the Urban Drainage sector described above, the Water Quality study also does not produce an annual time series of results. Therefore, an annual time series of damages needs to be constructed for each GCM and region combination based on available data (i.e., for the 2050 and 2090 eras). Linear interpolation is used to create an annual time series of values for each GCM and region combination for the period 1995-2099. Values are extrapolated for 2090-2099 using the linear trend observed between 2050 and 2090, and values for years prior to 2050 are estimated by using 1995 as a baseline year; i.e., impacts were assumed to be zero in 1995 and results are interpolated linearly between 1995 and 2050. Finally, impacts are binned by integer degrees of warming for each GCM and region combination. Impact estimates are calculated by applying regional population as a physical scalar.

FIGURE B-30. WATER QUALITY DATA PROCESSING FRAMEWORK

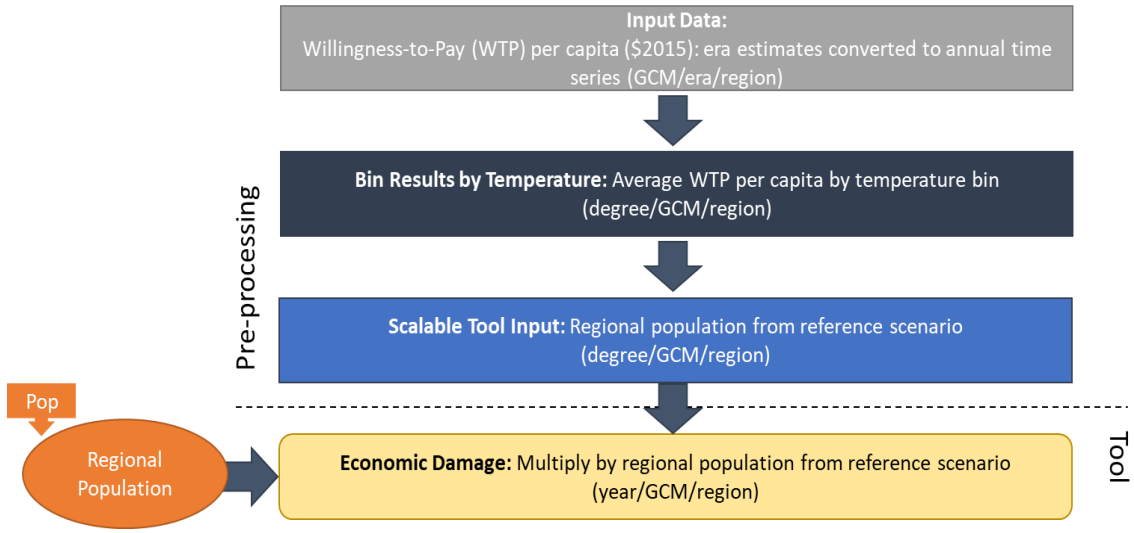

Limitations and Assumptions

- Decreases in water quality due to climate change will likely have adverse effects on human health and the environment that are not represented in the results of this section. For example, climate change impacts to water quality may affect ecological dynamics of freshwater systems, with cascading effects on ecosystem services and recreational opportunities.
- This analysis only considers four water quality parameters, and omits other constituents, such as sediment and heavy metals, that may be affected by changes in the climate system.
- The methods underlying the analysis do not consider the effects of climate change-induced extreme events on water quality, such as increased siltation and runoff following wildfire events.
- The analysis considers only a subset of all use/non-use values linked to water quality changes, therefore the damages reported here are likely underestimates of future impacts.
- By creating an annual time series for the period 1995 to 2100 based on values from 2050 and 2090 only, the Temperature Binning processing does not capture any non-linearities in the relationship between damages and temperature, particularly in the early years of the century.
- For further discussion of the limitations and assumptions in the underlying sectoral model, see Fant et al. (2017) and Boehlert et al. (2015).

Winter Recreation

This sector estimates lost revenue due to climate change to suppliers of three types of winter recreation occurring at 247 sites across the U.S.: alpine skiing, Nordic skiing, and snowmobiling.

Damages are based on the number of visits to winter recreational sites, entrance fees, and state-level

UNDERLYING DATA SOURCES AND LITERATURE

Wobus, C., Small, E. E., Hosterman, H., Mills, D., Stein, J., Rissing, M., Jones, R., Duckworth, M., Hall, R., Kolian, M., Creason, J., & Martinich, J. (2017). Projected climate change impacts on skiing and snowmobiling: A case study of the United States. Global Environmental Change, 45, 1-14. Doi:10.1016/j.gloenvcha.2017.04.006

average ticket prices. The model was run using both 2010 and 2090 ICLUSv2 population. A summary of results by temperature bin degree in 2010 and 2090 (the endpoints of socioeconomic modeling) is included in **Figure B-31**.

FIGURE B-31. WINTER RECREATION IMPACTS BY TEMPERATURE BIN DEGREE

A. 2010 SOCIOECONOMICS

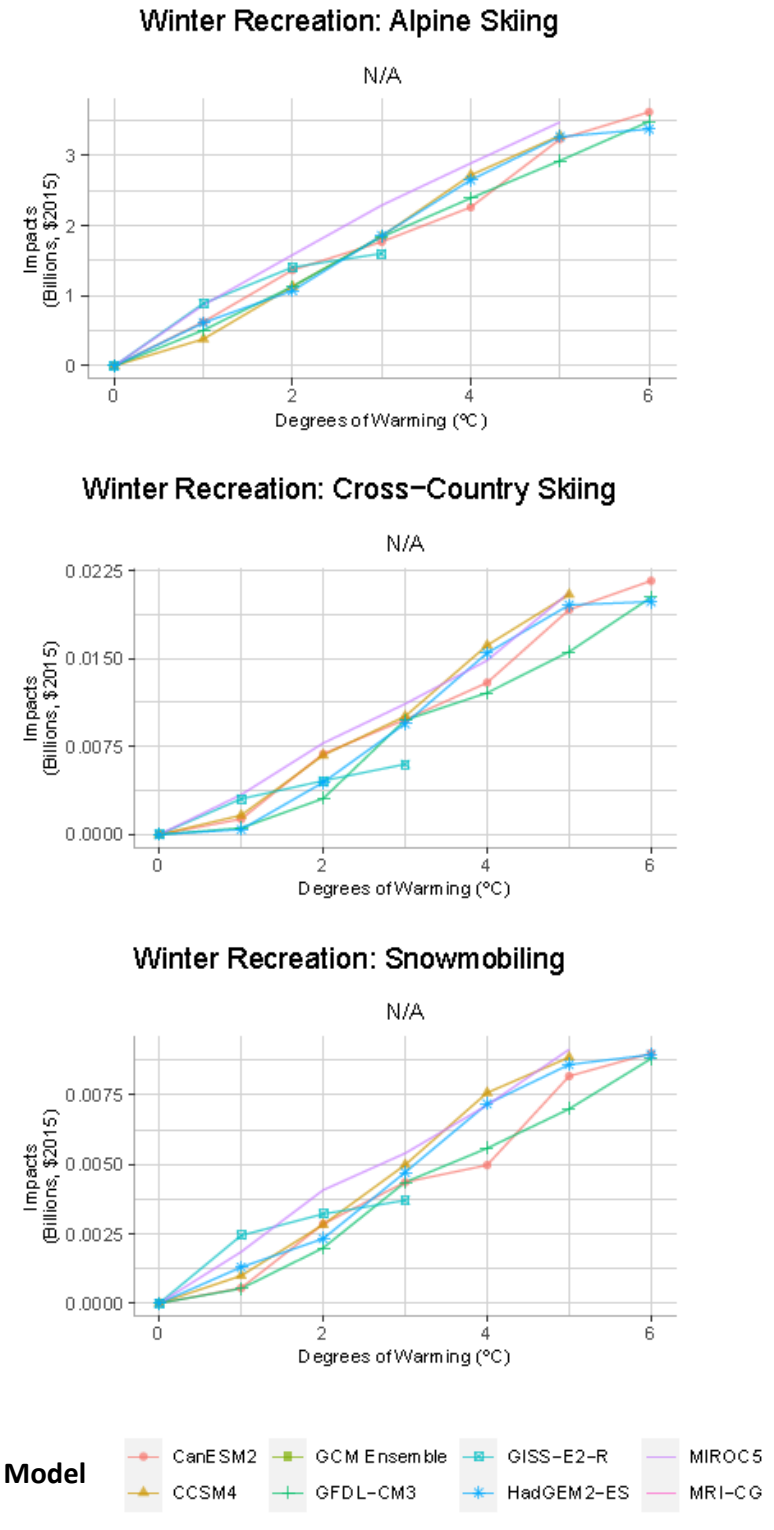

B. 2090 SOCIOECONOMICS

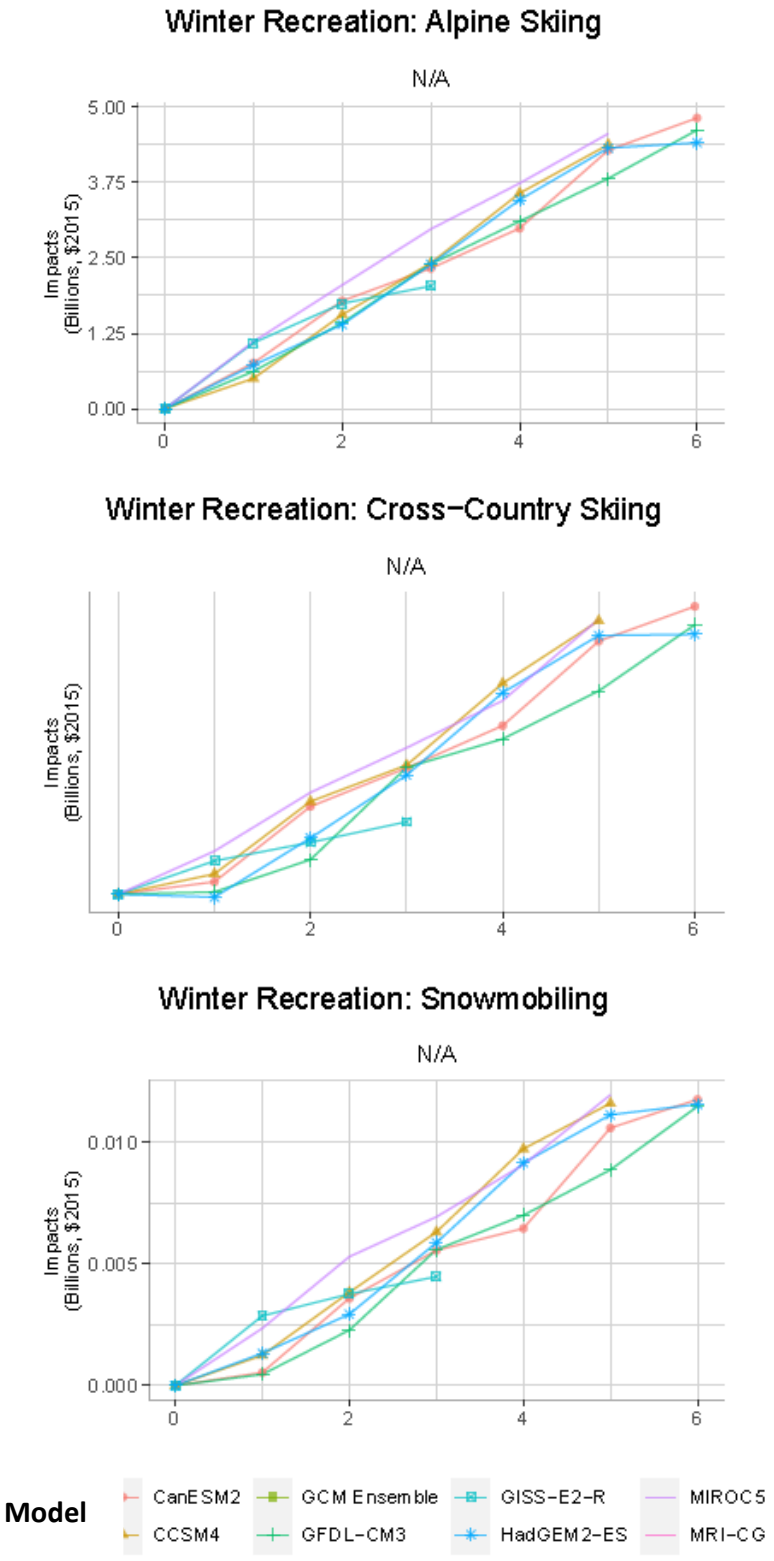

Processing steps

Processing steps are shown in **Figure B-32**. In step one, lost ticket sales are estimated across recreational activities (alpine skiing, Nordic skiing, and snowmobiling), GCMs, degrees, and regions, for both a 2010 and 2090 population.

In the second step, both the 2010 and 2090 regional estimates produced in step one are divided by regional population. Regional population estimates are based on ICLUSv2 population data. This produces a per capita estimate of forgone ticket sales for alpine skiing, Nordic skiing, and snowmobiling. The per capita cost estimates are multiplied against regional population to produce total lost revenue estimates.

FIGURE B-32. WINTER RECREATION DATA PROCESSING FRAMEWORK

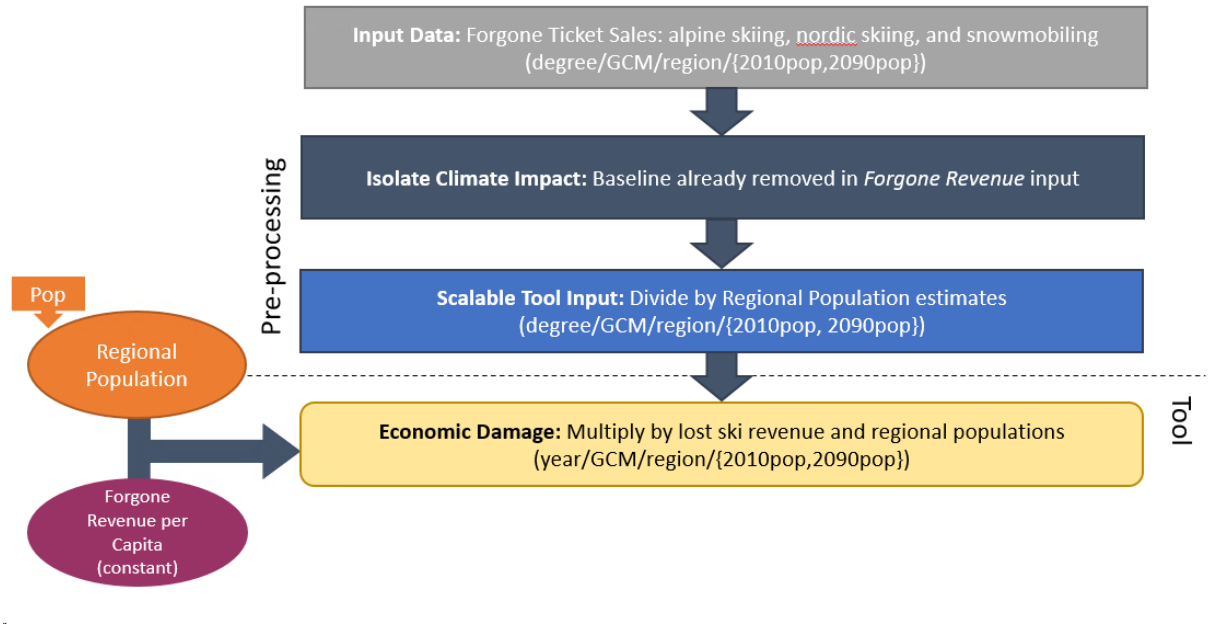

Limitations and Assumptions

- The scope of winter recreation loss for the tool is derived only from analysis of the alpine skiing, Nordic skiing, and snowmobile sub-sectors of the industry. Potential losses to other winter recreation activities (e.g., tubing) are not quantified in this study.
- Potentially compensating adaptations from the lost opportunity to engage in winter recreation (for example, with other forms of outdoor recreation, or with indoor recreation) are not considered.
- For further discussion of the limitations and assumptions in the underlying sectoral model, see Wobus et al. (2017) and EPA (2017).

B.5 Electricity Sectors Data Processing

Electricity Demand and Supply

This sector estimates increases in system costs to the power sector. These system costs include capital, fuel, variable operation and maintenance (O&M), and fixed O&M costs.

UNDERLYING DATA SOURCES AND LITERATURE

McFarland, J., Zhou, Y., Clarke, L., Sullivan, P., Colman, J., Jaglom, W. S., Colley, M., Patel, P., Eom, J., Kim, S. H., Kyle, G. P., Schultz, P., Venkatesh, B., Haydel, J., Mack, C., & Creason, J. (2015). Impacts of rising air temperatures and emissions mitigation on electricity demand and supply in the United States: a multi-model comparison. Climatic Change, 131, 111-125. Doi:10.1007/s10584-015-1380-8

Increased costs are based on projected changes in demand for and supply of electricity across generation types. Effects on energy demand reflect the net impact of increased demand for residential, commercial, and industrial space cooling during summer/warmer months, and decreased demand for space heating during winter/cooler months. Effects on supply reflect the decreased production capacity of thermal power plants, and transmission capacity of the transmission system, associated with higher temperatures.[22] The complex interplay of supply and demand, coupled with forecast changes in fuel and energy production technology availability and prices, are modeled using the Global Change Assessment Model (GCAM-USA), a detailed service-based building energy model with a 50-state domain.

Costs are provided for a static baseline run, in which climate is held as constant to the CIRA baseline while socioeconomic variables are dynamic, and a projection run in which both climate and socioeconomic variables are changing. Estimates of costs with- and without-climate change are provided in five-year intervals. A summary of results by temperature binning degree in 2010 and 2090 (the endpoints of socioeconomic modeling) is provided in **Figure B-33**.

FIGURE B-33. ELECTRICITY DEMAND AND SUPPLY IMPACTS BY TEMPERATURE BIN DEGREE

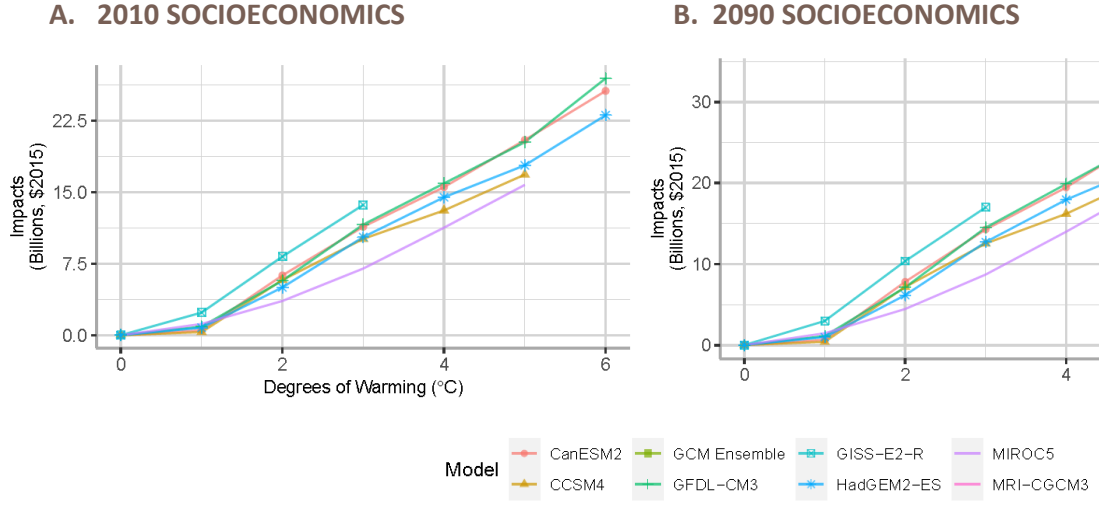

[22] Note that the transmission system effects in this sector are separate from those modeled in the Electricity Transmission and Distribution Infrastructure sector.

Processing steps

Processing steps for this sector are shown in **Figure B-34**. System costs for the power sector are provided for each GCM and a climate reference scenario for each region in 5-year intervals. Annual costs are interpolated between the 5-year interval data and costs are binned by degrees of warming for each GCM and region. To remove time dependencies, the final temperature binned estimates are the percentage change in costs from the reference scenario for each temperature bin, GCM, and region.

For a given input temperature trajectory, the percentage changes in system cost are multiplied by the reference scenario costs to produce total cost estimates across the century. That is, damages in a given year are dependent on warming, which maps a percentage change in costs from the reference scenario based on temperature binned damages, and the baseline system costs in the reference scenario for that year.

FIGURE B-34. ELECTRICITY DEMAND AND SUPPLY DATA PROCESSING FRAMEWORK

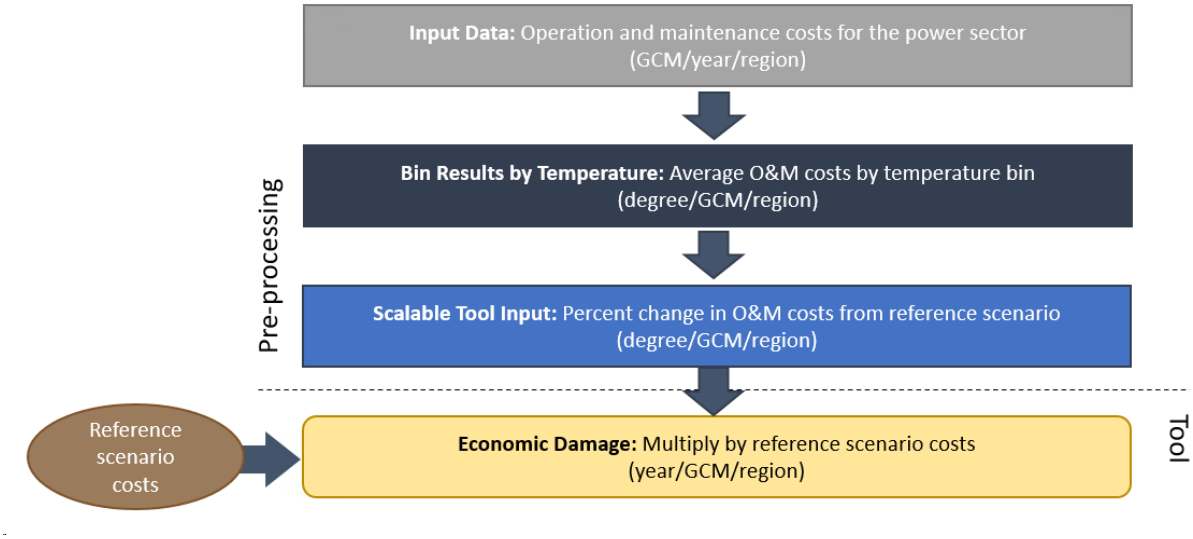

Limitations and Assumptions

- Projected changes in heating degree days (HDD) and cooling degree days (CDD) are based on a temperature set-point of 65°F, a common convention that may lead to a conservative energy demand estimate.
- The temporal aggregation of the underlying electricity supply model is too coarse to assess the impact of extreme temperature events that occur on only the very hottest days of the year. As a result, the underlying study focuses on a single aspect of climate change: average ambient air temperature, and therefore omits effects of extreme temperature effects on peak demands and the loads required to meet those changes. Effects from future changes in the frequency and magnitude of extreme temperatures may stress electric power systems, and these economic risks are not captured in this study.

- For further discussion of the limitations and assumptions in the underlying sectoral model, see McFarland et al. (2015).

Electricity Transmission and Distribution Infrastructure

UNDERLYING DATA SOURCES AND LITERATURE

Fant, C., Boehlert, B., Strzepek, K., Larsen, P., White, A., Gulati, S., Li, Y., & Martinich, J. (2020). Climate change impacts and costs to U.S. electricity transmission and distribution infrastructure. Energy, 195. Doi:10.1016/j.energy.2020.116899

This analysis estimates damages to the electric transmission and distribution infrastructure due to climate change. This multi-dimensional analysis considers a wide range of climate stressors, including extreme temperature, extreme rain, lightning, vegetation growth, wildfire activity, and coastal flooding. Impact receptors include transmission and distribution lines, poles/towers, and transformers.

Monetized damages for this sector are the costs of repair or replacement of damaged infrastructure. The impact model for this sector was run under two infrastructure system scenarios: one with expansion of infrastructure associated with demand growth, and one with static infrastructure. Increases in demand growth may be due to population growth, or increased demand due climatic change — in particular, warmer temperatures increase usage of air-conditioning. The model identifies changes in performance and longevity of physical infrastructure, such as power poles and transformers, and quantifies these impacts in economic terms. While certain climate stressors do cause power outages which have associated direct and indirect economic costs, these damages are not included in damage estimates.

Like other infrastructure sectors, the analysis is based on three adaptation scenarios. These include proactive adaptation, reactive adaptation, and no adaptation. Repair costs are also allocated based on the activity being performed. These activities include transmission line capacity, wildfire repair, tree trimming, substation seB-level rise, substation storm surge, wood pole decay, transmission transformer lifespan, and distribution transformer lifespan. **Figure B-31** below provides a summary of the results by temperature binning degree and adaptation scenario in 2010 and 2090 (the endpoints of socioeconomic modeling).

FIGURE B-35. ELECTRICITY TRANSMISSION AND DISTRIBUTION INFRASTRUCTURE IMPACTS BY TEMPERATURE BIN DEGREE

A. 2010 SOCIOECONOMICS

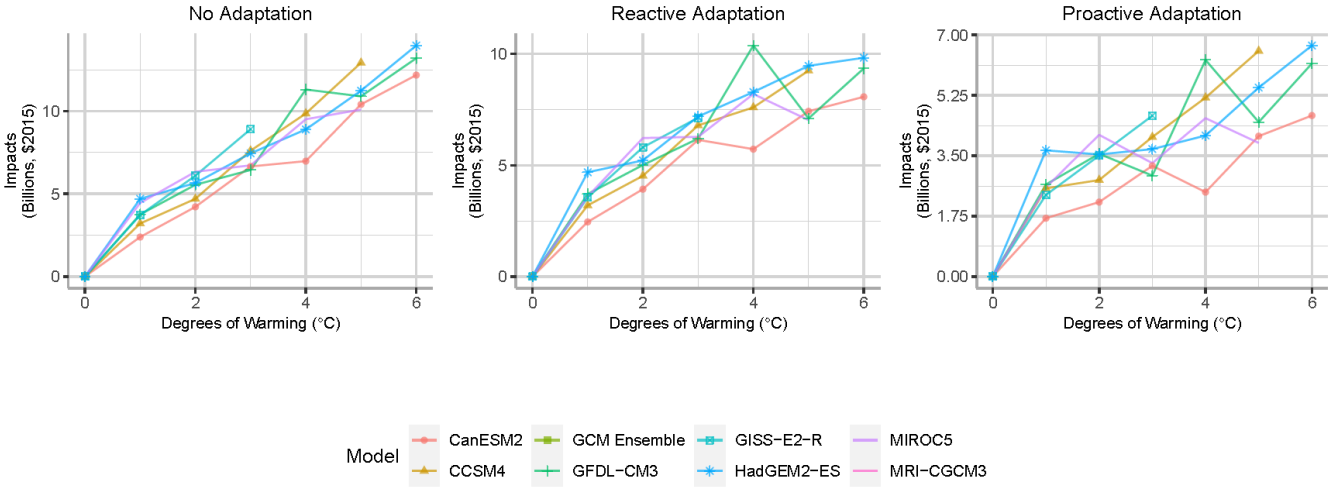

B. 2090 SOCIOECONOMICS

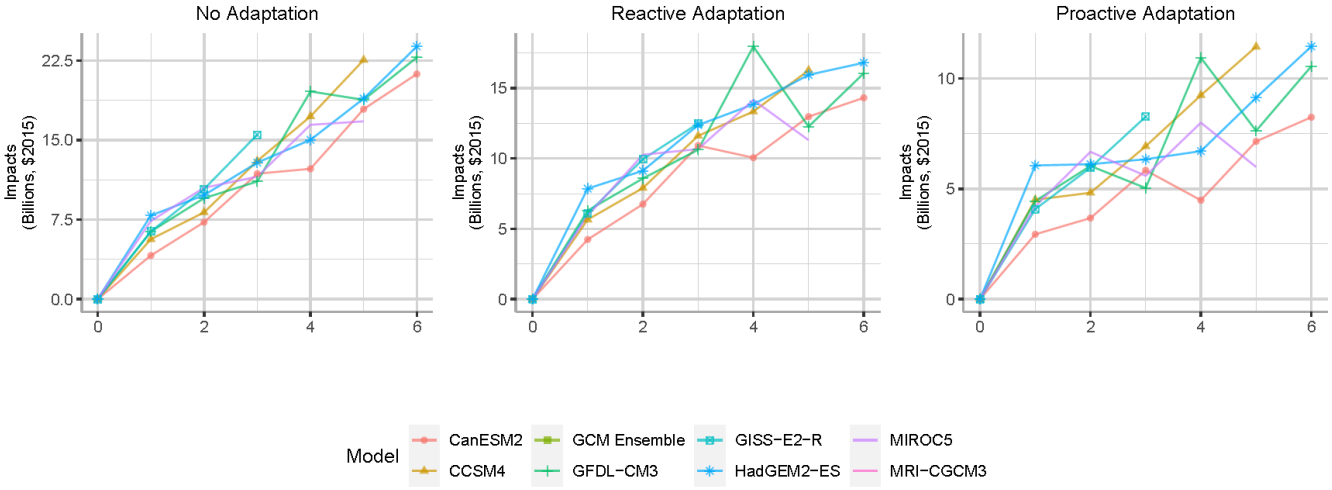

Processing steps

Processing steps are seen in **Figure B-36**. The underlying impact model produces damage estimates for each infrastructure type, GCM, and adaptation scenario. There are nine infrastructure types, seven of which grow with electricity demand. Therefore, damage estimates for these seven infrastructure types are influenced by both population and climate. To isolate damages associated with warming, damages associated with static demand are scaled by growth of demand attributable to warming. Demand attributable to warming is calculated based on the percentage increase in demand across the century for each GCM from a baseline demand across the century with a constant climate, as seen in **Figure B-37**.

After damages associated with climate driven infrastructure growth are calculated, results are aggregated for each GCM, infrastructure type, degree, and region combination. These costs are calculated for each adaptation scenario. Costs are then aggregated from individual infrastructure types to the sector total.

A population driven demand scalar is implemented to account for increases in demand for the grid as population grows. Thus, final damage estimates include expansion of electric grid infrastructure associated with a warming climate and with population growth. Note that because these damage estimates rely on an empirical relationship between damages with and without infrastructure growth in the underlying impact model, these damage estimates cannot be adjusted for custom input population trajectories.

FIGURE B-36. ELECTRICITY TRANSMISSION AND DISTRIBUTION INFRASTRUCTURE DATA PROCESSING FRAMEWORK

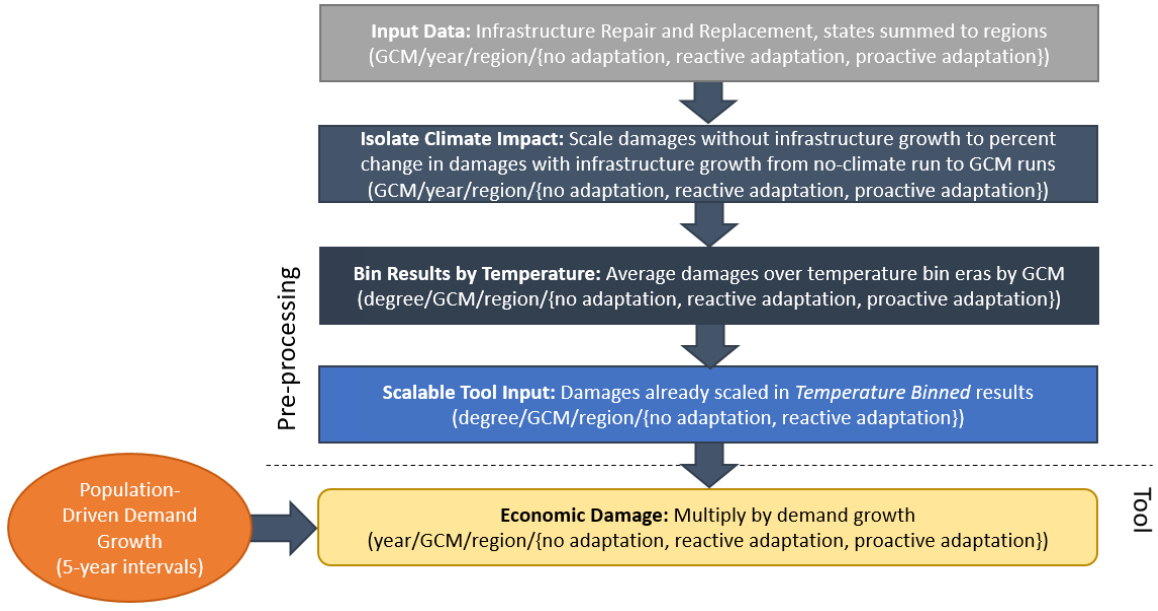

FIGURE B-37. ELECTRICITY TRANSMISSION AND DISTRIBUTION INFRASTRUCTURE DEMAND GROWTH SCALAR PROCESSING

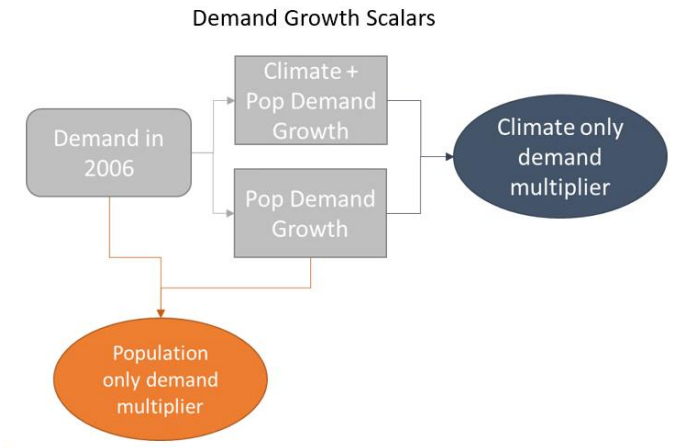

Limitations and Assumptions

- The model assumes that grid demand is controlled by population change and climatic factors; grid demand is assumed to not be influenced by economic growth. Future changes in the design and structure of electric grids are not considered in this study.
- Two of the nine infrastructure types considered in this study do not scale with changes in population; they are included in the overall results but not adjusted for population.
- For further discussion of the limitations and assumptions in the underlying sectoral model, see Fant et al. (2020)

APPENDIX C | EXAMPLE APPLICATION OF THE FREDI FRAMEWORK

This appendix presents example applications of FrEDI for evaluating impacts under a defined climate scenario and evaluating benefits of various emissions reduction scenarios compared to a reference scenario. The first section describes the emissions scenarios and climate models used to develop the global temperature trajectories evaluated in this example. The next section reports economic impacts associated with the temperature trajectories, following an evaluating in FrEDI. Finally, results are compared across scenarios to report the benefits of emissions reduction.

C.1 Climate Scenarios and Emissions Pre-processing

FrEDI requires analysts to define a temperature trajectory (global or CONUS), although many analyses may start from emissions trajectories. Analysts can use a variety of climate models to convert emissions scenarios into temperature trajectories. In this example, we use Hector, an open-source, object-oriented, reduced-form global carbon-cycle climate model (Hartin et al., 2015) to model temperatures associated with emissions scenarios from the Global Change Analysis Model v5.3 (GCAM). This step is not considered a part of the FrEDI framework, as analysts can use any model to process emissions scenarios.

Description of Hector

Hector, like other reduced form climate models, calculates concentrations of greenhouse gases from a given emissions pathway while modeling the carbon cycle and other gas cycles. Global emissions of greenhouse gases (CO_2, CH_4, N_2O, halocarbons) and aerosols (BC, OC, SO_2) are passed to Hector. Emissions are converted to concentrations where necessary and are used to calculate radiative forcing and then a global mean temperature change along with other Earth system variables (Hartin et al., 2015).

Hector has a three-part carbon cycle: atmosphere, land, and ocean. The atmosphere is treated as a single well-mixed box, where a change in atmospheric carbon is a function of anthropogenic fossil fuel and industrial emissions, land-use change emissions, and carbon fluxes between the atmosphere and ocean and the atmosphere and land. In Hector's default terrestrial carbon cycle, vegetation, detritus, and soil are linked to one another and to the atmosphere by first-order differential equations. Net primary production is a function of atmospheric CO_2 and temperature. Carbon flows from vegetation to the detritus and then down to soil, where some fraction is lost due to heterotrophic respiration.

The surface ocean carbon flux is dependent upon the solubility of CO_2 within high and low latitude surface boxes which are calculated from an inorganic chemistry submodule (Hartin et al., 2016). Hector calculates pCO_2, pH, and carbonate saturations in the surface boxes; once carbon enters the surface boxes, it is circulated through the intermediate and deep ocean layers via water mass advection and exchanges, simulating a simple thermohaline circulation.

Radiative forcing is calculated from each individual atmospheric constituent; CO_2, halocarbons, non-methane volatile organic carbons (NMVOCs), black carbon, organic carbon, sulfate aerosols, CH_4,

and N_2O, and forcing from tropospheric ozone and stratospheric water vapor. CO_2, CH_4, N_2O, and halocarbons are converted to concentrations, while NMVOC, and aerosols are left as emissions (Hartin et al., 2015).

Global atmospheric temperature is a function of a user-specified climate feedback parameter, which represents the equilibrium climate sensitivity for a doubling of CO_2 concentrations, total radiative forcing, and oceanic heat flux. Atmosphere–ocean heat exchange in Hector consists of a one-dimensional diffusive heat and energy-balance model, DOECLIM (Kriegler 2005; Vega-Westhoff et al., 2019). The code and detailed documentation can be found at https://jgcri.github.io/hector/

Description of GCAM

The Global Change Analysis Model v5.3 (GCAM) is an open source model that represents the linkages between energy, water, land, climate and economic systems (Calvin et al., 2019). GCAM is a market equilibrium model, global in scale and subdivided into 32 geopolitical energy and economic regions and 283 agriculture and land-use regions. GCAM is calibrated to a historical base year of 2010 and projects key variables forward in time through 2100. GCAM is a partial equilibrium model, representing the supply, demand and price for a variety of goods and services in the energy, agriculture and water sectors. A more complete documentation of GCAM is available at http://jgcri.github.io/gcam-doc/toc.html

Prices of energy, agriculture, and forest products are adjusted until supply and demand are in equilibrium. As a dynamic-recursive model, decision-makers base decisions on present prices assuming they will remain constant at those levels indefinitely as investment choices are made. GCAM computes emissions of 16 gases and short-lived species (CO_2, CH_4, N_2O, F-gases, SO_2, BC, OC, NOx, CO, NMVOCs) from a variety of human activities. These emissions are passed to a simple climate model, Hector, to calculate global mean temperature among other climate variables.

Description of climate scenarios used in this case study

This technical documentation provides a case study to illustrate the function and capabilities of FrEDI. The scenarios used in this case study are illustrative in nature and do not represent any actual policies or programs at domestic or international levels.

The GCAM v5.3 reference used in this case study represents a scenario with no additional future climate policies (for more information on GCAM see Calvin et al., 2019 and JGCRI 2020). When the emissions are run through Hector with an equilibrium climate sensitivity of 3°C the end of century radiative forcing is 4.66 Wm^{-2} and global mean temperature is 2.69 °C relative to a 1986-2005 baseline. Comparing the GCAM reference to EIA projections, GCAM fossil fuel and industrial CO_2 emissions are up to 2 GtC higher in 2025.[23]

[23] World carbon dioxide emissions by region:

For the emission reduction scenario used in this case study, CO_2 emission reductions were linearly interpolated between 2025 and 2100 based on the GCAM reference 2100 CO_2 emissions and run through Hector v2.5. Reductions begin in the next time step after 2025 (i.e., 2026). Only CO_2 emissions from fossil fuel and industry are reduced, not land use change emissions or other GHGs. The scenarios represent a reduction in emissions by 90 percent in 2100. For all scenarios, equilibrium climate sensitivity was varied [2.0, 2.5, 3.0, 4.0, 5.0], with an ECS value of 3.0 C as the default Hector parameter.

Figure C-1 shows the GCAMv5.3 reference scenario, with five different climate sensitivities (ECS) calculated within Hector. The bold line represents the central scenario (ECS 3 – reflecting global warming of 3°C for a doubling of atmospheric CO_2 concentrations), and the dotted lines show temperature pathways for the same scenario under alternative climate sensitivities (ECS 2, ECS 2.5, ECS 4, and ECS 5). The efficiency of the Framework allows for evaluation of multiple temperature pathways, which supports uncertainty analysis, for example, across climate sensitivities. The scenarios evaluated are for illustration purposes only, do not reflect analysis of any particular policy or action. Results should be interpreted with a consideration of the uncertainties and limitations described in Sections 2.6 and 2.7.

FIGURE C-1. EXAMPLE TEMPERATURE PATHWAYS FOR IMPACT EVALUATION FOR SIX CLIMATE SENSITIVITIES

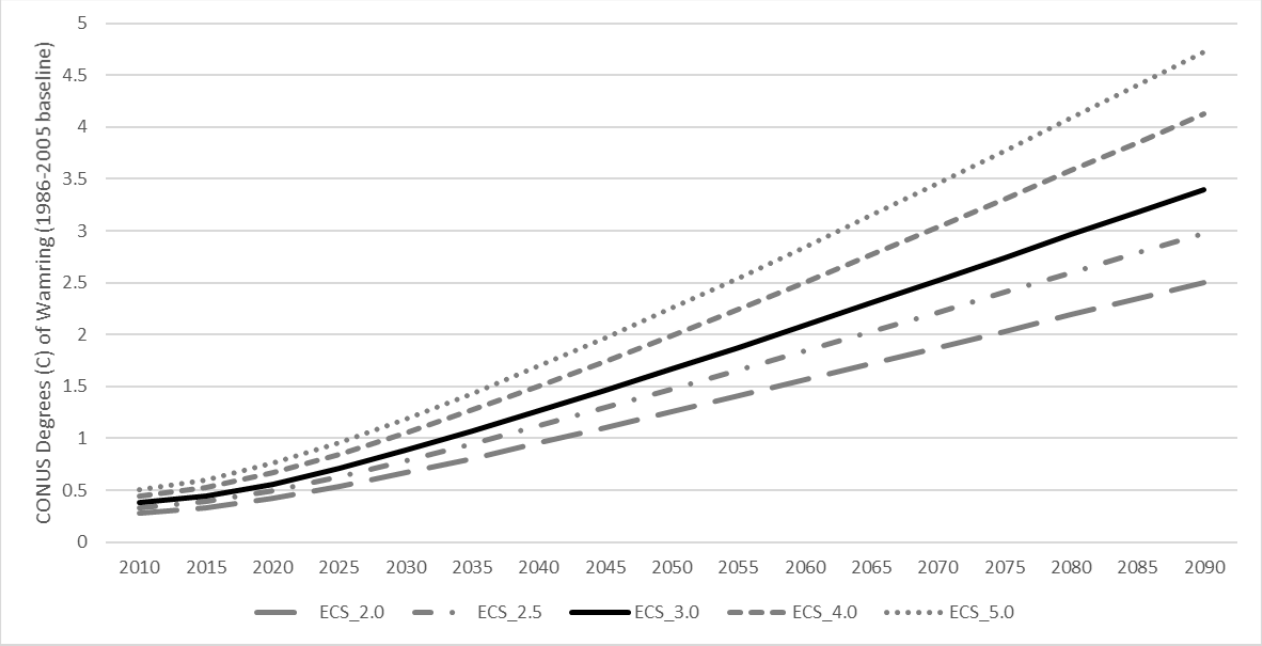

CONUS degrees of warming relative to a 1986-2005 baseline for the GCAMv5.3 reference scenario, across five climate sensitivities (ECS). ECS 3 is the central case.

Figure C-2 shows the GCAMv5.3 reference scenario along with five emissions reduction scenarios, ranging from 20 to 90 percent emissions reductions by the end of the century (ECS 3). The ability of the Framework

https://www.eia.gov/outlooks/aeo/data/browser/?src=-f1#/?id=10-IEO2019&region=0-0&cases=Reference&start=2010&end=2050&f=A&linechart=~Reference-d080819.26-10-IEO2019&map=&ctype=linechart&sid=Reference-d080819.26-10-IEO2019&sourcekey=0

to efficiency evaluate impacts of multiple temperature trajectories allows analysts to compare impacts across various scenarios, or under various policies.

FIGURE C-2. EXAMPLE TEMPERATURE PATHWAYS FOR VARIOUS EMISSIONS REDUCTION SCENARIOS

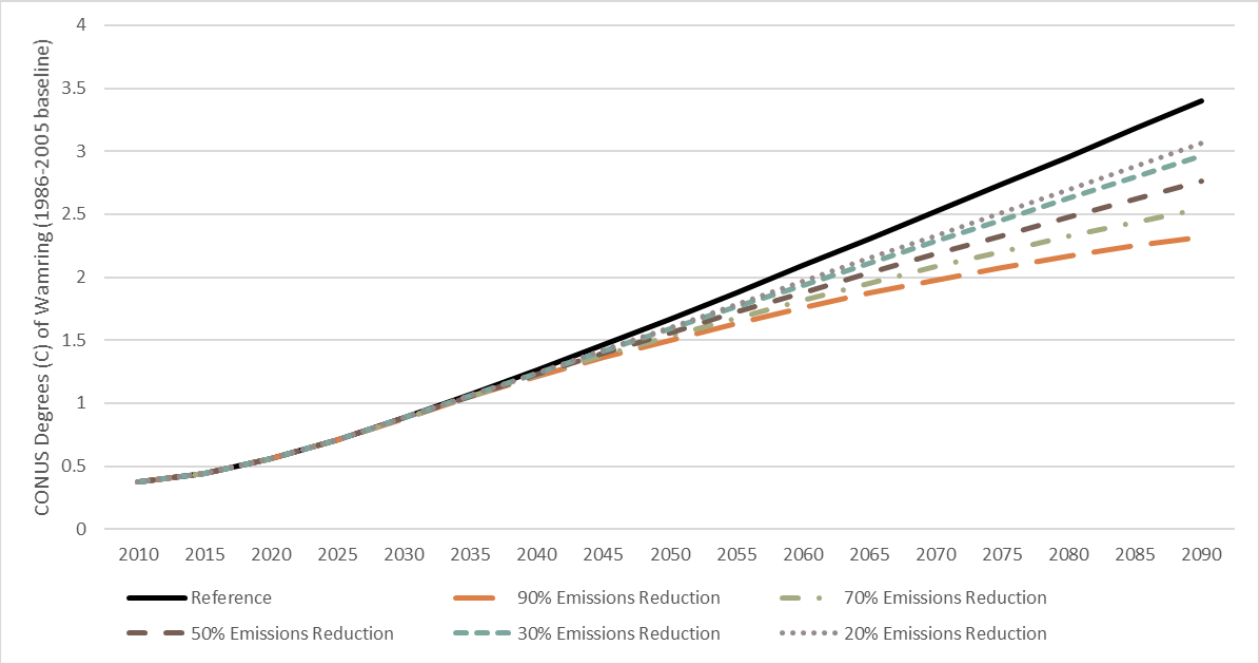

CONUS degrees of warming relative to a 1986-2005 baseline for the GCAMv5.3 reference scenario and five emissions reduction scenarios (ECS 3).

C.2 Evaluating Impacts of Climate Change

We first use FrEDI to evaluate impacts under the five climate sensitivity runs of the reference scenario. Running each of the five sensitivities through the Framework with the default socioeconomic inputs (see Appendix D), results in the impacts trajectories shown in **Figure C-3**. The impacts shown are annual impacts, summed across sectors and regions, that reflect the combination of temperature and socioeconomic condition trajectories. Sea level rise results are estimated using the temperature to sea level rise conversion function described in Section 2.1. The projections represent impacts across 17 modeled sectors (excluding Asphalt Roads which is an alternative method to the "All Roads" sector). Results from the underlying sectoral studies measure impacts through widely varying methods, including welfare economic measures, expenditure/direct cost measures, or a mix of these. These measures may not be strictly additive but are presented as a sum here consistent with practices for regulatory benefits analyses in EPA's Guidelines for Preparing Economic Analyses (2014). While the shapes of the impact curves appear similar to the shape of the temperature trajectories, they are much steeper. For the central case (ECS 3), temperatures range from 0.4 degrees to 3.4 degrees of warming through 2090 (a range of a factor of about nine), while impacts range from $23 billion to $530 billion (a factor of about 23) reflecting non-linearities of impacts in response to temperatures and changing socioeconomic conditions. **Figure C-4** shows total modeled impacts for each of the emissions reduction scenarios.

FIGURE C-3. PROJECTED NATIONAL ANNUAL ECONOMIC IMPACTS ASSOCIATED WITH THE GCAM REFERENCE SCENARIO

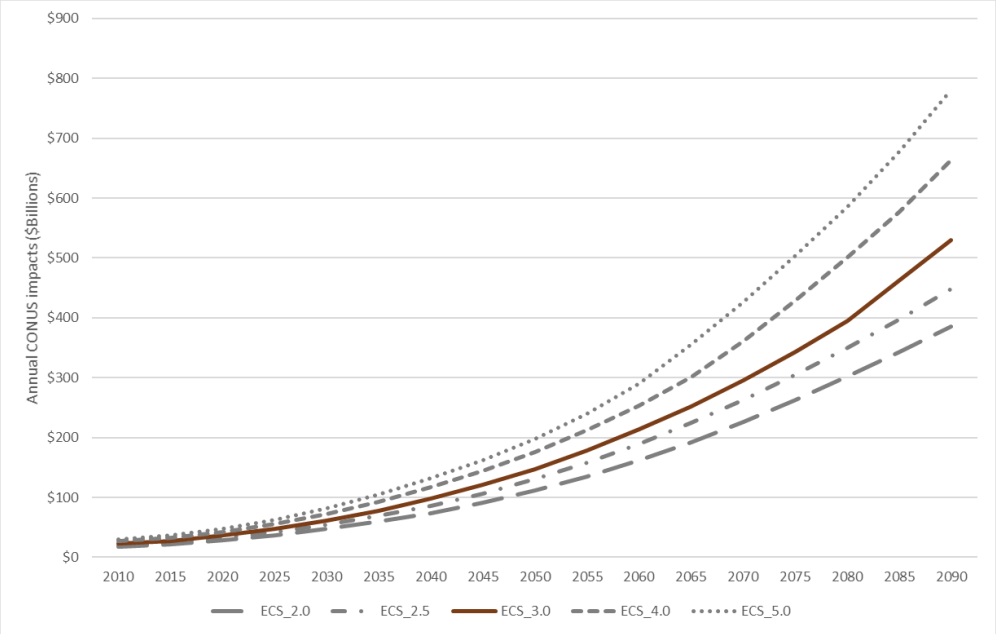

CONUS total annual impacts across 17 modeled sectors (excluding Asphalt Roads) for the GCAMv5.3 reference case with five climate sensitivities (ECS). ECS 3 is the central case. Impacts presented in billions of $2015.

FIGURE C-4. PROJECTED NATIONAL ANNUAL ECONOMIC IMPACTS ASSOCIATED WITH THE GCAM REFERENCE AND EMISSIONS REDUCTION SCENARIOS

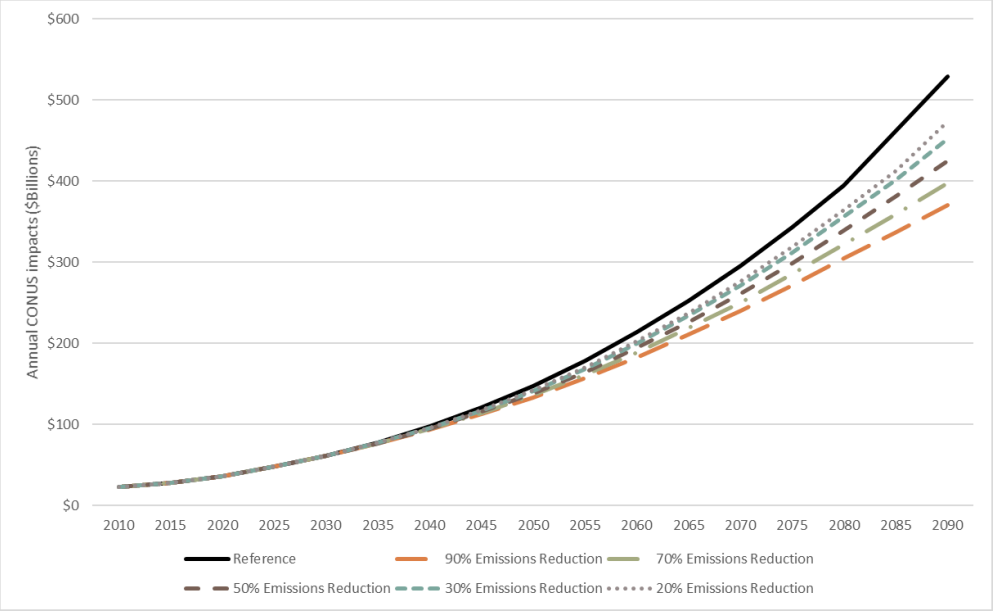

CONUS total annual impacts across 17 modeled sectors (excluding Asphalt Roads) for the GCAMv5.3 reference case and five emissions reductions scenarios (ECS 3). Impacts presented in billions of $2015.

FrEDI calculates impacts by year, region, sector, sub-impact, and adaptation scenario, allowing for analysis of custom scenarios across any of these dimensions. For example, **Figure C-5** shows projected annual impacts of the GCAMv5.3 reference scenario by sector.[32] Under this illustrative scenario, health-related impacts of climate change on Air Quality are the largest impacts in 2050 (28 percent of total modeled impacts). Air Quality experiences a 2.7-fold increase between 2050 and 2090 while High Tide Flooding and Traffic, the second largest modeled sector in 2050, increases 4-fold over the same period to become the largest impact sector by 2090. The largest five sectors make up approximately 74 percent of total annual impacts in 2090, though it is important to note that the modeled sectors only represent a portion of all impacts from climate change.

FIGURE C-5. CONUS ANNUAL ECONOMIC IMPACTS ASSOCIATED WITH A CUSTOM SCENARIO BY SECTOR

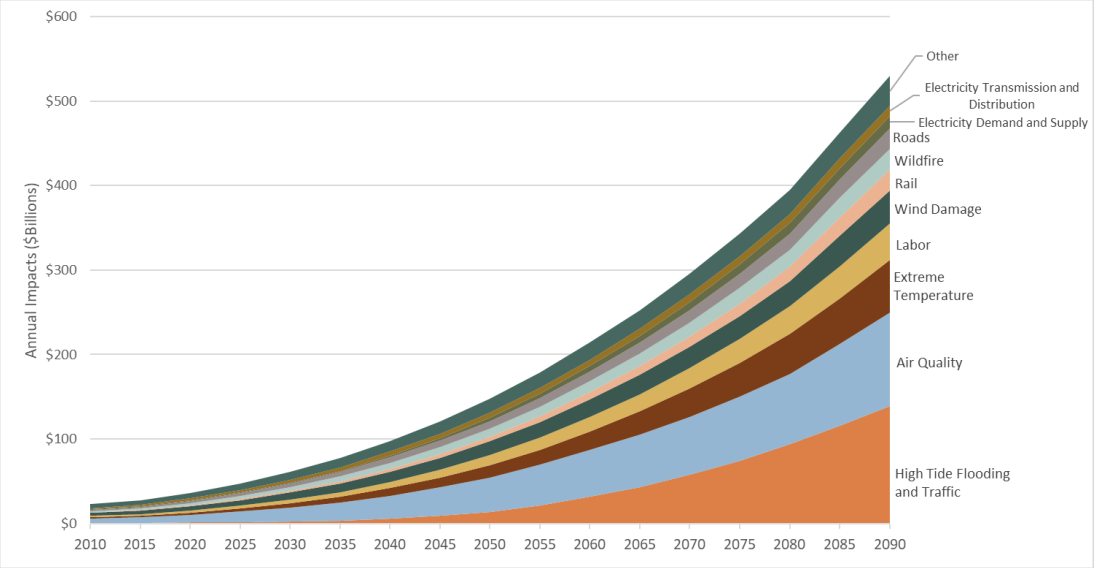

CONUS annual impacts by modeled sectors (excluding Asphalt Roads) for the GCAMv5.3 reference case for the central climate sensitivity (ECS 3). Impacts presented in billions of $2015.

C.3 Evaluating the Economic Benefits of Emission Reduction

This section demonstrates how FrEDI can be used to compare impacts between scenarios, using a comparison of the GCAMv5.3 reference and emissions reduction scenarios presented in the previous section. **Figure C-6** shows the decrease in temperatures associated with the emissions reduction scenarios compared to the reference scenario. The pathways begin diverging in 2030 and in 2090 represent a range of 0.3 to 1.0 degrees less of warming compared to the reference scenario (20 percent and 90 percent emission reduction, respectively). **Figure C-7** shows the resulting difference in projected economic impact between the illustrative emissions scenarios.[24] The projected difference in annual impacts reaches over $10 billion in all emissions reduction scenarios by 2050. The economic benefits per degree reduction from the

[24] Note that differences in annual impacts are calculated as the difference in projected impacts, not the impacts associated with the difference in temperature, the latter of which would not account for non-linearities in the sectoral impact functions.

reference scenario also increase over the century as impacts are non-linear, with more pronounced acceleration of benefits per degree at higher temperatures.

FIGURE C-6. DECREASE IN CONUS TEMPERATURE RELATIVE TO THE REFERENCE SCENARIO FOR EMISSIONS REDUCTION SCENARIOS

Decrease in CONUS degrees of warming relative to a 1986-2005 baseline for five emissions reduction scenarios defined by CO_2 emissions reduction in 2100 compared to the GCAMv5.3 reference scenario.

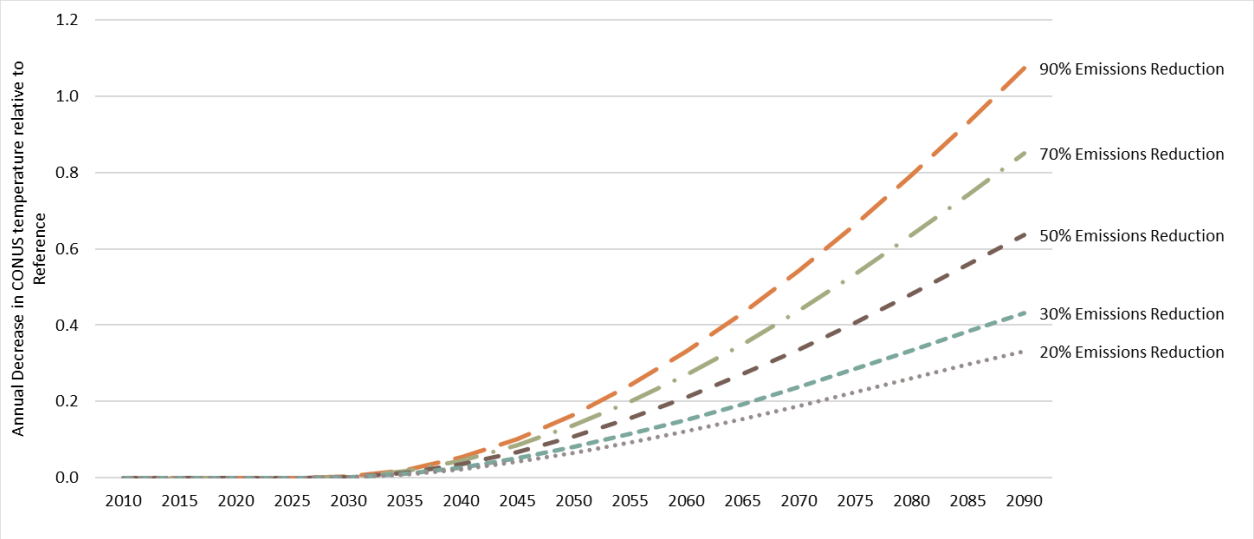

FIGURE C-7. PROJECTED NATIONAL ANNUAL ECONOMIC EFFECTS OF EMISSIONS REDUCTIONS

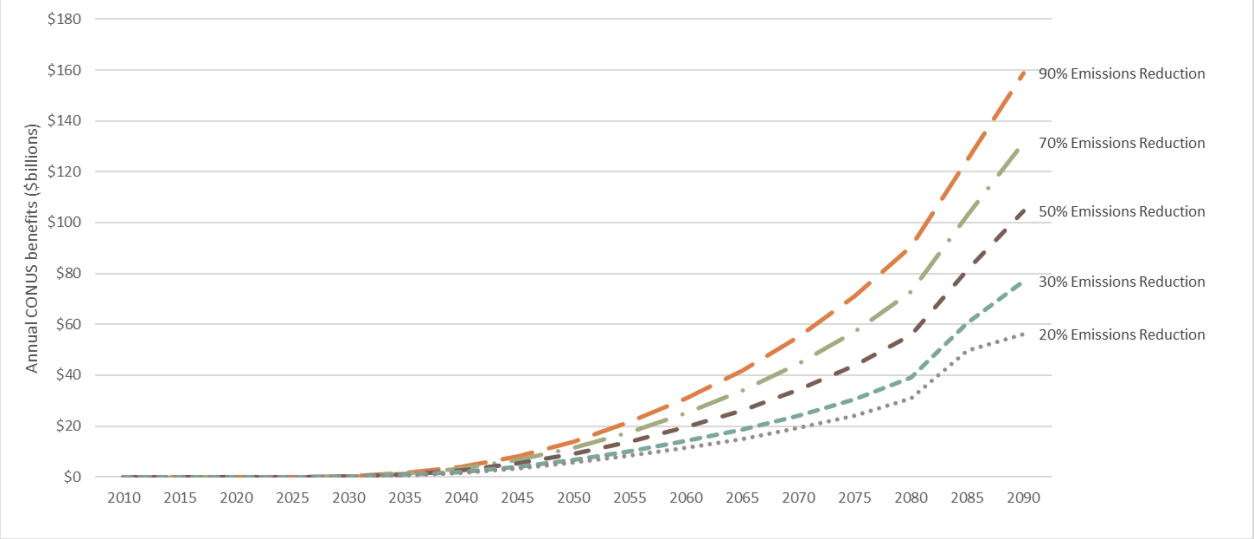

Reduction in CONUS total annual impacts across 17 modeled sectors (excluding Asphalt Roads) for five emissions reduction scenarios defined by CO2 emissions reduction in 2100 compared to the GCAMv5.3 reference scenario. Reduction in impacts presented in billions of $2015.

Figure C-8 shows the projected effects of emissions mitigation under each reduction scenario by sector. While the High Tide Flooding and Traffic sector is projected to experience the impacts in the reference scenario (see Figure C-4), both the Air Quality and Extreme Temperatures have larger benefits (i.e., avoided

damages) of mitigation. SLR-driven sectors show less sensitivity to mitigation measures due to the ways in which GMSL rise and temperature change interact over time. The ability to

FIGURE C-8. PROJECTED NATIONAL ANNUAL ECONOMIC BENEFITS OF HYPOTHETICAL EMISSIONS REDUCTIONS BY SECTOR ($BILLIONS)

Reduction in CONUS annual impacts by modeled sectors (excluding Asphalt Roads) for the illustrative GCAMv5.3 emissions reduction scenarios relative to the reference case for the central climate sensitivity (ECS 3). Sectors are ordered by magnitude of impacts under the reference scenario. Reduction in impacts presented in billions of $2015.

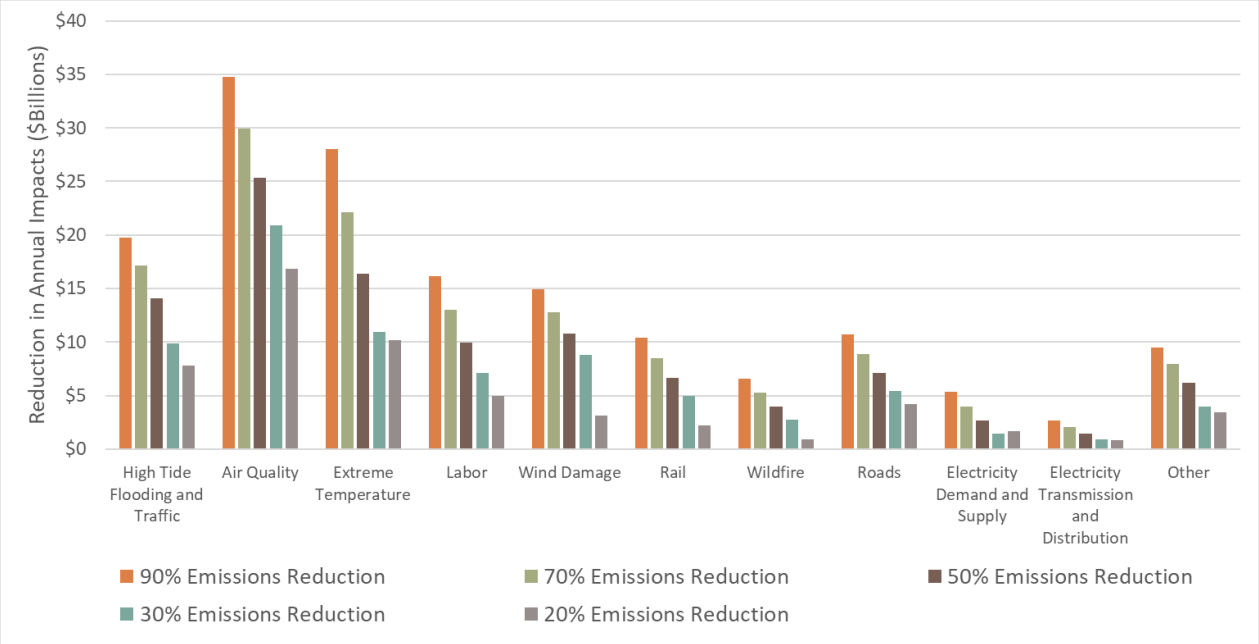

References:

Calvin, K., Patel, P., Clarke, L., Asrar, G., Bond-Lamberty, B., Cui, R.Y., Vittorio, A.D., Dorheim, K., Edmonds, J., Hartin, C. and Hejazi, M., 2019. GCAM v5. 1: representing the linkages between energy, water, land, climate, and economic systems. *Geoscientific Model Development*, *12*(2), pp.677-698.

EPA. 2014. Guidelines for Preparing Economic Analyses. Prepared by the National Center for Environmental Economics, Office of Policy, U.S. Environmental Protection Agency. Originally published December 17, 2010, updated May 2014. Available at: https://www.epa.gov/environmental-economics/guidelines-preparing-economic-analyses#new

Hartin, C.A., Bond-Lamberty, B., Patel, P. and Mundra, A., 2016. Ocean acidification over the next three centuries using a simple global climate carbon-cycle model: projections and sensitivities. *Biogeosciences*, *13*(15), pp.4329-4342.

Hartin, C.A., Patel, P., Schwarber, A., Link, R.P. and Bond-Lamberty, B.P., 2015. A simple object-oriented and open-source model for scientific and policy analyses of the global climate system–Hector v1. 0. *Geoscientific Model Development*, *8*(4), pp.939-955.

Kriegler, E. and Held, H., 2005. Utilizing belief functions for the estimation of future climate change. *International journal of approximate reasoning*, *39*(2-3), pp.185-209.

Vega-Westhoff, B., Sriver, R.L., Hartin, C.A., Wong, T.E. and Keller, K., 2019. Impacts of observational constraints related to sea level on estimates of climate sensitivity. *Earth's Future*, *7*(6), pp.677-690.

APPENDIX D | METHODS DETAILS

D.1 Calculation of global mean sea level

To calculate global mean sea level from global mean temperature we use a semiempirical sea level model from Kopp et al., 2006. This model relates the rate of global mean sea level rise (dh(t)/dt) to global mean temperature at time T(t), an equilibrium temperature $T_e(t)$, and a small residual trend arising from the long-term response to earlier climate change Ø(t), relative to 2000 using equation 10 from Kopp et al., 2016.

$$\frac{dh(t)}{dt} = a * \left(T(t) - T_e(t)\right) + \emptyset(t)$$

In the equation above, $T_e(t)$ and Ø(t) are functions of time, where:

$$\frac{dT_e(t)}{dt} = \frac{(T(t) - T_e(t))}{tau_1}$$

$$\frac{d\emptyset(t)}{dt} = \frac{-\emptyset(t)}{tau_2}$$

The parameter vales are estimated from the probability distributions of the semiempirical model parameters in Figure S5, and Dataset S1j, focusing on the posterior distribution calculated with the Mann et al., 2009 temperature data set. We use the median parameter values across the distributions for this calculation. We used HadCrUT4 to determine the appropriate temperature offset between the actual temperature and the equilibrium temperature in 2000.

TABLE D-1: PARAMETER VALUES USED IN THIS ANALYSIS, FROM KOPP ET AL., 2016, MEDIAN AND 5TH AND 95TH PERCENTILES.

Parameter	Value	Units
$\emptyset(2000)$	0.14 (0.05, 0.29)	mm/yr
tau_1	174 (87, 366)	Year
tau_2	4175 (1140, 17670)	Year
a	4.0 (3.2, 5.4)	mm/yr/K
$T_e(2000)$	-0.05 (-0.12, 0.07)	K

Future versions of FrEDI may use several different approaches for addressing uncertainty. Some of these approaches include: using the parameter distributions in S1j using a Monte Carlo approach to sample the parameters distributions provided in Kopp et al., 2016, both Mann et al., 2009 and Marcott et al.,;

calibrating T_e(2000) and alpha parameters to emulate the range of sea level rise from AR6; and examine low-probability high impact outcomes such as the sea level rise projection including ice sheet instability from AR6 or the higher Sweet et al., 2017 scenarios. Some approaches (such as using the normal distributions for parameters or the alternate parameter set calibrated against Marcott et al.) will be straightforward, but others may be more challenging to implement. The semi-empirical approach was not designed to incorporate future sea level rise processes that were not observed in historical data such as ice sheet instability and may not be accurate for multi-century applications. We note that the user can supply FrEDI with exogenous global mean sea level rise scenarios instead of calculating them from global mean temperature.

Figure D-1 shows the projected global mean sea level rise from RCP 2.6, RCP 4.5 and RCP 8.5 using the updated sea level rise model. Global mean temperature was calculated with Hector v2.5. The colored bars represent the 5th and 95th percentile projections of global mean sea level driven by the Mann et al., 2009 temperature data set (Table S1i in the supplementary material of Kopp et al., 2016).

FIGURE D-1. GLOBAL MEAN SEA LEVEL RISE PROJECTIONS

Global mean sea level rise projections using the updates method for RCP 2.6, 4.5, and 8.5. The colored bars represent the 5th and 95th percentile and the symbols represent the median projections using the calibration to the Mann et al., 2009 temperature data set.

D.2 Global to CONUS Temperature Translation

One of the flexibilities of FrEDI is its ability to generate impact estimates from either global or CONUS temperature inputs. FrEDI contains a translation function, derived from global and CONUS temperatures from six CMIP5 GCMs (i.e., the suite of GCMs used in the CIRA project). **Figure D-2** plots the global and CONUS temperatures for the six GCMs, under RCP8.5 (the pathway used in FrEDI analyses), where each

point represents an era (i.e., 2030, 2050, 2070, 2090) and GCM combination. All temperature changes presented are relative to the 1985-2006 baseline period.

FIGURE D-2. GLOBAL AND CONUS TEMPERATURES, RCP8.5

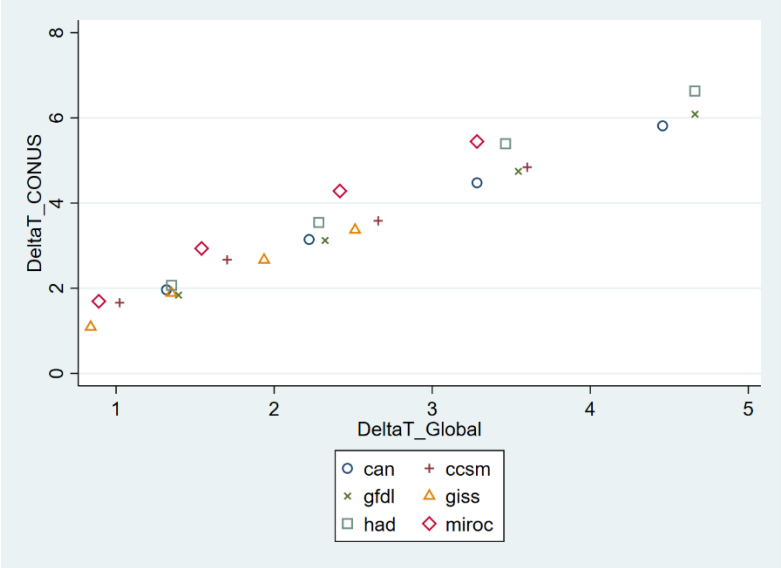

This plot shows global and CONUS temperatures for the six GCMs, under RCP8.5. Each data point is an era-GCM combination.

The relationship between CONUS and global temperatures is relatively stable across GCMs and over time, allowing us to use these available datapoints to develop a generalized relationship between global and CONUS temperature anomalies. Using this data, we estimate a linear translation function specified as:

$$\Delta T_{CONUS} = \beta_1 \Delta T_{GLOBAL} + \varepsilon$$

The coefficients of this equation are as follows, in **Table X**. Using the estimated coefficients, FrEDI calculates CONUS temperatures from Global temperatures as:

$$\Delta T_{CONUS} = 1.42 \Delta T_{GLOBAL}$$

TABLE D-2. CONUS TO GLOBAL TEMPERATURE TRANSLATION COEFFICIENT ESTIMATES

Regression estimates relating CONUS and global temperature changes, relative to a 1986-2005 baseline.

	ΔT_{CONUS}	
ΔT_{GLOBAL}	1.421	***
	(0.000)	
R-squared	0.990	
Adjusted R-squared	0.990	
N	24	

Standard errors listed below coefficients, in parentheses. * p<0.05; ** p<0.01; *** p<0.001

These coefficients are used most commonly in the Tool to translate global temperature inputs into CONUS temperatures for binning indexing, however if a user inputs CONUS temperatures, the inverse of the formula can be used to generate global temperatures, which are used to derive GMSL as described in the previous section.

References:

Kopp, R. E. et al. Temperature-driven global sea-level variability in the Common Era. PNAS 113, E1434–E1441 (2016).

JGCRI/hector. GitHub https://github.com/JGCRI/hector/releases.

Mann, M. E. et al. Global Signatures and Dynamical Origins of the Little Ice Age and Medieval Climate Anomaly. Science 326, 1256–1260 (2009).

Marcott, S. A., Shakun, J. D., Clark, P. U. & Mix, A. C. A Reconstruction of Regional and Global Temperature for the Past 11,300 Years. Science (2013).

Met Office Hadley Centre observations datasets. https://www.metoffice.gov.uk/hadobs/hadcrut4/data/current/download.html.

Sweet, W. V. and Horton, R. and Kopp, R. E. and LeGrande, A. N. and Romanou, A. Climate Science Special Report: Fourth National Climate Assessment, Volume I. (U.S. Global Change Research Program, 2017).

APPENDIX E | METHODS SENSITIVITY TESTS

E.1 Sensitivity to GHG emissions scenarios

Since FrEDI uses only RCP8.5 results to establish impacts at integer degrees of national warming, it is important to understand the sensitivity of the results to a single GHG emissions scenarios—i.e., would the impacts by degree of warming be significantly different under a more moderate GHG emissions scenario? It is possible that using RCP8.5 results only may bias the results because of the land-sea warming differences that have been established (Herger et al. 2015) between higher and lower GHG mitigation, among other potential differences.[1]

The roads sector is ideal for this comparison because it includes both precipitation and temperature drivers, as most of the sectors in FrEDI are largely temperature-driven with some that are entirely precipitation-driven. **Table E-1** shows the impacts for the roads sector for CONUS for six GCMs and two GHG emissions scenarios by integer degrees. Note that none of the RCP4.5 GCMs exceed 4 degrees of national (CONUS) warming and two of the GCMs (CCSM4 and GISSE2R) never exceed 2 degrees of warming. For each GCM, there are differences between the RCPs at the same degrees of warming. Of the four GCMs with values for all three degrees of warming, two of the GCMs (CanESM and HadGEM2ES) show higher impacts for RCP8.5 than RCP4.5 and the other two GCMs (MIROC5 and GFDLCM3) show lower impacts for RCP8.5 than RCP4.5. In addition, differences between impacts across the two RCPs for the same GCM are well within the range of differences between GCM results with the same RCP, indicating that uncertainty is similar between GCMs and these two RCPs.

Differences in the mean across the six GCMs for the two RCPs are similar for 1 through 3 degrees, where RCP4.5 is higher by 16% for 1 degree, lower by 27% for 2 degrees, and higher by 6% for 3 degrees. As such, there is not a clear bias, high or low, in using a single RCP for the roads sector.

[1] Herger, N., B. M. Sanderson, and R. Knutti (2015), Improved pattern scaling approaches for the use in climate impact studies, Geophys. Res. Lett., 42, 3486–3494, doi:10.1002/2015GL063569

TABLE E-1. CONUS IMPACTS FOR ROADS SECTOR BY GCM AND GHG EMISSIONS SCENARIO

Roads impacts (bill. $2015 / year) for six GCMs and two GHG emissions scenarios (RCP4.5 and RCP8.5), as well as the mean across the six GCMs for each GHG emissions scenario for 1-3 degrees of national (CONUS) warming (Celsius) from 1986-2005 average baseline. Difference between the RCP means are also shown.

GCM	RCP	Impacts ($2015 bill. / year)		
		1 Deg	2 Deg	3 Deg
CanESM	RCP4.5	-$4	$10	$62
CanESM	RCP8.5	-$1	$15	$105
CCSM4	RCP4.5	$33		
CCSM4	RCP8.5	$1	$103	$196
GISSE2R	RCP4.5	$7		
GISSE2R	RCP8.5	$1	$20	$74
HadGEM2ES	RCP4.5	$59	$131	$302
HadGEM2ES	RCP8.5	$80	$211	$325
MIROC5	RCP4.5	$2	$21	$102
MIROC5	RCP8.5	$4	$28	$51
GFDLCM3	RCP4.5	$5	$35	$149
GFDLCM3	RCP8.5	$2	$28	$116
Mean	***RCP4.5***	***$17***	***$49***	***$154***
Mean	***RCP8.5***	***$15***	***$68***	***$145***
Difference between RCP mean		*16%*	*-27%*	*6%*

Note: none of the RCP4.5 GCMs exceed 4 degrees of national (CONUS) warming and two of the GCMs (CCSM4 and GISSE2R) never exceed 2 degrees of warming.

E.2 Sensitivity to binning window

The FrEDI Framework uses an 11-year binning window, which is essentially an 11-year moving average, for assigning integer degrees of warming. The main purpose of the binning window is to smooth out inter-annual variability to establish the arrival year of integer degrees of warming. An 11-year window is composed of a center year with 5 years on each side. 11 years are used because this provides a balance between longer windows that use temperatures from years far from the center year and shorter windows that may reach or not reach temperature thresholds because of the noise from year-to-year temperature variability. Longer windows, especially a 30-year period, often used to establish a climatology, would cause issues or at least inconsistencies near the end or the beginning of the timeseries. For example, the first degree of warming is often within the first 10 years of the projection, which would not allow a full 30-year window. However, it is important to establish the consequences of using 11 years instead of using a shorter or longer period.

FIGURE E-1. CONUS DEGREES OF WARMING WITH 11-YEAR MOVING AVERAGE

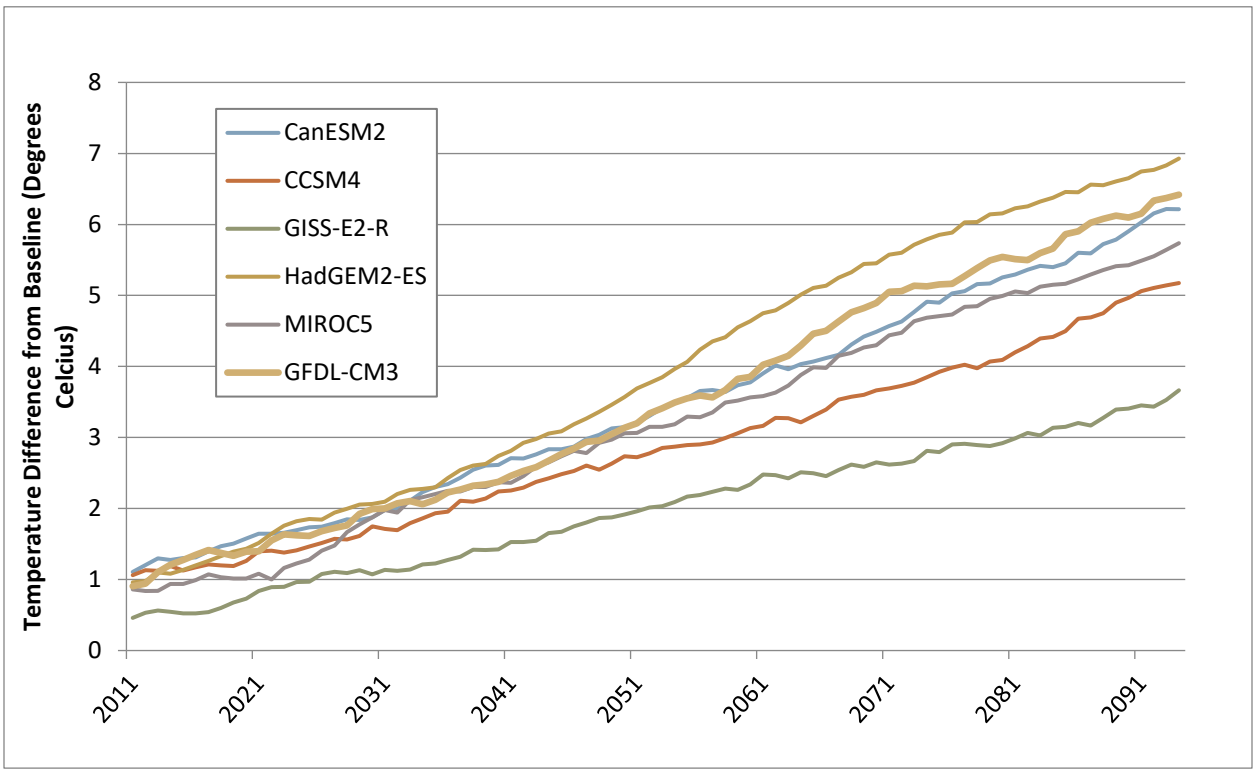

Annual degrees of warming (Celsius) from 1986-2005 average baseline for CONUS after an 11-year moving average is applied. All six CIRA GCMs are shown.

Figure E-1 shows the 11-year moving average CONUS temperature trajectory as a difference from the 1986-2005 baseline. As shown, the majority of the inter-annual variability is removed with an 11-year averaging window. However, some variability remains. To investigate the effect of an 11-year moving average as opposed to a shorter or longer period, the following tables indicate how the arrival years would differ for a 5-year window (**Table E-2**) or a 15-year window (**Table E-3**). As shown, in most cases, arrival years only differ by 1 to three years and differences are greater for the 5-year window than the 15-year window.

TABLE E-2. DIFFERENCE IN ARRIVAL TIMES FOR A 5-YEAR WINDOW

Differences between arrival times (years) if a 5-year window is used compared to an 11-year window.

GCM	Difference between arrival times for a 5-year window (years)					
	1 Deg	2 Deg	3 Deg	4 Deg	5 Deg	6 Deg
CanESM2	2	1	0	3	1	1
CCSM4	2	1	3	2	1	N/A
GISS-E2-R	3	1	3	N/A	N/A	N/A
HadGEM2-ES	1	3	1	1	0	1
MIROC5	3	3	1	0	0	0
GFDL-CM3	1	3	0	1	3	1

TABLE E-3. DIFFERENCE IN ARRIVAL TIMES FOR A 15-YEAR WINDOW

Differences between arrival times (years) if a 15-year window is used compared to an 11-year window.

GCM	Difference between arrival times for a 5-year window (years)					
	1 Deg	2 Deg	3 Deg	4 Deg	5 Deg	6 Deg
CanESM2	2	2	1	2	1	0
CCSM4	2	0	1	0	0	N/A
GISS-E2-R	1	0	0	N/A	N/A	N/A
HadGEM2-ES	0	0	0	0	1	0
MIROC5	2	0	0	1	0	N/A
GFDL-CM3	0	0	0	0	2	1

E.3 Sensitivity to socioeconomic factors

Two primary socioeconomic factors are explicitly incorporated into FrEDI: projected total population changes and projected changes in GDP. The Framework was designed based on a conclusion that these two are the primary drivers of socioeconomic change on the resulting economic impact. For some sectors, these are the only socioeconomic drivers—e.g., Roads, Labor, High Tide Flooding, and Coastal Properties. For some other sectors, secondary socioeconomic factors are embedded in the underlying study results. For example, the sectoral studies underlying Southwest Dust, Valley Fever, and Temperature Mortality include projections of population age distribution. Temperature Mortality impacts are based on city-specific functions, each of which capture demographic information embedded in the functional relationships that relate mortality to weather conditions, such as age distribution and baseline mortality rates. For this reason, and because Extreme Temperature mortality impacts tend to be larger in magnitude than many of the other sectors, Extreme Temperature mortality is a suitable sector to evaluate the influence of these

secondary socioeconomic factors, comparing them to the influence of the two primary factors: population and GDP.

Table E-4 shows the drivers of changes from the 2010 impacts to the 2090 values as ratios (or factors) of 2090 impacts to 2010 impacts where a 1.2 would indicate 2090 values are 20 percent higher than the equivalent 2010 values. This table effectively isolates the socioeconomic influence on the final impacts into three categories. As such, multiplying the *Population*, *GDP/Capita*, and *Secondary Socioeconomic* columns gives the value in the *Total Socioeconomic* column. Note that GDP/Capita, which influences VSL, uses national scale GDP and population (rather than regional or city-scale population) so is consistent across regions.

Secondary socioeconomic factors influence the total socioeconomic influence factor by about 2 to 5 percent across regions. In contrast, the two primary socioeconomic factors each influence the total factor by 20 to 76 percent, indicating that the influence of the two factors used explicitly in the framework—population and GDP—are considerably higher than the secondary factors. Note that the effects of secondary socioeconomic factors will vary by sector. However, temperature mortality provides a relatively straightforward means to test the influence of these factors since they are implicitly imbedded in the underlying relationship of weather conditions and mortality, which vary by location.

TABLE E-4. FACTORS OF CHANGE BETWEEN 2010 AND 2090 IMPACTS FOR TEMPERATURE MORTALITY AT 2-DEGREES

Factors of change (2090 over 2010 value) for all socioeconomic conditions that influence temperature mortality impacts at 2 degrees of warming above the 1986-2005 CIRA baseline, mean across the six GCMs.

Region	Population	GDP/Capita	Secondary Socioeconomic	Total Socioeconomic
Midwest	1.20	1.55	1.04	1.95
Northeast	1.44	1.55	0.95	2.11
Northwest	1.24	1.55	0.98	1.90
Southeast	1.52	1.55	0.97	2.29
Southern Plains	1.71	1.55	1.02	2.71
Southwest	1.76	1.55	1.02	2.80
Total	1.50	1.55	0.98	2.27

E.4 Errors from year-specific adjustment factors

This section attempts to quantify errors associated with using 2010 and 2090 year-specific socioeconomic adjustment factors. There are three sectors that use this approach—Temperature Mortality, Valley Fever, and Southwest Dust. Since all of these are health sectors, the primary socioeconomic drivers are population growth and GDP/capita, which effects VSL. Both of these drivers are used in all three sectors.

In FrEDI, a linear interpolation between 2010 and 2090 is used to estimate the effect of socioeconomic growth on impacts between these two points in time. Using a linear approach will result in some discrepancy in FrEDI estimated impacts between 2010 and 2090 and estimates that use annual projections

of population and GDP. **Figure E-2** shows the factors that influence impacts when a population projection is used compared to a linear version on the left and the same for VSL on the right. The VSL factor is calculated as the ratio of change in GDP per capita from 2010 raised to an elasticity of 0.4, which follows the VSL equation in Appendix B.

FIGURE E-2. PROJECTED AND LINEAR FACTORS OF POPULATION GROWTH AND VSL

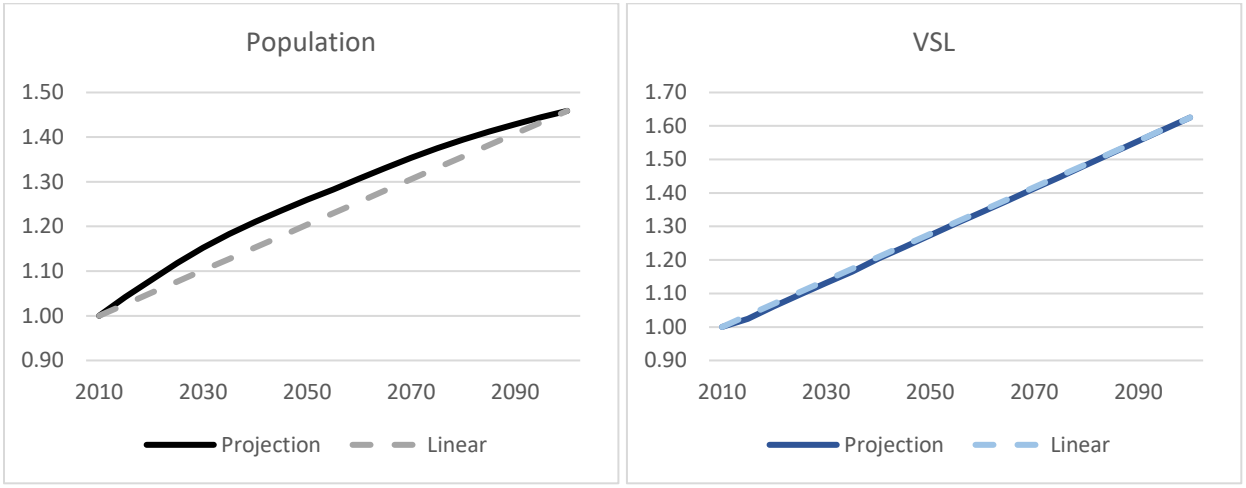

Growth factors for population and VSL with a projection of population and GDP and the linear counterpart. Growth factors represent the multiplier on impacts to account for socioeconomic growth from 2010. The VSL factor is calculated as the ratio of change in GDP per capita from 2010 raised to an elasticity of 0.4, which follows the VSL equation in Appendix B.

As shown in **Figure E-2**, the population projection is inreasing at a decreasing rate and the linear approximation underestimates the factor for all years. The projected VSL, on the other hand, almost follows a linear approximation. **Figure E-3** shows the difference in the linear approximation from the projection, where positive values indicate the linear approximation overestimates the growth factor and negative values indicate the linear approach underestimates the growth factor. The linear approach underestimates the population growth factor by slightly less than zero in years close to 2010 or 2090 and up to 4.8 percent in 2035. For VSL, the linear approach only slightly overestimates the growth factor peaking in 2015 at 1.1 percent. This indicates that the linear approach is less impactful for VSL than population although even for the population growth factor the difference is relatively small.

FIGURE E-3. DIFFERENCE IN LINEAR APPROACH TO POPULATION AND VSL PROJECTION

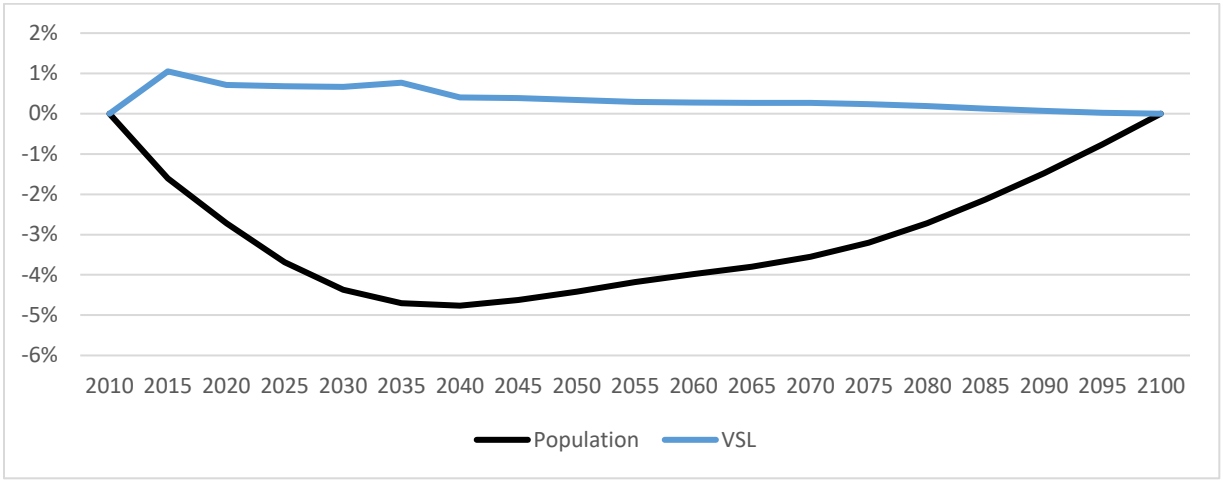

Percent difference in socioeconomic growth factors between a linear approach and a projection approach (used in most underlying studies) for 5-year increments from 2010 to 2090. Negative values indicate the linear approach produces an underestimate compared to the projection approach and positive values indicate the linear approach overestimates the growth factor.

APPENDIX F | R CODE DOCUMENTATION

The EPA has implemented the FrEDI framework in an R package called `FrEDI`, which consists of one main function, several pre- and post- processing functions, and additional helper functions. The package is currently available for download through GitHub and may eventually be submitted for dissemination through the Comprehensive R Archive Network (CRAN).[26] The `FrEDI` package depends on several additional, widely used R packages - `dplyr`, `tidyr`, and `ggplot2`. All package dependencies are available through CRAN.

The FrEDI package implements the Framework described in this report. The first section in this appendix presents an overview of the main elements of the FrEDI package. The second section provides detailed descriptions of each of the functions in the package. For more details on the underlying methodology, refer to the main documentation report.

F.1 `FrEDI' Overview

The R package implements the FrEDI framework in one main function (`run_fredi()`) and provides additional pre- and post-processing functions. The primary functions and their main arguments are highlighted in the table below. The function dependencies are shown in the following figure.

Function Name	Function Type	Inputs
run_fredi	Main temperature- and SLR-projection function	Custom scenarios for temperature, global mean sea level rise (GMSL), population, and gross domestic product (GDP)
import_inputs	Function for importing custom scenarios from CSV files	Paths to CSV files containing custom scenarios
get_plots	Create plots of impacts produced using `run_fredi()` (heatmaps and impacts over time)	Outputs of FrEDI, aggregated to impact types

Function dependencies are shown in the **Figure F-1**.

[26] For more information on CRAN, visit https://cran.r-project.org/.

FIGURE F-1 FUNCTION DEPENDENCIES IN THE `FREDI' R PACKAGE

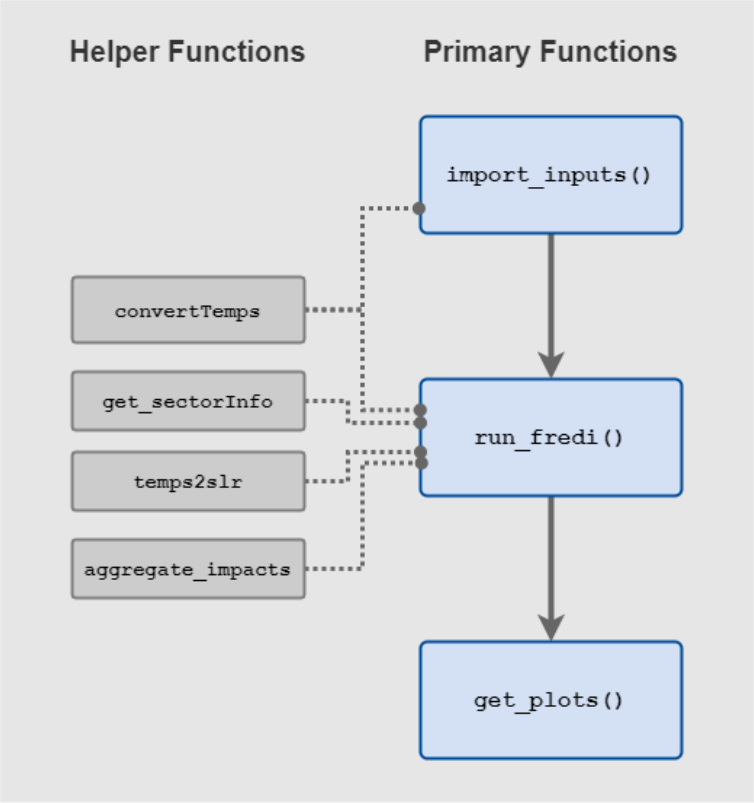

Main function for projecting climate impacts

- `run_fredi()` - Project annual average climate change impacts throughout the 21st century for available sectors.

Pre-processing functions

Primary functions:

- `import_inputs()` - Import custom scenarios for climate and socioeconomics (temperature and global mean sea level rise (GMSL), population, and GDP) from user-specified file names.

Helper functions:

- `convertTemps()` - Convert contiguous U.S. (CONUS) temperatures to global temperatures or vice versa.
- `temps2slr()` - Convert global temperature change in degrees Celsius to global mean sea level rise (GMSL) in centimeters.
- `get_sectorInfo()` - Access information about sectors in FrEDI as a vector or dataframe.

Post-processing functions

Primary functions:

- `get_plots()` - Create plots for FrEDI outputs.
- `aggregate_impacts()` - Summarize and aggregate impacts from FrEDI. Calculate national totals, average across models, sum impact types, and interpolate between impact year estimates.

Included datasets (default outputs)

The FrEDI R package contains a dataset with default results `defaultResults`, which contains annual impacts produced by `run_fredi()` for the default scenarios (i.e., default temperature, GDP and regional population trajectories), and can be loaded into the R workspace (`load(defaultResults)`).

F.2 `FrEDI' Function Details

F.2.1 Primary Functions

F.2.1.1 run_fredi

Project annual average climate change impacts throughout the 21st century for available sectors.

Description

This function allows users to project annual average climate change impacts throughout the 21st century (2010-2090) for available sectors. Users may specify an optional list of custom scenarios using `inputsList`. The output of `run_fredi()` is an R data frame object containing annual average impacts, by year, for each sector, adaptation, impact type, model (GCM or SLR scenario), and region.

Usage

```
run_fredi(inputsList=NULL, sectorsList=NULL, aggLevels="all",
pv=FALSE, baseYear=2010, rate=0.03, silent=TRUE)
```

Arguments

inputsList	A list of named elements (`names(`inputsList)= c("tempInput", "slrInput", "gdpInput", "popInput")`), each containing dataframes of custom temperature, global mean sea level rise (GMSL), gross domestic product (GDP), and/or population scenarios, respectively, over the period 2010 to 2090. For more information, see `import_inputs()`. Values for each scenario type must be within reasonable ranges. For more information, see the details, below, for `run_fredi()` and documentation for `import_inputs()`.
sectorsList	A character vector indicating a selection of sectors for which to calculate results. If `NULL`, all sectors are included.
aggLevels	Levels of aggregation at which to summarize data: one or more of `c("national", "modelaverage", "impactyear", "impacttype", "all")`. Defaults to all levels (i.e., `aggLevels="all"`). Uses the same aggregation levels as `aggregate_impacts()`).
pv	A `TRUE/FALSE` value indicating whether to calculate present values for the annual impacts. Defaults to `pv=FALSE`.
baseYear	Base year used for calculating present values of annual impacts (i.e., discounting). Defaults to `baseYear=2010`.
rate	Annual discount rate used in calculating present values (i.e., discounting) annual impacts. Defaults to `rate=0.03` (i.e., 3% per year).

silent	A `TRUE/FALSE` value indicating the level of messaging desired by the user (default=`FALSE`).

Details

This function allows users to project annual average climate change impacts throughout the 21st century for available sectors. `run_fredi()` is the main function in the FrEDI R package. The FrEDI package implements the methods of the Framework, as described in this report.

Users can specify an optional list of custom scenarios with `inputsList` and specify a selection of sectors with `sectorsList`. `run_fredi()` uses default scenarios for temperature, population, and GDP when no inputs are specified (i.e., `inputsList` is `NULL`) or for empty elements of the inputs list. If the user does not specify an input scenario for GMSL (i.e., `inputsList= list(slrInput=NULL)`) , `run_fredi()` first converts the CONUS temperature scenario to global temperatures and then converts the global temperatures to a global mean sea level rise (GMSL) height in centimeters. For more information on the conversion of CONUS temperatures to global temperatures, see `convertTemps()`. For more information on the conversion of global temperatures to GMSL, see `temps2slr()`.

Values for input scenarios must be within reasonable ranges. If a user inputs a custom scenario with values outside the allowable ranges, `run_fredi()` will not run the scenarios and will instead stop and return an error message. Temperature and GMSL inputs must begin in 2000 or earlier. Values for population and GDP scenarios can start in 2010 or earlier. For more information, see F.2.1.2 `import_inputs()`.

The input temperature scenario (passed to `run_fredi()` via the `inputsList` argument) requires temperatures for the contiguous U.S. (CONUS) in degrees Celsius relative to 1995 (degrees of warming relative to the baseline year). Temperature values must be greater than or equal to zero and less than or equal to 10 degrees Celsius (CONUS temperatures). Users can convert global temperatures to CONUS temperatures using `convertTemps(from="global")` or by specifying `import_inputs(temptype="global")` when importing a temperature scenario from a CSV file.

Values for the sea level rise (SLR) scenario are for global mean sea level rise (GMSL) must be in centimeters (cm) and values must be greater than or equal to zero and less than or equal to 250 cm.

Population and gross domestic product (GDP) values must be greater than or equal to zero.

If `inputsList=NULL`, `run_fredi()` uses defaults for all scenarios. Otherwise, `run_fredi()` looks for a list object passed to the argument `inputsList`. Within that list, `run_fredi()` looks for list elements `tempInput`, `slrInput`, `gdpInput`, and `popInput` containing dataframes with custom scenarios for temperature, GMSL, GDP, and regional population, respectively. `run_fredi()` will default back to the default scenarios for any list elements that are `NULL` or missing. In other words, running `run_fredi(inputsList= list())` returns the same outputs as running `run_fredi()`. For help importing custom scenarios from CSV files, refer to the pre-processing function `import_inputs()`.

For all inputs, `run_fredi()` linearly interpolates missing annual values using non-missing data points. Temperatures are interpolated using 1995 as the baseline year (i.e., the central year of the 1986-2005 baseline period). The temperature input series must begin in 2000 or earlier. GMSL is interpolated using 2000 as the baseline year. In other words, the temperature (in degrees Celsius) is set to zero for the year 1995 and GMSL is set to zero for the year 2000. The interpolated temperature and GMSL scenarios are combined into a column called `driverValue`, along with additional columns for the driver unit (`driverUnit` in "degrees Celsius" and "cm" for temperature and GMSL, respectively). FrEDI joins the driver scenarios with annual values for each sector by the model type associated with the sector ("GCM" or "SLR").

The population scenario must provide annual regional values for population, with national totals calculated from regional values. FrEDI uses the national population scenario and the GDP scenario to calculate GDP per capita. Values for regional population, national population, national GDP (in 2015$), and national per capita GDP (in 2015$/capita) are provided in the results dataframe in columns "reg_pop", "national_pop", "gdp_usd", and "gdp_percap", respectively.

Annual impacts for each sector, adaptation, impact type, and impact year combination included in the model are calculated by multiplying scaled climate impacts by a physical scalar and economic scalars and multipliers.

`run_fredi()` aggregates or summarizes results to levels of aggregation specified by the user (passed to `aggLevels`) using the post-processing helper function `aggregate_impacts()` (see `aggregate_impacts()`). Users can specify a single aggregation level or multiple aggregation levels by passing a single character string or character vector to `aggLevels`. Options for aggregation include calculating national totals (`aggLevels="national"`), averaging across model types and models (`aggLevels="modelAverage"`), summing over all impact types (`aggLevels="impacttype"`), and interpolate between impact year estimates (`aggLevels="impactyear"`). Users can specify all aggregation levels at once by specifying `aggLevels="all"` (default) or no aggregation levels (`aggLevels="none"`).

For each of the `aggLevels`, `run_fredi()` performs the following summarization (using `aggregate_impacts()`):

- `"national"`: Annual values are summed across all regions present in the data. I.e., data is grouped by columns `"sector"`, `"adaptation"`, `"impactType"`, `"impactYear"`, `"model_type"`, `"model"`, and `"year"`. Years which have missing column data for all regions return as `NA` (missing). The rows of the dataframe of national values (with column `region="National Total"`) are then added as rows to the regional values.
- `"modelAverage"`: Annual results are averaged across all models present in the data, i.e., data is grouped by columns `"sector"`, `"adaptation"`, `"impactType"`, `"impactYear"`, `"model_type"`, `"region"`, and `"year"` and averaged across models. Averages exclude missing values. Years which have missing column data for all models return as `NA` (missing). The rows of the dataframe of model averages (with `model="Average"` for temperature-driven sectors and `model="Interpolation"` for SLR-driven sectors) are then added as rows to individual model results.
- `"impactType"`: Annual results are summed across all impact types by sector present in the data. I.e., data is grouped by columns `"sector"`, `"adaptation"`, `"impactYear"`,

`"model_type", "model", "region",` and `"year"` and summed across impact types. Mutates column `impactType="all"` for all values. Years which have missing column data for all impact types return as `NA` (missing). If results are aggregated across impact types, information about physical impacts (dataframe columns `"physicalmeasure"` and `"physical_impacts"`) are dropped.

- `"impactYear"`: Annual results for sectors with only one impact year estimate (i.e., `impactYear=="N/A"`) are separated from those with multiple impact year estimates. For sectors with multiple impact years, annual results are interpolated between impact year estimates for applicable sectors i.e., data is grouped by columns `"sector"`, `"adaptation"`, `"impactType"`, `"model_type"`, `"model"`, `"region"`, and `"year"` and interpolated across years with the 2010 run assigned to year 2010 and the 2090 run assigned to year 2090. The interpolated values are bound back to the results for sectors with a single impact year estimate, and column `impactYear` set to `impactYear="Interpolation"` for all values.

Users can choose to calculate present values of annual impacts (i.e., discounted impacts), by setting `pv=TRUE` (defaults to `pv=FALSE`). Discounted impacts are calculated using a base year and annual discount rate as `discounted_impacts=annual_impacts/(1+rate)^(year-baseYear)`. Set base year and annual discount rate using `baseYear` (defaults to `baseYear=2010`) and `rate` (defaults to 3% i.e., `rate=0.03`), respectively.

Outputs

The output of `run_fredi()` is an R data frame object containing annual average impacts, by year (2010-2090), for each sector, adaptation, model (GCM or SLR scenario), and region.

Examples

```
### Path to example scenarios
scenariosPath <- system.file(package="FrEDI") %>%
file.path("extdata","scenarios")
### View example scenario names
scenariosPath %>% list.files
### Temperature Scenario File Name
tempInputFile <- scenariosPath %>% file.path("GCAM_scenario.csv")
### SLR Scenario File Name
slrInputFile  <- scenariosPath %>% file.path("slr_from_GCAM.csv")
### Population Scenario File Name
popInputFile  <- scenariosPath %>% file.path("pop_scenario.csv")
### Import inputs
example_inputsList <- import_inputs(
  tempfile = tempInputFile,
  slrfile  = slrInputFile,
  popfile  = popInputFile
)
### Run custom temperature scenario and output impacts without aggregation
and with present values (default base year and discount rate)
df_tempExOut <- run_fredi(inputsList= tempBin_inputs, aggLevels="none",
pv=TRUE, silent=TRUE)
```

F.2.1.2 import_inputs

Import custom scenarios for temperature, sea-level rise, population, and GDP from user-specified file names.

Description

This function enables users to import data on custom scenarios for use with FrEDI (supplied as to `run_fredi()`. Users specify path names to CSV files containing temperature, global mean sea level rise (GMSL), gross domestic product (GDP), and population scenarios. `import_inputs()`reads in and formats any specified files as data frames and returns a list of dataframes for imported scenarios.

Usage

```
import_inputs(tempfile=NULL, slrfile=NULL, popfile=NULL, gdpfile=NULL,
popform="wide", temptype="conus")
```

Arguments

tempfile	A character string indicating the location of a CSV file containing a custom temperature scenario (first column contains years in the interval 2000 to 2090; second column contains temperatures, in degrees Celsius, above the 1995 baseline year). The temperature scenario must start in 2000 or earlier.
slrfile	A character string indicating the location of a CSV file containing a custom sea level rise scenario (first column contains years in the interval 2000 to 2090; second column contains values for global mean sea level rise (GMSL), in centimeters, above the 2000 baseline year). The SLR scenario must start in 2000 or earlier.
popfile	A character string indicating the location of a CSV file containing a custom population scenario for NCA regions. The first column contains years in the interval 2010 to 2090. The number of additional columns, column names, and column contents depend on the population format set by `popform`. For more details, see `popform `.
gdpfile	A character string indicating the location of a CSV file containing a custom scenario for gross domestic product (GDP) (first column contains years in the interval 2010 to 2090; second column contains values for GDP, in total 2015$).
temptype	A character string indicating whether the temperature values in the temperature input file (specified by `tempfile` represent global temperature change (`temptype= "global"`) or temperature change for the contiguous U.S. (`temptype="conus"`) in degrees Celsius. By default, the model assumes temperatures are CONUS temperatures (i.e., `default="conus"`).
popform	A character string indicating whether the populations in the population input file specified by `popfile` are spread across multiple columns (wide format i.e., `popform="wide"`) or are combined in a single column (long format i.e., `popform="long"`). For both formats (`popform="wide"` or `popform="long"`), the first column contains values for the associated value year. If `popform= "wide"` (default), the second through eighth columns of `popfile` must contain population values for each NCA region, with the associated NCA

	region as the column name. If `popform= "long"`, the second column must contain NCA region names and the third column must contain values for the associated region population.

Details

This function enables users to import data on custom scenarios for use with FrEDI (supplied as to `run_fredi()`. Users specify path names to CSV files containing temperature, global mean sea level rise (GMSL), population, and gross domestic product (GDP) scenarios (`tempfile`, `slrfile`, `gdpfile`, and `popfile`, respectively). `import_inputs()` reads in and format any specified files as data frames and returns a list of dataframes for imported scenarios. Users can specify whether the temperature input is for the contiguous U.S. (CONUS) or global using `temptype` (`temptype="cons"` or `temptype="global"`, respectively) and specify the format of the population scenario using `popform` (`popform="wide"` or `popform="long"`).

Values for input scenarios must be within reasonable ranges. Temperatures must be in degrees Celsius and values must be greater than or equal to zero and less than or equal to 10 degrees of warming. Values for GMSL must be in centimeters (cm) and values must be greater than or equal to zero and less than or equal to 250 cm. Population and GDP values must be greater than or equal to zero. If a user inputs a custom scenario with values outside the allowable ranges, `import_inputs()` will not import that scenario and will instead stop and return an error message.

`import_inputs()` drops missing values . The main function, `run_fredi()`, linearly interpolates missing values between available data points. For more information, see `run_fredi()`.

If the temperature type is specified as global (`temptype="global"`), `import_inputs()` converts input global temperatures in to CONUS temperatures (both in degrees Celsius relative to the baseline year of 1995) using `convertTemps()`. For more information, see F.2.2.1. `convertTemps()`.

If the population input is spread across multiple columns (wide format i.e., `popform="wide"`), columns must be named according to the NCA regions. If the population input is in the long format (i.e., `popform="long"`), the region value must be in the second column. The NCA region names for population inputs must be in the following character vector: `c("Midwest", "Northeast", "Northern.Plains", "Northwest", "Southeast", "Southern.Plains", "Southwest")`. All regions must be present in the population input file.

`import_inputs()` outputs a list of dataframes that can be passed to `run_fredi()` using the `inputList` argument. For example, specify `run_fredi(inputsList=x)` to generate impacts for a custom scenario `x` (where `x` is a list of dataframes such as that output from `import_inputs()`) . For more information and examples, see `run_fredi()`. All inputs to `import_inputs()` are optional. If the user does not specify a file path for `tempfile`, `slrfile`, `gdpfile`, or `popfile` (or if there is an error reading in inputs from those file paths), `import_inputs()` outputs a list with a `NULL` value for the associated list element. When the resulting list is passed as an argument to `run_fredi()`, `run_fredi()` defaults back to the default scenarios for any list elements that are `NULL` or missing. In other words, running `run_fredi(inputsList=list())` returns the same outputs as running `run_fredi()`.

Outputs

`import_inputs()` returns a list of named elements containing dataframes with custom scenarios for temperature, GMSL, GDP, and regional population, respectively:

`tempInput`	Dataframe containing a custom temperature scenario imported from the CSV file specified by `tempfile`, with missing values removed. `tempInput` has two columns with names `c("year", "temp_C")` containing the year and CONUS temperatures in degrees Celsius, respectively.
`slrInput`	Dataframe containing a custom GMSL scenario imported from the CSV file specified by `slrfile`, with missing values removed. `slrInput` has two columns with names `c("year", "slr_cm")` containing the year and global mean sea level rise (GMSL) in centimeters, respectively.
`gdpInput`	Dataframe containing a custom GDP scenario imported from the CSV file specified by `gdpfile`, with missing values removed. `gdpInput` has two columns with names `c("year", "gdp_usd")` containing the year and the U.S. national GDP in 2015$, respectively.
`popInput`	Dataframe containing a custom temperature scenario imported from the CSV file specified by `popfile`, with missing values removed. `popInput` has and three columns with names `c("year", "region", "reg_pop")` containing the year, the NCA region name, and the NCA region population, respectively.

Examples

```
### Path to example scenarios
scenariosPath <- system.file(package="FrEDI") %>%
file.path("extdata","scenarios")
### View example scenario names
scenariosPath %>% list.files
### Temperature Scenario File Name
tempInputFile <- scenariosPath %>% file.path("GCAM_scenario.csv", sep="/")
### SLR Scenario File Name
slrInputFile  <- scenariosPath %>% file.path("slr_from_GCAM.csv", sep="/")
### Population Scenario File Name
popInputFile  <- scenariosPath %>% file.path("pop_scenario.csv")
### Import inputs
example_inputsList <- import_inputs(
  tempfile = tempInputFile,
  slrfile  = slrInputFile,
  popfile  = popInputFile
)
```

A snapshot of the dataframes comprising the output list from the example above (`example_inputsList`) is shown below:

```
example_inputsList$tempInput %>% head
```

```
##   year    temp_C
## 1 2010 0.7706176
## 2 2015 0.8879051
## 3 2020 1.0331185
## 4 2025 1.1999864
## 5 2030 1.3806500
## 6 2035 1.5674594
```

```
example_inputsList$slrInput %>% head
```

```
##   year slr_cm
## 1 1970      0
## 2 1980      2
## 3 1990      5
## 4 2000      8
## 5 2010     13
## 6 2020     19
```

```
example_inputsList$popInput %>% head
```

```
##   year          region reg_pop
## 1 2010 Northern.Plains 4956777
## 2 2020 Northern.Plains 5348266
## 3 2030 Northern.Plains 5879482
## 4 2040 Northern.Plains 6458399
## 5 2050 Northern.Plains 7090174
## 6 2060 Northern.Plains 7860014
```

F.2.1.3 get_plots

Create and save plots for summarized FrEDI outputs.

Description

This function creates plots for the summarized FrEDI outputs. `get_plots()` returns a list with heatmaps for model types present in the data (GCMs and SLR scenarios) and annual results for all sectors and adaptations. Results from FrEDI must be summed across impact types before using `get_plots()` (use `run_fredi()` with the defaults, use `run_fredi(aggLevels="impacttype")`, or run `aggregate_impacts(aggLevels="impacttype")` on the output from `run_fredi()`).

Usage

```
get_plots(data, column="annual_impacts", undiscounted=TRUE,
directory=NULL, save=FALSE, plotTypes="all")
```

Arguments

data	Dataframe of summarized outputs produced by `run_fredi()`. Do not change column names of the `run_fredi()` output before running `get_plots()`.
column	A character string indicating the name of the numeric column in the data for which to create plots (e.g., `"annual_impacts"`).
undiscounted	A `TRUE/FALSE` value indicating whether the values in specified column represent undiscounted values (e.g., if `column="annual_impacts"`) or discounted values (i.e., present values). Defaults to `undiscounted=TRUE`.
directory	A character string indicating the location of a directory in which to save the report objects. No default (i.e., `directory=NULL`).
save	A `TRUE/FALSE` value indicating whether to save results. If a directory value is supplied (i.e., `!is.null(directory)`), defaults to `save=TRUE`. Otherwise, default is `save=FALSE`.
plotTypes	Character string or character vector indicating which types of plots to produce. Options are `c("heatmaps", "ribbon", "all")`. Set `plotTypes="all"` (default) to produce both types of plots.

Details

This function processes the results from FrEDI (outputs from `run_fredi()`) after the results have been summarized for impact year estimates and impact types (use `run_fredi()` with the defaults, use `run_fredi(aggLevels= "impacttype")`, or run `aggregate_impacts(aggLevels="impacttype")` on the output from `run_fredi()`).

By default, `get_plots()` plots results from the `"annual_impacts"` column. Alternatively, users can specify a column name in the data with `column` (defaults to (`column="annual_impacts"` for undiscounted impacts or `column="discounted_impacts"` for discounted impacts).

The argument `undiscounted` is used by `get_plots()` for plot labels and in file and directory names for saving results.

Users can specify which plot types to produce by setting `plotTypes`. Set `plotTypes="all"` (default) to produce both heat maps and annual results) or specify a single type (`plotTypes="heatmaps"` and `plotTypes="ribbon"`, respectively). `get_plots()` produces heatmaps (`plotTypes="heatmaps"`) for the outputs of FrEDI and/or plots the average value and range of impacts as a time series (`plotTypes="ribbon"`) for each sector-adaptation-region combination.

The heatmaps display the numeric values in the specified column (e.g., "annual_impacts") as a grid of colored pixels. Each row in the grid corresponds to a sector-adaptation combination (e.g., "Coastal Properties, No Adaptation"), while columns in the grid correspond to years. In other words, the heatmaps display the relative intensity of the impacts of a sector and adaptation compared to others. The colors in the heatmap are a gradient ranging from dark blue (impacts with values below zero) to dark red (impacts with values above zero), with a midpoint at zero (missing values appear as grey pixels). The scale of the gradient is determined from the underlying data, with the darkest points corresponding to the minimum and maximum values.

If temperature-driven (GCM sectors) and SLR-driven (SLR sectors) sectors are both present in the data, `get_plots()` will produce a separate heatmap for each. Each heatmap displays panels for each region (stacked vertically) and underlying models (organized horizontally). An example heatmap for the SLR-driven sectors is shown in Figure F-2 (SLR sectors have a single model value, "Interpolation").

FIGURE F-2 EXAMPLE OF A HEATMAP PRODUCED BY `get_plots()` FOR THE SLR-DRIVEN SECTORS

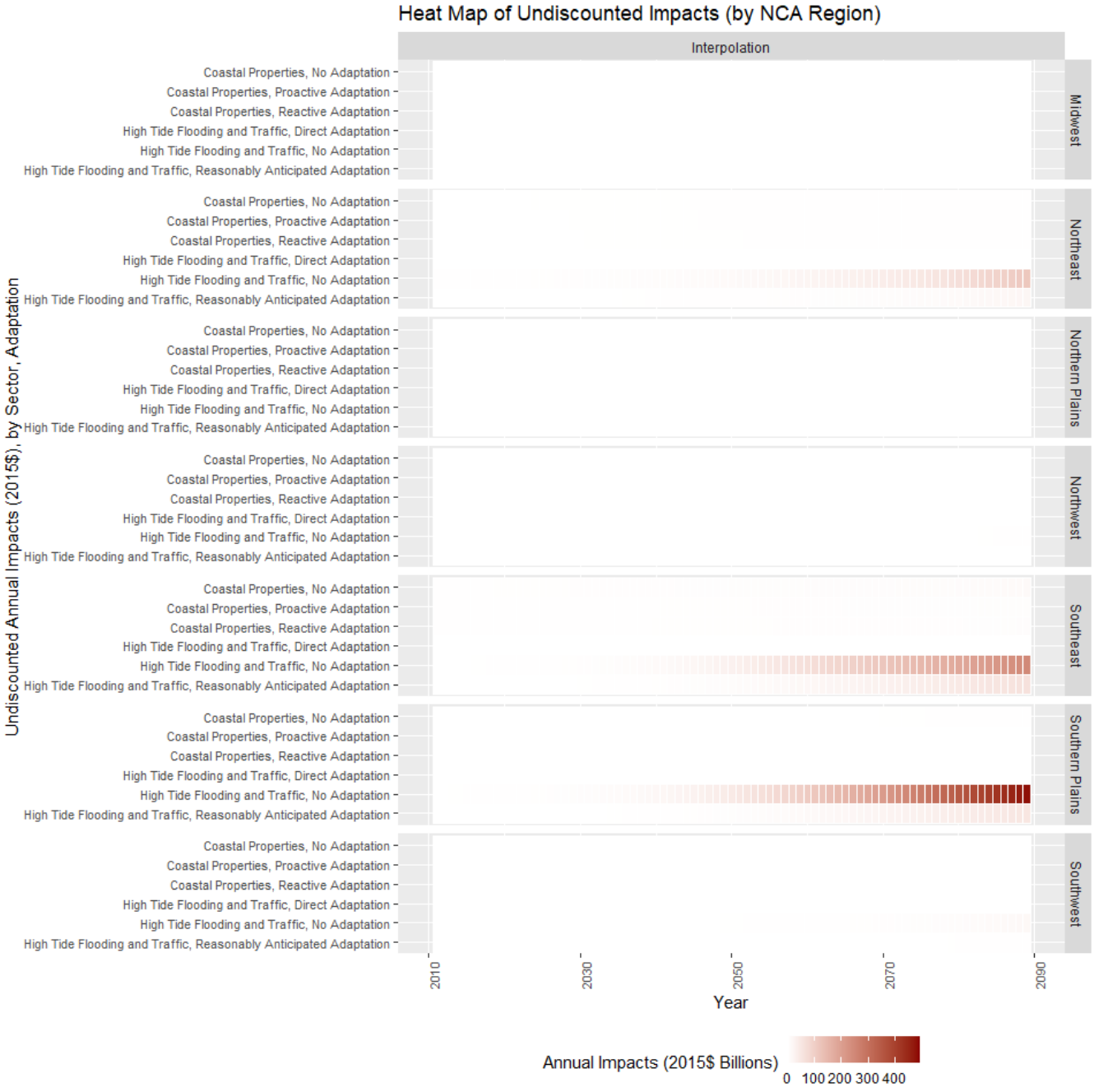

Annual values (`plotTypes="ribbon"`) plots the annual impacts as time series:

- For temperature-driven sectors, the model average is plotted as a line and the range of model values (minimum and maximum) are plotted as a ribbon or area plot. Figure F-3 shows an example of a plot of annual impacts produced by `get_plots()` for a temperature-driven sector (Labor) with a single adaptation (i.e., `adaptation="N/A"`), with the model average plotted as a line and the model range plotted above and below the average.
- For the SLR-driven sectors, the interpolated impacts are plotted as a line. Figure F-4 shows an example of a plot of annual impacts produced by `get_plots()` for a SLR-driven sector (Coastal Properties) with multiple adaptations, with interpolated values plotted as a line.
  For sectors with multiple adaptations, seen in Figure F-4, impacts for individual adaptations are displayed in separate panels (organized horizontally).

FIGURE F-3 EXAMPLE OF A PLOT OF ANNUAL IMPACTS PRODUCED BY `get_plots()` FOR A TEMPERATURE-DRIVEN SECTOR (LABOR)

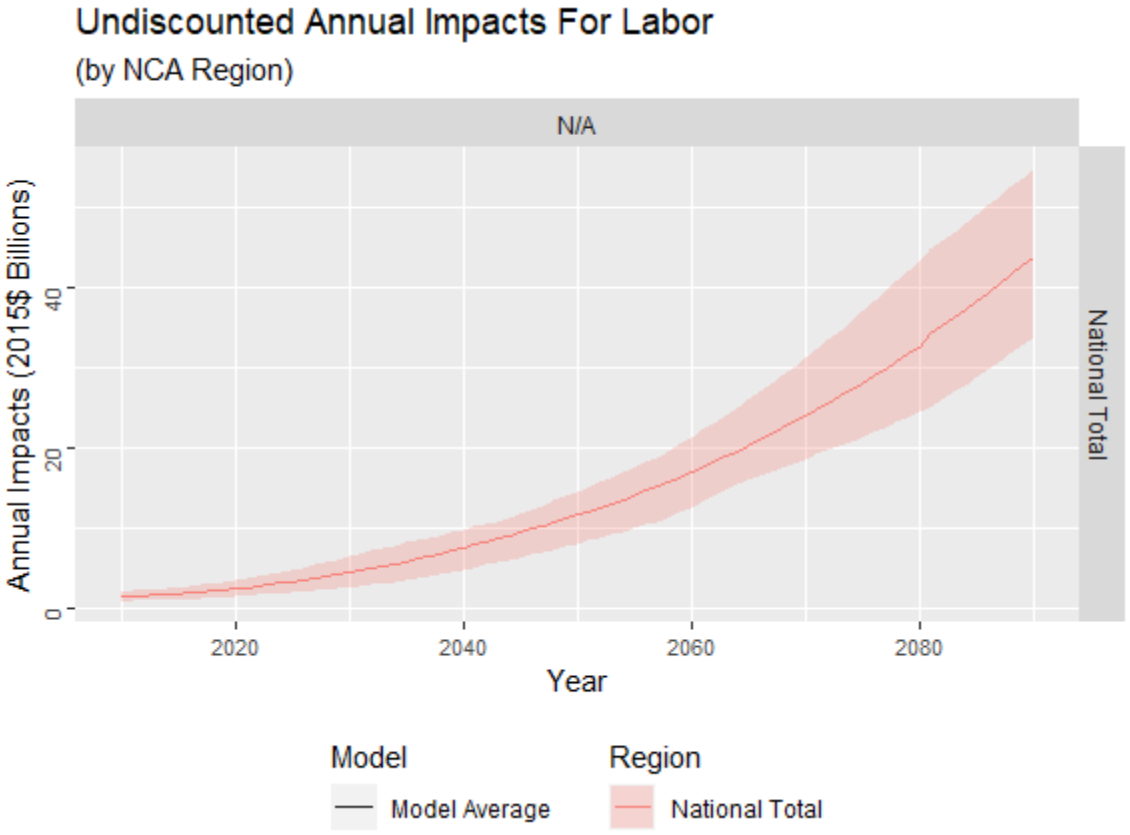

FIGURE F-4 EXAMPLE OF A PLOT OF ANNUAL IMPACTS PRODUCED BY `get_plots()` FOR A SLR-DRIVEN SECTOR (COASTAL PROPERTIES)

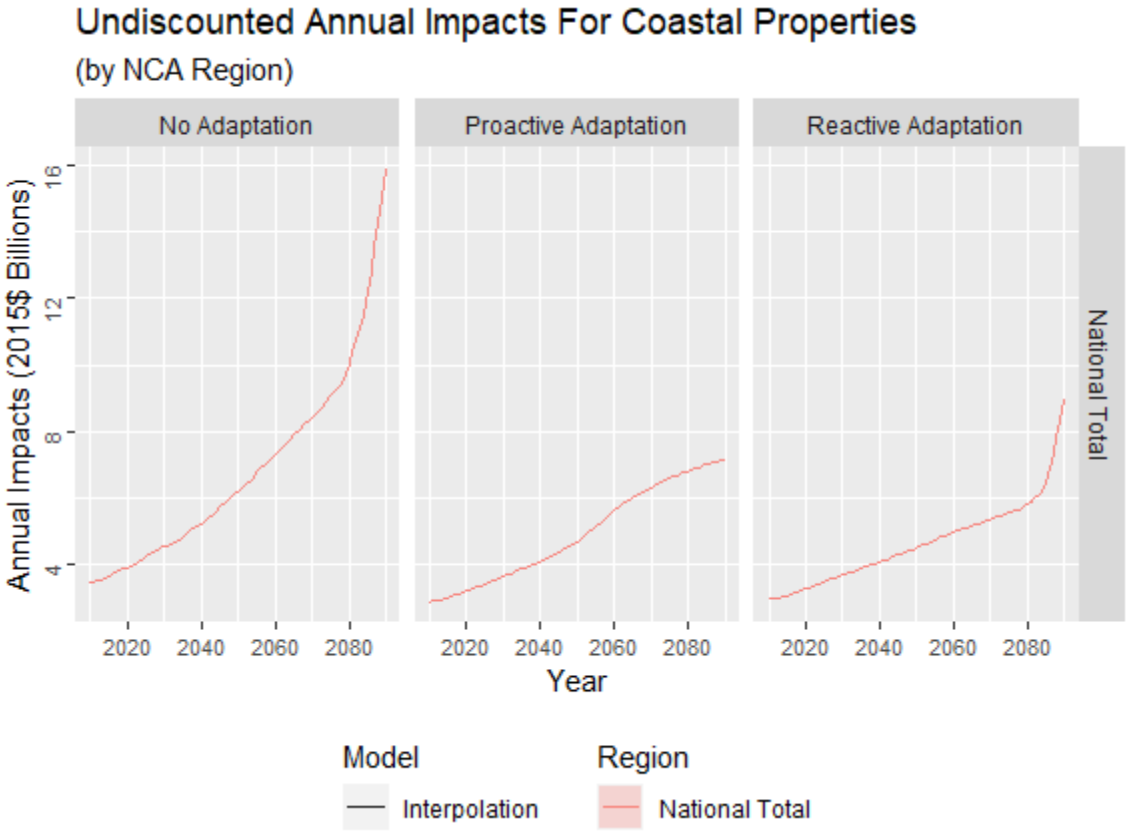

If `save=TRUE` and the user supplies a path to a directory (i.e., `!is.null(directory)`), `get_plots()` will try to save the images as PDF files in the specified directory. `get_plots()` will create separate directories within the specified directory for heatmaps and annual results.

Outputs

heatmaps	List of heatmaps with list elements for all unique values for model types present in data (i.e., `"GCM"` for results calculated with temperature as the driver value and `"SLR"` for results calculated with GMSL as the driver value.
ribbon	List of lists of annual results. List of annual plots contains a list of sectors. Each sector contains a list of adaptations for that sector. Each sector-adaptation combination contains a list of nested regional plots.

Examples

```
### Create input scenarios for FrEDI
df_tempExOut <- run_fredi(aggLevels="none", pv=TRUE, silent=TRUE)

### Aggregate FrEDI impacts for multiple columns
agg_tempExOut <- df_tempExOut %>%
aggregate_impacts(columns=c("annual_impacts", "discounted_impacts"))
```

```
      ### Create list of plots for aggregated results
      agg_plotList <- agg_tempExOut %>% get_plots()

      ### Create list of heatmaps for regional values only:
      reg_plotList <- agg_tempExOut %>% filter(region!="National Total") %>%
get_plots(plotTypes="heatmaps")

      ### Create list of annual plots for national values only:
      nation_plotList <- agg_tempExOut %>% filter(region=="National Total") %>%
get_plots(plotTypes="annual")
```

F.2.2 Helper Functions

F.2.2.1 convertTemps

Convert contiguous U.S. (CONUS) temperatures to global temperatures or vice versa.

Usage

```
convertTemps(temps, from=c("conus", "global"))
```

Arguments

`temps`	A numeric vector of CONUS or global temperatures in degrees Celsius. The temperature series and corresponding years must begin in 2000 or earlier.
`from=c("conus", "global")`	A character string (one of `` `c("conus", "global")` ``), indicating whether users are converting from CONUS to global temperatures (`` `from="conus"` ``) or from global to CONUS (`` `from="global"` ``).

Description/Details

This pre-processing helper function converts a list of warming temperatures in degrees Celsius (`` `temps` ``) from global to CONUS (`` `from="global"` ``) or vice versa (`` `from="global"` ``). The equations for converting between CONUS and global temperatures and back again are described elsewhere in this report.

Outputs

Outputs a numeric vector of temperatures in degrees Celsius.

Examples

```
      ### Create a numeric vector of CONUS integer temperatures from
      ### 1 to 7 degrees of warming (degrees Celsius)
      conusTemps  <- seq(1:7)
      ### Convert from CONUS temperatures to global temperatures
      globalTemps <- conusTemps %>% convertTemps(from="conus")
```

F.2.2.2 temps2slr

Convert global temperature change to global mean sea level rise (GMSL) in centimeters

Arguments

`temps`	A numeric vector of global temperatures in degrees Celsius.

`years`	A numeric vector of years (common era) corresponding to the temperatures provided to `temps`. The temperature series and corresponding years must begin in 2000 or earlier.

Description/Details

This function converts a temperature scenario (global temperatures in degrees Celsius) into an SLR scenario to use for estimate impacts of global mean sea level rise (GMSL) on affected sectors. `temps2slr()` implements the method described by Kopp et al., 2016, "Temperature-driven global sea-level variability in the Common Era" (see references, below).

Outputs

Outputs a dataframe with two columns: `year`, which has the years from the `years` input that fall within the range from 2000 through 2090 (interpolated to annual values) and a second column, `slr_cm`, which has the GMSL in centimeters.

Examples

```
### Path to example scenarios
scenariosPath <- system.file(package="FrEDI") %>%
file.path("extdata","scenarios")

### View example scenario names
scenariosPath %>% list.files

### Temperature Scenario File Name
tempInputFile <- scenariosPath %>% file.path("GCAM_scenario.csv")

### Import example temperature scenario
example_inputsList <- import_inputs(tempfile = tempInputFile)

### Extract the example temperature scenario dataframe from the list
### Example has global temperatures in degrees Celsius
x_tempInput <- example_inputsList$tempInput

### Calculate global mean sea level rise in cm from global
temperatures
x_slr <- temps2slr(temps=x_tempInput$temp_C, years=x_tempInput$year)
```

F.2.2.3 get_sectorInfo

Get information about the sectors in FrEDI

Usage

```
get_sectorInfo(description=FALSE, gcmOnly=FALSE, slrOnly=FALSE)
```

Arguments

`description`	Logical value indicating whether to return the list of sectors as a character vector (`description=FALSE`, default) or to include information about each sector (`description=TRUE`, returns a dataframe).
`gcmOnly`	Logical value indicating whether to return only temperature-driven sectors (`gcmOnly=TRUE`). Defaults to `gcmOnly=FALSE`.
`slrOnly`	Logical value indicating whether to return only SLR-driven sectors (`slrOnly=TRUE`). Defaults to `slrOnly=FALSE`.

Description/Details

If `description=FALSE` (default), this helper function returns a character vector of sector names, which the user can supply to the `sectorList` argument to `run_fredi()`. If `description=TRUE`, `get_sectorInfo()` returns dataframe of sectors with related information returns a dataframe containing the sectors available for FrEDI along with additional information. Sector names are in the first column, with additional columns for the associated model type ("GCM" or "SLR"), adaptations, impact years, and impact types in the remaining columns. Adaptations, impact years, and impact types vary by sector.

Users can specify whether to return only GCM (temperature-driven) sectors *or* SLR (SLR-driven) sectors by setting `gcmOnly=TRUE` or `slrOnly=TRUE`, respectively. `get_sectorInfo()` will return the sectors in the form specified by `description` (see above).

Outputs

- If `description=FALSE` (default), outputs a character vector containing the names of sectors available for FrEDI.
- If `description=TRUE`, outputs a dataframe containing the names of sectors available for FrEDI in one column, with information about the sector model type, adaptations, impact years, and impact types in the remaining columns.

Examples

```
### Return a character vector with the names of all of the sectors in FrEDI:
get_sectorInfo()

### Return a dataframe of all of the sectors in FrEDI (sector names and
additional information)
get_sectorInfo(description=T, gcmOnly=T)

### Return a character vector with only the names of the temperature-driven
sectors:
get_sectorInfo(gcmOnly=T)

### Run FrEDI for only the temperature-driven sectors and view results:
df_x <- run_fredi(sectorList=get_sectorInfo(gcmOnly=T))
```

F.2.2.4 aggregate_impacts

Summarize and aggregate impacts from FrEDI (calculate national totals, average across models, sum impact types, and interpolate between impact estimate years).

Usage

```
aggregate_impacts(data, columns= c("annual_impacts"),
aggLevels=c("all"))
```

Arguments

data	Dataframe of results from FrEDI (outputs from `run_fredi()`
columns	Character vector of columns for which to aggregate results (defaults to columns=c("annual_impacts"))
aggLevels	Levels of aggregation at which to summarize data: one or more of `c("national", "modelaverage", "impactyear", "impactType", "all", "none")`. Defaults to all levels (i.e., `aggLevels="all"`).

Description/Details

This post-processing helper function aggregates and summarizes the FrEDI results to levels of aggregation specified by the user (passed to `aggLevels`). Users can specify a single aggregation level or multiple aggregation levels by passing a single character string or character vector to `aggLevels`. Options for aggregation include calculating national totals (`aggLevels="national"`), averaging across model types and models (`aggLevels="modelaverage"`), summing over all impact types (`aggLevels="impacttype"`), and interpolate between impact year estimates (`aggLevels="impactyear"`). Users can specify all aggregation levels at once by specifying `aggLevels="all"` (default) or no aggregation levels (`aggLevels="none"`).

Before aggregating impacts for national totals and/or model averages, `aggregate_impacts()` will drop any pre-summarized results (i.e., values for which `region="National Total"` and/or for which `model="Average"`, respectively) that are already present in the data and then reaggregate at those levels.

For each of the `aggLevels`, `run_fredi()` performs the following summarization (using `aggregate_impacts()`):

- `"national"`: Annual values are summed across all regions present in the data. I.e., data is grouped by columns `"sector"`, `"adaptation"`, `"impactType"`, `"impactYear"`, `"model_type"`, `"model"`, and `"year"`. Years which have missing column data for all regions return as `NA` (missing). The rows of the dataframe of national values (with column `region="National Total"`) are then added as rows to the regional values.
- `"modelAverage"`: Annual results are averaged across all models present in the data, i.e., data is grouped by columns `"sector"`, `"adaptation"`, `"impactType"`, `"impactYear"`, `"model_type"`, `"region"`, and `"year"` and averaged across models. Averages exclude missing values. Years which have missing column data for all models return as `NA` (missing). The rows of the dataframe of model averages (with `model="Average"` for temperature-driven sectors and `model="Interpolation"` for SLR-driven sectors) are then added as rows to individual model results.
- `"impactType"`: Annual results are summed across all impact types by sector present in the data. I.e., data is grouped by columns `"sector"`, `"adaptation"`, `"impactYear"`, "model_type", "model", "region", and "year" and summed across impact types. Mutates column `impactType="all"` for all values. Years which have missing column data for all impact types return as `NA` (missing). If results are aggregated across impact types, information about physical impacts (dataframe columns `"physicalmeasure"` and `"physical_impacts"`) are dropped.
- `"impactYear"`: Annual results for sectors with only one impact year estimate (i.e., `impactYear=="N/A"`) are separated from those with multiple impact year estimates. For sectors with multiple impact years, annual results are interpolated between impact year estimates for applicable sectors i.e., data is grouped by columns `"sector"`, `"adaptation"`, `"impactType"`, `"model_type"`, `"model"`, `"region"`, and `"year"` and interpolated across years with the 2010 run assigned to year 2010 and the 2090 run assigned to year 2090. The interpolated values are bound back to the results for sectors with a single impact year estimate, and column `impactYear` set to `impactYear="Interpolation"` for all values.

Note that `aggregate_impacts()` drops columns not used in grouping or aggregation.

Outputs

Outputs a dataframe of results produced using FrEDI, summarized at the specified aggregation levels.

Examples

```
### Run FrEDI using the default scenario
df_tempExOut <- run_fredi(aggLevels="none", pv=TRUE, silent=TRUE)

### Aggregate FrEDI results for multiple columns
agg_tempExOut <- df_tempExOut %>%
aggregate_impacts(columns=c("annual_impacts", "discounted_impacts"))
```